Materials Advances

Accepted Manuscript

This article can be cited before page numbers have been issued, to do this please use: V. D. Nguyen, T. Luu, G. Chang-Chien and V. G. Le, *Mater. Adv.*, 2025, DOI: 10.1039/D5MA00872G.

ROYAL SOCIETY OF CHEMISTRY

rsc.li/materials-advances

View Article Online
DOI: 10.1039/D5MA00872G

Progress in Biochar Derived Adsorbents: Preparation, Modification Strategies, and Applications for Remediation of Antibiotics from Wastewater

Van Doan Nguyen,[1] The Anh Luu,[1] Guo-Ping Chang-Chien,[2,3] Van Giang Le,[1,]*

[1] Central Institute for Natural Resources and Environmental Studies, Vietnam National University, Hanoi, Viet Nam.

[2] Center for Environmental Toxin and Emerging-Contaminant Research, Cheng Shiu University, Kaohsiung 833301, Taiwan.

[3] Super Micro Mass Research and Technology Center, Cheng Shiu University, Taiwan.

[*]*Corresponding Author: levangiangcres@.vnu.edu.vn (Van-Giang Le)*

View Article Online
DOI: 10.1039/D5MA00872G

HIGHLIGHTS

- A comprehensive review of recent advances in biochar-based materials for the removal of emerging antibiotic pollutants from aqueous environments.
- Systematic classification and critical analysis of adsorption mechanisms, including hydrogen bonding, electrostatic attraction, π–π interactions, and complexation.
- Comparative evaluation of functionalization strategies (chemical, thermal, and nano-enabled) to enhance adsorption performance and selectivity toward antibiotics.
- In-depth discussion of regeneration techniques and the challenges related to recyclability and stability of biochar-based adsorbents in long-term applications.
- Identification of knowledge gaps and future research directions toward developing next-generation biochar composites with high efficiency and environmental sustainability.

Abstract

The increasing presence of antibiotic compounds in aquatic environments has become a serious concern due to their potential to promote antibiotic resistance and adversely affect ecosystems. Conventional treatment methods are often insufficient for the complete removal of these pollutants. In this context, biochar a porous carbonaceous material derived from biomass pyrolysis has attracted significant attention as a promising material for the remediation of antibiotics in wastewater. This review systematically highlights recent advances in the study of biochar including its sources and synthesis techniques such as pyrolysis, gasification, hydrothermal carbonization, and mild pyrolysis. It also explores various activation and modification strategies including physical and chemical activation, electrochemical techniques, and environmentally friendly modification approaches. Furthermore, the effects of operational parameters such as pH, temperature, duration time, biochar dosage, and pollutant concentration on uptake performance are thoroughly examined. The underlying adsorption mechanisms such as electrostatic interactions, ion exchange, π–π interactions, surface complexation, and capillary diffusion, are analyzed in detail. In addition, quantum chemical approaches, particularly density functional theory (DFT) are discussed for their role in elucidating the fundamental interactions between antibiotics and biochar materials. Finally, the review

View Article Online
DOI: 10.1039/D5MA00872G

addresses current challenges, potential risks, and emerging trends in the development of hybrid biochar materials, particularly those incorporating MOFs and MXenes for effective antibiotic pollution control.

Keywords: *Biochar, chemical activation, modification, antibiotics, wastewater treatment*

View Article Online
DOI: 10.1039/D5MA00872G

1. Introduction

Biochar, also known as “black gold”, is a solid substance abundant in carbon fabricated via the pyrolysis of biomass including sludge, agricultural and livestock waste under low oxygen environments [1]. The name “biochar” refers to the combination of the prefix “bio” representing biomass and the suffix “char” originating from charcoal. Since its name, the concept has been mentioned in many research works [2]. Alternatively, biomass is a general term for the collection of organic materials originating from living entities or a mixture of related substances [3]. In fact, biomass is formed by the process of photosynthesis and is commonly present in both terrestrial and aquatic plants. Among them, lignocellulosic biomass consists of three fundamental parts like hemicellulose, lignin, and cellulose. Owing to its low cost, renewable ability, and carbon neutrality, this type of biomass is considered a promising option in solving energy problems. Its origin can come from natural materials or through intermediate effects [4].

Thermal processes including incineration, pyrolysis or hydrothermal carbonization (HTC) can be utilized to fabricate biochar from biomass wastes such as manure, rice husk, sawdust or leaves [5]. Among these techniques, pyrolysis stands as the most commonly utilized method to fabricate biochar under oxygen-free and high-temperature conditions [6-8]. This method also generates by-products such as heat energy, syngas, liquid fuel, and wood vinegar (pyroligneous acid) [9, 10]. HTC technology represents a new method for synthesizing carbonaceous materials such as biochar, which is receiving much attention due to its environmental friendliness, reasonable cost, and relatively simple process [11, 12]. During this process, the crude material is heated at high pressure and temperature to create hydrochar, a carbon-rich material with high calorific value, low moisture, and good combustion properties [13, 14]. Hydrochar can be used for many purposes such as providing energy for gas storage [15], soil improvement [16], catalysis [17], fuel cells [13] or adsorbing pollutants in water including antibiotics [18] and heavy metals [19].

Biochar is a widely utilized and effective material globally for removing pollutants from water thanks to its porous structure similar to activated carbon (AC). As opposed to AC, biochar refers to a new, low-cost but highly efficient material. While activated carbon requires a complex activation process and high temperature, biochar is easier to produce and more energy-efficient [2]. Therefore, biochar may be employed as an initial precursor for the fabrication of AC [20]. However, due to being produced under low-energy conditions and without an activation stage, biochar usually exhibits a smaller surface area and reduced

View Article Online
DOI: 10.1039/D5MA00872G

mechanical strength compared to AC. While the fabrication of AC requires chemical activation of the input material along with gas activation during pyrolysis, biochar hardly needs these steps [21].

Biochar is considered an effective soil additive due to its ability to retain nutrients and enhance soil stability, thereby contributing to increased crop yields. In addition to its role in agriculture, biochar also brings great benefits in environmental remediation, especially in controlling soil pollution. Currently, soil pollution caused by heavy metals [22, 23] and persistent organic pollutants (such as chlorinated furans (PCDFs), chlorinated biphenyls (PCBs), brominated flame retardants (BFRs), and chlorinated dioxins (PCDDs)) [24-26] is a serious global problem, directly threatening human health and ecosystems. Contaminants persist in soil and water for extended periods because they are not biodegradable, causing soil quality deterioration and hindering agricultural activities. The treatment of these pollutants is often very expensive and lengthy. Nevertheless, biochar can stabilize pollutants through enhanced removal mechanisms (including electrostatic attraction, coordination, and surface complexation) and chemical precipitation (arising from the increase in soil pH as well as the addition of carbonate ash and phosphate ash) [27-29]. Physicochemical attributes of biochar therefore effectively support the remediation of metal species and antibiotic contaminants in soil, helping to reduce their mobility and potential for harm [30-33]. Thus, the utilization of biochar not only contributes to soil quality restoration but is also a sustainable solution in minimizing the environmental impact caused by soil pollution.

To address the pressing need for water conservation under global environmental strain, biochar is being used as a water purifier in various agricultural and industrial applications [29, 34-36]. The quality of aquatic ecosystems is continuously declining due to a growing array of pollutants stemming from human activities [37, 38]. These include common contaminants like pesticides, heavy metals, pathogens, antibiotics, dyes, pharmaceuticals, and personal care products [37, 39-42]. Notably, antibiotics frequently occur in aquatic environments at comparatively high levels [43, 44], making their pollution a widespread global environmental concern [45]. Water and wastewater systems can be contaminated with antibiotics from various natural and human-related sources including medical waste, urine and feces from humans, and animals treated with antibiotics, and runoff from livestock farms [46, 47]. The primary sources include hospital waste, pharmaceutical manufacturing facilities, livestock farms using antibiotics as growth promoters, and inadequately treated municipal wastewater [48]. Measured concentrations of these antibiotics in the environment often exceed safe limits,

View Article Online
DOI: 10.1039/D5MA00872G

posing a risk of drug resistance and affecting the ecosystem [48]. For example, antibiotic concentrations in some polluted water sources can reach extremely high levels. A study in India detected ciprofloxacin (CIP) concentrations in streams near pharmaceutical factories as high as 296 mg/L, over 1500 times the recommended safety limit [49]. In Pakistan, CIP levels in wastewater reached 331.15 mg/L while hospital wastewater in Egypt contained amoxicillin, ampicillin, and dicloxacillin at concentrations of 99.04, 70.06, and 119.24 mg/L, respectively [50]. In Vietnam, sulfamethoxazole (SMX) levels in the To Lich, Lu, and Kim Nguu rivers were measured at 0.585, 1.09, and 0.535 mg/L, respectively [51]. The persistent presence of these antibiotics in aquatic environments promotes the emergence of antibiotic-resistant bacterial strains, posing serious risks to ecosystems and human health [52].

As depicted in **Figure 1**, multiple approaches can be employed to eliminate antibiotics from water like solvent extraction, chemical precipitation, membrane filtration, ion exchange, sedimentation, coagulation, and both electrochemical and genetic approaches [53-56]. Among these, adsorption using natural and eco-friendly materials stands out as a promising solution owing to its user-friendliness, low expense, high performance, and environmental sustainability [57-59]. Traditional approaches like coagulation and sedimentation are inexpensive and straightforward to implement, yet they typically offer low removal efficiency and pose significant challenges in managing the generated sludge. In contrast, advanced oxidation processes can break down pollutants that resist conventional treatment methods. However, they demand substantial chemical inputs, leading to higher operational costs and the risk of secondary pollution. Techniques such as electrodialysis, ion exchange, and membrane separation tend to achieve high selectivity and efficiency, but their reliance on complex equipment and high energy consumption makes them costly solutions. Unlike many complicated approaches, adsorption is a straightforward method that relies on physical or chemical interactions to capture pollutants on the surface of an adsorbent, offering both high removal efficiency and environmental compatibility [60-62]. From a cost perspective, adsorption remains a much more economical option, with expenses under $200 per million liters of treated water and considerably lower than methods like electrodialysis or ion exchange, which can cost up to $450 [63]. Consequently, adsorption continues to be regarded as a promising approach for eliminating antibiotics from aqueous environments. The global research trend related to biochar, adsorption and treatment of antibiotics in aquatic environments is also increasing markedly over the years, as shown in **Figure 2**.

View Article Online
DOI: 10.1039/D5MA00872G

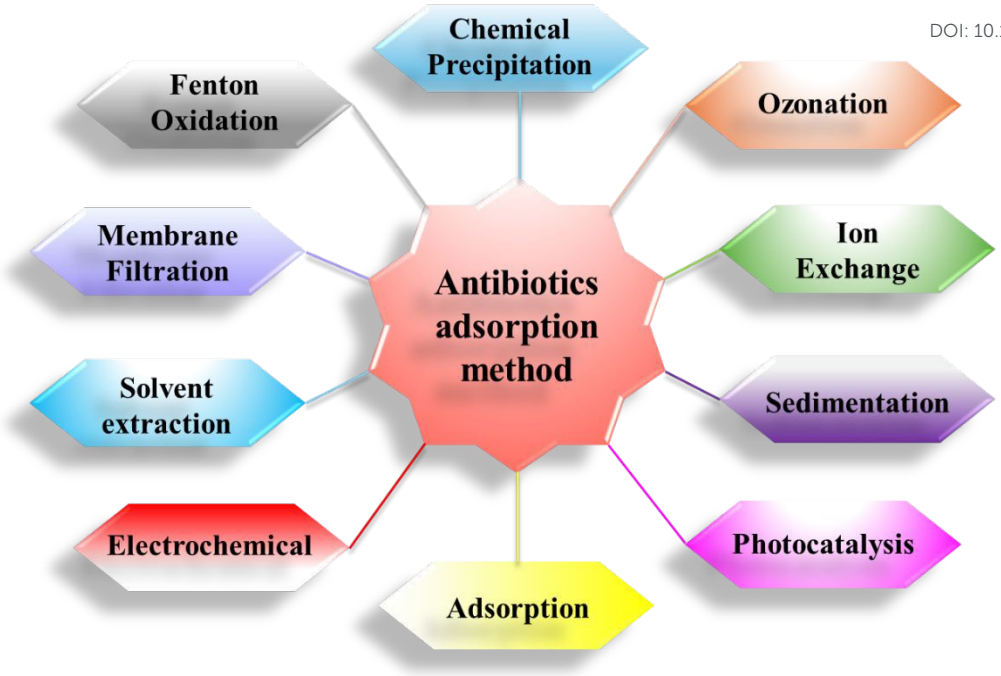

Figure 1. Multiple technique for the treatment of antibiotics

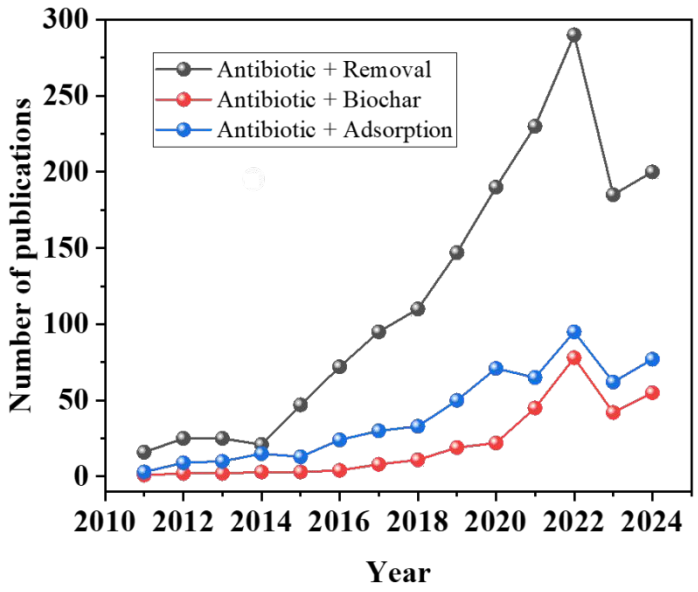

Figure 2. Number of articles published from 2011–2024 with the keywords "Antibiotic + Removal", "Antibiotic + Adsorption" and "Antibiotic + Biochar" on the Web of Science

In the context of increasing environmental pressures and the proliferation of organic pollutants including antibiotics, biochar has emerged as an environmentally friendly and cost-effective material. However, most current research remains primarily focused on heavy metal treatment [64-66] while the application of biochar for antibiotic elimination, a group of highly

View Article Online
DOI: 10.1039/D5MA00872G

toxic pollutants with significant potential to induce antimicrobial resistance has not yet been fully explored. Furthermore, biochar is not only enhanced by traditional chemical modification methods but is also being studied for performance improvement through advanced techniques such as electrochemical modification [67, 68], plasma treatment [68], or integration with novel nanomaterials like MXene and MOFs. These approaches significantly increase the material's removal capacity and selectivity toward challenging organic pollutants, including antibiotics. In addition to experimental studies, recent years have seen a growing trend in utilizing computational models, such as Density Functional Theory (DFT) to elucidate adsorption mechanisms on biochar at the atomic level. This approach generates novel insights into the nature of interactions between biochar and pollutants, including antibiotics, which are challenging to observe through conventional experimental methods.

Unlike many reviews that focus solely on material aspects such as biomass origin, synthesis methods, and conventional biochar modification, this paper offers a more integrated perspective by connecting material development with practical insights into pollutant adsorption. Beyond detailing feedstocks and fabrication methods like pyrolysis and HTC, it highlights advanced surface engineering strategies including nanomaterial incorporation and novel activation techniques that enhance adsorption performance. A key feature of this work is its focused analysis on the elimination of antibiotics from wastewater, supported not only by experimental evidence but also by computational modeling. Specifically, density functional theory (DFT) is employed to elucidate adsorption mechanisms at the atomic level, offering insights into interactions that conventional methods often overlook. This comprehensive approach bridges material innovation with real-world application, contributing to the development of next-generation, sustainable water purification technologies.

2. Biochar: Precursors, Preparation Approaches, and Structural Features

Biochar is a carbon-dense substance that typically makes up 60 to 90 % of the material's composition [69]. It could also comprise elements like oxygen, inorganic ash, and hydrogen, which depends on the biomass source [70]. Producing biochar is seen as more environmentally sustainable than burning coal, as biomass is naturally carbon neutral. Its surface area is generally large, often surpassing 100 m^2/g, which effected by both the synthesis conditions and crude materials [71]. This property makes biochar useful in various non-fuel applications, including chemical adsorption [72] for water purification and long-term carbon storage [70]. It has also been explored and applied as a soil amendment to enhance fertility [73].

View Article Online
DOI: 10.1039/D5MA00872G

2.1. Precursors for biochar preparation

Biomass refers to organic substances sourced from living or once-living organisms, with the potential for regeneration and widespread application in environmental and energy-related fields. It may be utilized to fabricate electricity and heat, produce organic fertilizers, biofuels, pharmaceuticals, chemicals, and biological materials such as biochar. Virtually all types of organic matter including bark, seed coats, agricultural residues, and manure can be converted into biochar with appropriate processing equipment [74-76]. The original source of biomass may come from plant, animal, or human waste, including domestic and industrial wastewater [77, 78]. Contingent on the specific biomass chosen, the resulting biochar will exhibit different physical and chemical characteristics, enabling the flexible application of carbon materials for various specific purposes.

Biomass feedstocks are commonly categorized into two main types: non-woody and woody biomass [79]. The study by Shrivastava et al. focused on rubberwood sawdust (RWS) as a representative of woody biomass and oil palm fronds (OPF) as a representative of non-woody biomass [80]. The initial assessment of these materials covering moisture content, fixed carbon, volatile matter, and ash shows that woody biomass typically contains 75.97 % volatile matter, 15.22 % fixed carbon, 7.14 % moisture, and 1.69 % ash (by weight), while the corresponding values for non-woody biomass are 72.31, 15.68, 6.44, and 5.34 %, respectively. Similarly, ultimate analysis reveals that woody biomass comprises approximately 47.65 % carbon, 6.12 % hydrogen, 0.33 % nitrogen, 45.90 % oxygen, and 0.03 % sulfur compared to 44.96, 5.79, 0.41, 48.72, and 0.07 % in non-woody biomass. Woody biomass mainly originates from forest residues and wood processing waste, which is characterized by minimal moisture and ash content while demonstrating elevated energy content, significant mass per unit volume, and limited pore space [79]. Conversely, non-woody biomass sources such as farm residues, bioenergy crops, animal manure, and household refuse or industrial solid waste typically exhibit higher moisture and ash content, lower heating values, lower bulk densities, and greater porosity [79]. These significant differences underscore the importance of selecting appropriate raw materials when producing biochar for specific environmental applications.

View Article Online
DOI: 10.1039/D5MA00872G

Figure 3. Widely utilized raw materials for biochar synthesis

Biomass includes living or previously living organic matter which is a versatile renewable resource with applications in environmental and energy sectors such as heat or electricity generation. It also serves as a raw material for producing organic fertilizers, biofuels, chemicals, pharmaceuticals, and biomaterials like biochar. The characteristics of biochar-based materials vary depending on the presursor, enabling tailored use of carbonaceous materials for specific purposes. This primary resource can originate from plant, animal, or human waste, including sewage sludge, food wastes, forestry waste (e.g., wood chips), farm waste (e.g., animal manure), and industrial byproducts [77, 78]. Nearly any organic material such as seed coats, bark, crop residues, or manure can be converted into biochar with suitable processing methods [74, 81]. **Figure 3** lists the most common feedstocks for biochar fabrication, which range from plant matter to industrial byproducts.

In recent years, various raw materials including animal tissue, algae, manure, and food waste have been explored for the generation of biochar [82-84]. These investigations have produced notable findings regarding both the physicochemical characteristics and the potential uses of the resulting biochar. Although biochar is primarily derived from plant-based waste, commonly referred to as cellulosic biomass such as firewood or rice husks, not all organic-rich materials are suitable for its synthesis. Municipal solid waste (MSW) or wastewater, despite

View Article Online
DOI: 10.1039/D5MA00872G

their high biomass content, often contain contaminants that may decrease the performance of biochar in soil and water remediation applications [2].

2.2. Approaches to synthesizing biochar

2.2.1. Traditional pyrolysis

The pyrolysis method and its resulting products are illustrated in **Figure 4**, which highlights the diversity of biomass precursors utilized in biochar fabrication. Pyrolysis generally refers to the heat-driven breakdown of biomass under heat in an oxygen-limited environment, typically at evevated temperatures spanning from 300 to 900 °C [85]. This conditions result in the fragmentation of hemicellulose, lignin, and cellulose as well as depolymerization and cross-linking reactions, resulting in the formation of biomass-derived products. Furthermore, pyrolysis produces liquid, solid, and gaseous products, named as bio-oil, biochar, and biogas, respectively. The physicochemical properties and yields of these products may vary depending on the type of pyrolysis applied. Based on heating rateand residence duration, pyrolysis could be classified into two fundamental modes like fast and slow pyrolysis. Fast pyrolysis is primarily employed to produce high concentrations of liquid products (such as biofuels) with superior physicochemical properties including lower volatile organic compound (VOC) concentration and a higher content of long-chain hydrocarbons [86]. It usually requires brief residence times under 10 seconds and rapid heating rates above 200 °C/min [15]. Nonetheless, fast pyrolysis typically produces biochar with reduced yields and smaller surface areas, which may be due to tar-like substances becoming lodged within the pores [87]. In addition, fast pyrolysis tends to produce biochar with hydroxyl and carboxylic acid groups as the dominant functional groups, whereas slow pyrolysis generates biochar rich in aromatic C–H groups [88]. Slow pyrolysis typically involves extended durations for material retention during the process (more than 1 h) and lower heating rates (3–10 °C/min). While it produces a larger amount of biochar, it also yields gases and liquids with lower concentrations but containing significant amounts of VOCs, which are considered pollutants [89].

High treatment temperatures during pyrolysis not only promote transformation reactions but also generate the activation energy necessary to facilitate the generation of carbonaceous frameworks with a higher order's degree [90]. Increasing the treatment temperature significantly enhances pore development on the surface's biochar, a key factor in improving specific surface area. For example, a work by Lua et al. [91] revealed that enhancing the temperature of the pyrolysis from 250 to 500 °C raised the surface area from 170 to 480 m^2/g.

This increase was attributed to the intense development of volatiles in pistachio shells, which contributed to the generation of a porous frameworks with a high pore volume of 0.469 cm^3/g at 500 °C, more than double the 0.192 cm^3/g observed at 250 °C.

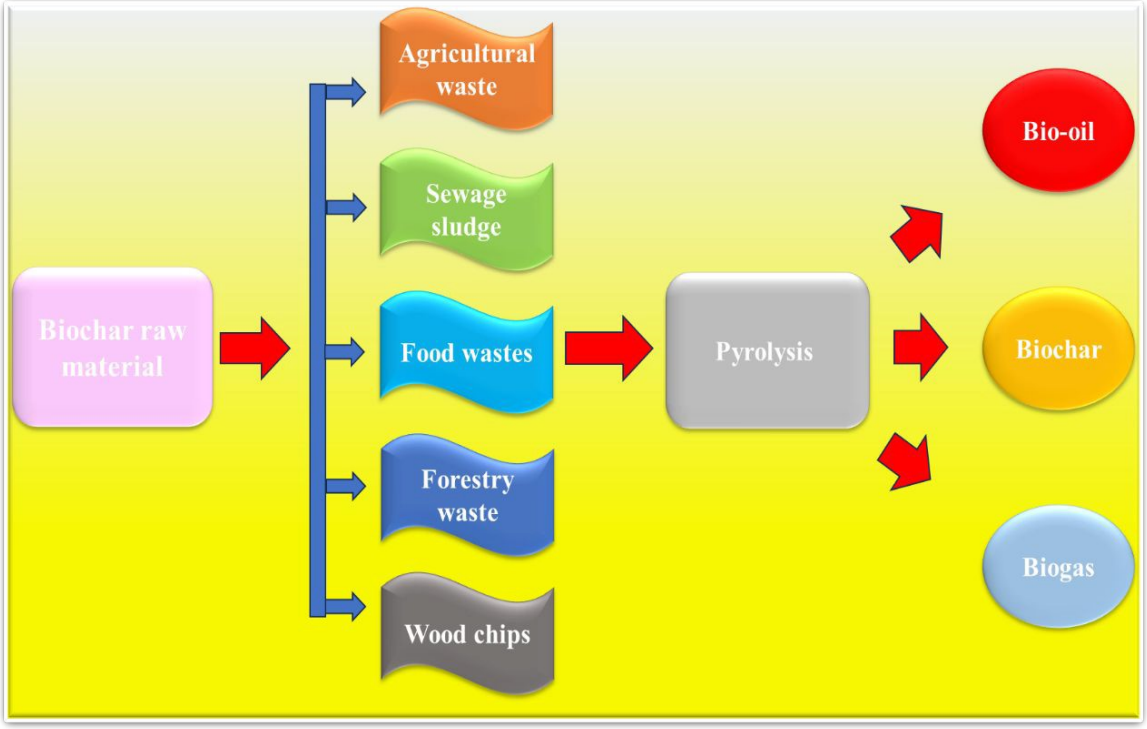

Figure 4. Schematic diagram of biochar fabrication from multiple biomass sources through pyrolysis.

In general, higher processing temperatures have a more pronounced effect on the physicochemical properties of the resulting products. Therefore, to obtain high-efficiency and high-quality biochar, the pyrolysis process should be conducted within the temperature range of 400 – 800 °C [92, 93]. The changes in the size and arrangement of carbon structures that occur during biomass pyrolysis are key contributors to the enhancement of the physicochemical parameters of the ultimate products [94].

2.2.2. Gasification

Gasification operates as an advanced thermal treatment method, typically occurring at elevated temperatures around 800 °C in the occurrence of reactive gases like air and oxygen [6], where carbon-rich materials are transformed into gaseous, liquid, and solid samples. This process involves four fundamental stages such as pyrolysis, partial oxidation, reduction, and drying. Among the resulting products are carbon monoxide, carbon dioxide, nitrogen, hydrogen, tar, ash, and charcoal. Charcoal, which represents a solid output, typically makes up only approximately 10 % of the initial precursor weight [95, 96].

View Article Online
DOI: 10.1039/D5MA00872G

While the original purpose of gasification was to enhance energy recovery by generating large volumes of synthesis gas, increasing interest has recently been directed toward the charcoal produced during the process. This carbon-rich material, typically identified as biochar, is now recognized as a valuable secondary product. However, balancing the dual objectives of maximizing energy recovery and increasing biochar yield presents a technical challenge. This requires careful adjustment of operational parameters including temperature, pressure, and the nature of the input gas mixture [95]. Additionally, the chemical-physical profile of input feedstocks are fundamentally important to the overall efficiency, as well as to both the amount and characteristics of the resulting biochar produced by gasification techniques.

2.2.3. Hydrothermal carbonization - HTC

Hydrothermal carbonization (HTC) refers to a thermochemical technique utilized to efficiently treat high-moisture biomass in an aqueous environment under high temperature and pressure conditions [12]. The method also known as wet roasting, occurs within a sealed environment at temperature ranges between 120 and 260 °C and under pressures between 2 and 10 MPa without the need for pre-drying of the precursor [97]. HTC typically takes place over a period of 30 min to 8 h under either autogenous or externally applied pressure and could be employed for diverse feedstock sources such as crop byproducts, industrial wastes, sewage sludge, and aquatic biomass [98-100].

HTC primarily produces hydrochar as its end product, a carbon-rich form of biochar formed in the solid phase. In addition to hydrochar, the process also produces an aqueous phase rich in organic matter and nutrients as well as a small mass of gas, mainly consisting of carbon dioxide [101]. Compared to biochar obtained through other thermochemical methods, hydrochar typically has lower fixed carbon and ash contents along with a smaller pore volume and S_{BET} surface area [102]. However, hydrochar possesses large energy density, making it a promising fuel for the application in energy [103].

A key benefit of HTC lies in its capacity to directly process wet biomass without the need for energy-intensive drying stages, which are commonly required in pyrolysis or other high-temperature technologies [16, 104]. This process not only enhances carbon recovery efficiency but also improves product quality compared to conventional technologies. In addition, HTC helps limit the formation of toxic compounds and micropollutants that often arise under the harsh conditions of pyrolysis [105]. However, the performance of the HTC process depends largely on the properties of the precursors, size of particles, and residence time in the reactor.

Particle sizes larger than 2 cm or reaction times shorter than 30 minutes can reduce the efficiency of heat and mass transfer [16]. Therefore, to achieve uniform heat distribution and optimize conversion efficiency, careful control of particle size and feedstock homogeneity is necessary. In the case of sludge treatment, dewatering steps including filtration or centrifugation are also required to facilitate the conversion reaction. Depending on the intended end use, hydrochar can serve as a coal substitute, a feedstock for gasification processes, a soil amendment to enrich nutrients or a freestock to fabricate adsorbents and activated carbon [106]. The selection of appropriate feedstocks and operating conditions will determine the efficiency, quality, and potential applications of the products derived from the HTC process.

2.2.4. Torrefaction

Torrefaction operates at relatively low temperatures (200–300 °C) under oxygen-free conditions, primarily yielding biochar, a material with inferior physicochemical properties compared to pyrolysis-derived products [84, 107, 108]. While both torrefaction and pyrolysis are thermochemical conversion techniques that transform biomass into value-added outputs (e.g., biooil, biogas, biochar) [70], they exhibit distinct differences in processing parameters and end products.

2.3. Approaches to biochar activation and functionalization

2.3.1. Physical activation

Biochar experiences both increased pore development on its surface and chemical property changes when subjected to physical activation (e.g., hydrophobicity, polarity, and surface functional groups). At temperatures ranging from 700–1100 °C [109], gas/steam expands and develops the porous structure of carbonaceous materials, thereby creating materials with high porosity and large surface areas. Conversely, research findings have demonstrated the ability of biochar activated by gas/steam to remove heavy metals and antibiotics. Research by Rong et al. [110] demonstrated that biochar produced from sludge through pyrolysis and physical activation with steam has excellent SMX uptake capacity. Specifically, the specific surface area reached 1583.07 m^2/g after activation while the SMX adsorption capacity increased to 204.07 mg/g in 90 min. The maximum Cu^{2+} adsorption efficiency (93 %) was only achieved when biochar was activated at an appropriate steam flow rate, according to Lima and Marshall [111]. In addition, Mondal et al. [112] utilized biochar derived from mung bean hulls which is activated by superheated steam to adsorb ranitidine hydrochloride in a fixed-bed column. The data revealed that the adsorption efficiency reached

99.16 % at an inlet content of 100 mg/L, demonstrating the effectiveness of steam-activated biochar for the elimination of pharmaceuticals from aqueous environments. High temperature (>500 °C) combined with oxidants (ozone, steam, air, or CO_2) [113] when treating biochar will create two effects: (1) gasification of carbon atoms and (2) expansion of the previously inaccessible pore system [114]. This activation method not only increases the biochar surface area but also significantly adds surface oxygen functional groups, which are considered effective adsorption centers for pollutant treatment [114].

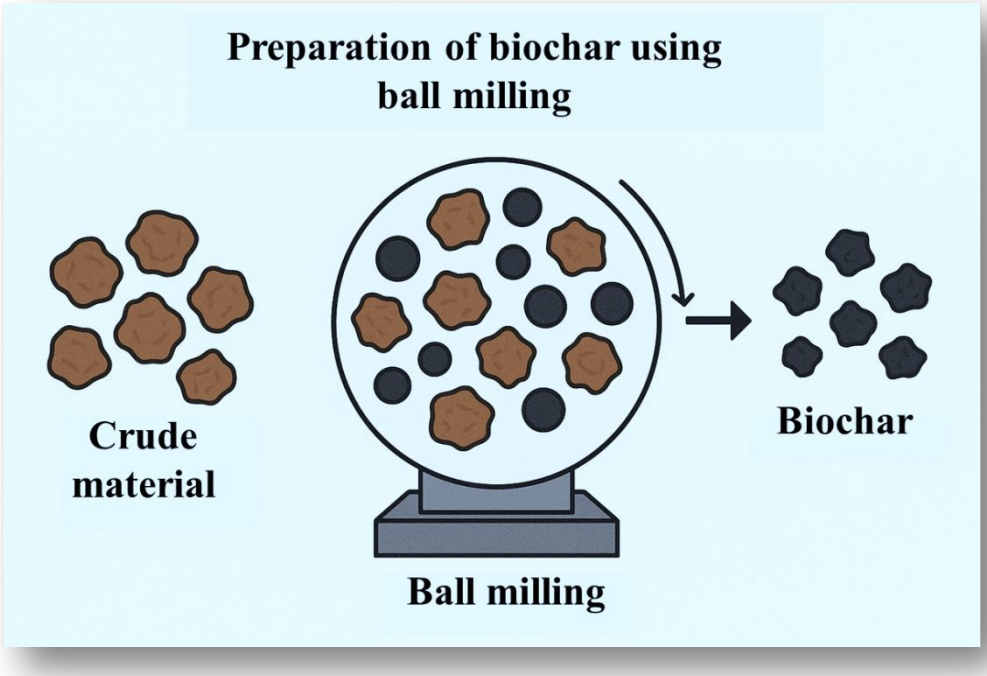

Figure 5. Ball milling synthesis of biochar

Another uncomplicated but productive physical approach involves the use of ball milling (**Figure 5**). The procedure harnesses the momentum of oscillating grinding elements to fracture chemical linkages, transform particle morphology, and synthesize nanomaterials [115]. As a result, biochar obtained after ball milling exhibits many superior properties, including increased pore volume, large specific surface area (SSA), low surface charge (negative), the presence of oxygen functional groups, and superior adsorption capacity [36]. Biochar from bagasse after ball milling has demonstrated superior removal of Ni^{2+} and methylene blue (MB) in water compared to conventional biochar [116]. The reason is that the ball milling technique increases the surface area (both internal and external) while exposing the graphitic structure and oxygen functional groups on the carbon's surface [117]. Additionally, Peterson and

View Article Online
DOI: 10.1039/D5MA00872G

colleagues demonstrated that optimizing the grinding conditions using a ball mill could increase the surface area of corn stover biochar up to 194 m^2/g, which is 60 times larger than that of the original material [118]. A notable drawback involves the high water dispersibility of ball-milled biochar, potentially causing environmental contamination.

2.3.2. Chemical activation

2.3.2.1. Utilizing of acids, bases, inorganic salts for activation

Chemical treatment techniques including acid treatment (HNO_3, H_2SO_4, HCl, etc.), alkali treatment (NaOH, KOH, etc.), oxidation ($KMnO_4$, H_2O_2), metal salts ($FeCl_3$, $MgCl_2$), inorganic-organic polymers (clay, chitosan), amines, cationic surfactants (e.g., cetyltrimethylammonium bromide), and ethylenediaminetetraacetic acid (EDTA) are utilized to modify the chemical properties and surface structure of biochar [119, 120]. Depending on their chemical nature, these agents impart distinct characteristics such as pore development, increased surface area, enhanced cation exchange capacity, and the introduction of functional groups. For example, oxidation with HNO_3 increases the mass of acidic functional groups and improves hydrophilicity but may also degrade the structure and reduce surface area [121].

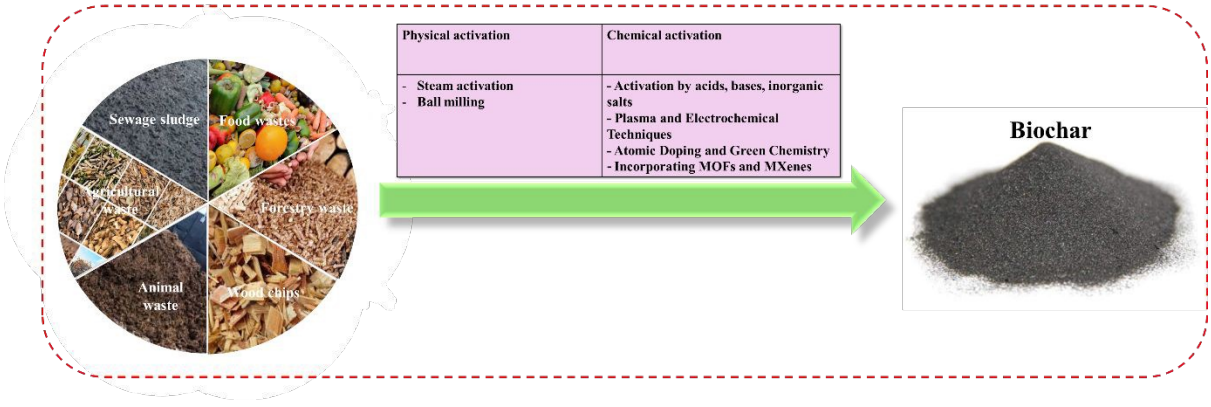

Figure 6. Strategy for converting biomass into biochar

In contrast, alkaline treatment typically yields a larger surface area than acid treatment [122]. KOH modifies the porous structure, as demonstrated in a work by Han et al. [123] on peanut shell-derived biochar, which achieved a BET surface area of 640.57 m^2/g. Similarly, NaOH enhances thermal stability and antibiotic adsorption capacity [124], while 30 % H_2SO_4 boosts sulfadiazine adsorption efficiency [125]. In oxidation treatments, $KMnO_4$ combined with KOH increases the specific surface area (SSA), improving tetracycline (TC) adsorption [126], whereas H_2O_2 introduces oxygen-containing functional groups, enhancing heavy metal removal [127]. Additionally, the choice of decontamination agents depends on factors

View Article Online
DOI: 10.1039/D5MA00872G

including low decomposition temperature, short carbonization time, or the ability to form a mesoporous structure [128]. Common techniques are illustrated in **Figure 6**.

2.3.2.2. Plasma and electrochemical techniques

In the current scientific climate, the issue of antibiotic contamination in aquatic environments has become a global concern. Traditional treatment methods often prove ineffective due to the complex nature of antibiotic molecules. In this context, advanced plasma and electrochemical biochar modification techniques have emerged as promising solutions, offering significant advantages over conventional chemical methods. Plasma treatment is considered a breakthrough technology in the surface modification of materials, particularly in the formation of specific functional groups. Cold plasma at atmospheric pressure can be applied within a short period (5–30 min), yet induces remarkable structural transformations. The main mechanisms include: (1) surface activation through collisions with high-energy particles, (2) oxidation to form functional groups including –COOH, –OH, and C=O, and (3) microstructural modification of the surface, increasing pore volume and surface area.

A work by Zhang et al. [129] employed a cold plasma system using NH_3 gas to treat corn straw biochar (CS-300), demonstrating that CIP removal efficiency increased from 31.8 to 85.7 %. This improvement was attributed to the dense formation of amine and amide groups on the biochar's interface. These nitrogen-containing functional groups not only enhanced the π electron density within the conjugated system of the biochar, thereby promoting π–π stacking interactions with the aromatic ring of CIP but also contributed to strong ionic and hydrogen bonding interactions at high-energy sites (above 10 kJ/mol). Similarly, Lou et al. (2021) combined seaweed-derived biochar (from Enteromorpha prolifera) with a dielectric barrier discharge (DBD) plasma system [130]. They discovered an enhance in biochar surface area from 415.84 to 486.32 m^2/g after treatment. The concentration of oxygen-based functional moieties such as hydroxyl (–OH) and carboxyl groups was significantly enhanced, which results in a tetracycline hydrochloride (TCH) removal efficiency of 89.36 % in just 5 min. This approach not only yielded high elimination efficiency but also improved energy efficiency, reaching 6.21 g/kWh, significantly higher than that of the plasma-only system.

Recent developments in electrochemical techniques have also advanced the modification of adsorbent materials, particularly biochar. A notable example is the work by Benis et al. [131], in which an electrochemical process involving an iron anode was used to modify biochar derived from rapeseed straw. This method produced goethite (α-FeOOH) coatings on the

material surface without the need for external chemical agents. The modified biochar achieved a nearly 37-fold increase in arsenic (As(V)) adsorption capacity (from 25 to 922 μg/g) under optimized conditions such as pH 3, drying temperature 60 °C, and 20 min of electric current application. The elimination mechanism involved multilayer heterogeneous adsorption and chemical bonding, with iron-containing functional groups playing a key role in creating selective active sites. A review by Tian et al. [132] further confirmed that electroactive functional groups including –C=O, –COOH, –OH, and persistent free radicals (PFRs) function as electron donors or acceptors in redox processes. Electrochemical modification of biochar can optimize the density of these groups, thereby enhancing its capacity to eliminate a wide range of organic and inorganic contaminants. In particular, activation with KOH, treatment with HNO_3, and heteroatom doping with elements like nitrogen and sulfur significantly improve electron transport capacity and create selective uptake sites on the biochar surface. A comparison of the two techniques reveals that each has distinct advantages. Plasma treatment is characterized by a short processing time (usually under one hour), the absence of toxic chemicals, and feasibility for pilot-scale application. Meanwhile, electrochemical techniques offer precise control over the degree of modification via adjustable electrochemical parameters and the simultaneous generation of diverse functional groups. However, both methods face challenges, including high initial investment costs, the need for specialized equipment, and the necessity for further research into material reusability.

2.3.2.3. Atomic Doping and Green Chemistry

A summary of the investigations is presented in **Table 1**. Biochar modified via atomic doping has proven to be an effective strategy for enhancing elimination performance by introducing additional active functional groups, modifying surface charge, and increasing surface area. A representative example is boron (B)-doped biochar synthesized through microwave pyrolysis using H_3BO_3 which achieved a surface area of 933.39 m^2/g and a TC uptake capacity of up to 413.22 mg/g [133]. This capacity surpasses that of many commercial and previously studied biochars such as straw-derived biochar modified with H_3PO_4 (267 mg/g) or peat-derived biochar (94 mg/g). Mechanistic investigations revealed that the $–BCO_2$ functional group, formed from B doping and served as the primary adsorption site through π–π electron interactions. Similarly, phosphorus (P)-doped biochar prepared by pyrolyzing H_3PO_4-impregnated straw at 600 °C, formed C_3–P–O functional groups, which exerted the greatest effect in the adsorption of SMX, achieving a capacity of 148.62 mg/g [134]. This

performance exceeds that of commercial materials such as activated carbon (27–94 mg/g) or sludge-derived carbon. Furthermore, P-doped biochar demonstrated operational stability in continuous flow columns and showed good agreement with practical models such as the Thomas and BDST models, indicating strong potential for industrial-scale applications [134]. In the case of nitrogen (N)-doped biochar, N species including pyridinic, pyrrolic, and graphitic nitrogen were found to increase local electron density, facilitating the generation of active functional groups and enhancing the adsorption of persistent pollutants including bisphenol A (BPA), norfloxacin (NOR), and CIP [135, 136]. Lian et al. [137] revealed that N-doped biochar derived from straw exhibited excellent adsorption capacity for phenolic pesticides. Particularly, Fe/N co-doped biochar revealed outstanding performance owing to the synergistic effect and resonance between the doped atoms. For example, Fe/N-doped biochar synthesized from sawdust achieved a NOR uptake capacity of 107.5 mg/g, significantly higher than that of the pristine biochar (35.3 mg/g) and Fe-doped biochar (58.2 mg/g) [137]. Ahmad et al. (2022) further confirmed that Fe/N biochar exhibited a faster adsorption rate and markedly enhanced efficiency compared to other carbon-based adsorbents in treating micropollutant-containing wastewater [138].

Table 1. Atomic doping strategies at the biochar interface

Feedstock	Dopant(s)	Synthesis Conditions	Contaminant (Efficiency)	Adsorption mechanism	Ref.
Coconut husk	B (H_3BO_3)	Microwave-assisted pyrolysis, 600–1000 °C, 1h, N_2 atmosphere	TC (413.22 mg/g)	π–π EDA interaction, H-bonding, –BCO_2 active sites	[133]
Rice straw	P (H_3PO_4)	Pyrolysis at 600 °C, 2 h, solid–liquid ratio 1:2, N_2 atmosphere	SMX (148.62 mg/g)	H-bonding (C_3–P–O), electrostatic, π–π EDA	[134]
Maize straw	Fe/N ($FeCl_3$ + urea)	Pyrolysis at 700 °C, 2 h, 1-step mixing process	MOR (107.5 mg/g), CIP (85.1 mg/g)	π–π interaction, electrostatic, surface complexation	[137]

Coconut shell	Fe/B ($FeSO_4$ + $NaBH_4$)	Microwave pre-treatment 5 min + pyrolysis at 1000 °C, 1 h, N_2 atmosphere	TC (107.32 mg/g)	π–π interaction, electrostatic, H-bonding	[139]
Wood chips	Fe/Ti	Co-pyrolysis at 600 °C, 2 h, N_2 atmosphere	CIP (88.4 %), NOR (88.0 %)	π–π interactions, polar interactions	[140]
Rice husk	Cu	Hydrothermal carbonization at 180 °C, 8 h	Congo red dye (437.40 mg/g)	π–π interaction, electrostatic attraction, hydrogen bonding	[141]
Rape straw	Fe/N	Pyrolysis at 600 °C, 2 h, N_2 atmosphere	CIP (46.45 mg/g), Cu^{2+} (30.77 mg/g)	Electrostatic interaction, π–π interaction, H-bonding	[142]
Loofah waste	Mn/N	One-step pyrolysis with $NaHCO_3$ activation	BPA (351 mg/g)	Pore filling, hydrophobicity, π–π EDA interaction	[143]
Maize straw	$FeCl_3$	Pyrolysis at 500-900 °C, 2 h, N_2 atmosphere	Extended-chain PFAS (per- and polyfluoroalkyl substances) (>95 %)	Complexation, Electrostatic interactions	[144]
Corn stalk	N	Pyrolysis at 600 °C, 1 h, N_2 atmosphere, 5 °/min	NOR (46.27 mg/g)	Pore-filling, H-bond, π-π electron donor-acceptor	[145]
Tea residue biochar	S/N	Carbonization at 220 °C, 6h	TC (140.76 mg/g)	Electrostatic interactions	[146]

Additionally, Fe/B co-doped biochar synthesized using $NaBH_4$ as the B source, which exhibited uniform distribution of B and Fe atoms within the carbon matrix. This configuration enhanced TC adsorption via π–π interactions and hydrogen bonding [139]. Literature also highlights that atomically doped biochars outperform conventional materials like carbon nanotubes or activated carbon. For instance, in the work by Ma et al. [147], a sludge biochar–

View Article Online
DOI: 10.1039/D5MA00872G

carbon nanotube composite achieved only ~70 mg/g for SMX whereas P-doped biochar reached over 140 mg/g. In summary, whether doped with single elements such as B, P, N, or with combinations such as Fe/N and Fe/B, biochar has demonstrated substantial improvements in adsorption efficiency, stability, and practical applicability, surpassing both unmodified biochar and many commercial adsorbents reported in the literature.

A sustainable approach that continues to draw interest from researchers in wastewater treatment is the application of green chemistry techniques in both the fabrication and activation of biochar. In particular, the use of plant extracts to reduce metal precursors has proven to be an effective method for generating metal nanoparticles (NPs). These nanoparticles can be dispersed and immobilized within plant-derived biochar (BC) matrices, resulting in environmentally friendly, low-cost, and chemically non-toxic BC–NP composites [148]. Numerous studies have demonstrated the synthesis and characterization of NPs through biological methods involving either microorganisms or plant-based extracts. These include a range of metal nanoparticles (Al, Ag, Au, Pd, Fe, Cu) [149], metal oxides (ZnO, CeO_2, CuO, TiO_2, Fe_3O_4) [150], and metal sulfides (PbS, CdS) [151]. Inorganic salts such as $AgNO_3$ and $FeSO_4$ are commonly reduced using plant extracts to synthesize isolated nanoparticles [152] or to co-synthesize NPs in situ within biochar frameworks, forming composite materials [153]. For example, silver nanoparticles have been generated via the decrease of $AgNO_3$ using plant extracts derived from pine, rose, ginkgo, magnolia, and platanus, with applications in biomedicine and antimicrobial treatments [152].

Additionally, the incorporation of physical attributes such as magnetism into biosorbents has been reported [153]. A representative case is the preparation of magnetic bioadsorbents through the use of rosemary leaf extract to generate Fe_3O_4 nanoparticles. In this method, rosemary leaves were initially activated with phosphoric acid (H_3PO_4) and subjected to thermal treatment at 220 °C to yield acid-modified biochar. This modified biochar was then mixed with rosemary extract, followed by the dropwise addition of $FeSO_4$ solution, facilitating the in situ formation of Fe_3O_4 nanoparticles within the biochar matrix. The integration of magnetic properties into such bioadsorbents enhances pollutant separation from aqueous media and promotes their reusability and practical waste management at scale.

The use of plant-derived reducing agents in nanoparticle synthesis further contributes to lowering the toxicity of the final materials, enhancing their safety and environmental compatibility. Kumar et al. represented a green synthesis route for biochar using seeds of

View Article Online
DOI: 10.1039/D5MA00872G

Abelmoschus esculentus (AESB) to eliminate Direct Blue 86 dye [154]. The dried seeds were chemically activated with 88 % H_3PO_4 at 100 °C for 90 min, leading to the development of mesoporous and microporous structures on the surface via pyrolytic degradation mechanisms [155]. Subsequent pyrolysis at 600 °C in a nitrogen environment facilitated the formation of additional functional pores, significantly increasing the material's active surface area [156]. The high-temperature thermal decomposition of lignin, cellulose, and hemicellulose is considered pivotal in generating a porous structure with enhanced adsorption efficiency [157].

More recently, the focus of biochar research has shifted from terrestrial biomass to marine algal biomass, which offers advantages such as rapid growth and ease of harvesting. Algal species including U. ohnoi (Chlorophyta), S. hemiphyllum (Phaeophyceae), and A. subulata (Rhodophyta) have been explored as promising precursors for green biochar synthesis aimed at wastewater decontamination [158-161]. In U. ohnoi, functional groups like carboxyl and sulfate present in cell wall polysaccharides are known to assist in alkali-mediated modification of BC using agents like NaOH or KOH [162]. The biomass of A. subulata contains a variety of bioactive compounds including fibers, carotenoids, lipids, and proteins [163] whereas S. hemiphyllum possesses functional constituents including fucoxanthin, phlorotannins, polyphenols, and sulfoglycolipids, which provide chemically active sites for further modification [161]. An additional example is the study by Mosaffa et al., who developed a highly porous green sorbent by integrating hydrogel and biochar derived from Borassus flabellifer. Using a carbonization temperature control approach (350–700 °C), they achieved a BET of 80.34 m^2/g [164]. The resulting material demonstrated remarkable adsorption capacities for both cationic (malachite green –10,596 mg/g at pH ~10) and anionic (Congo red – 7,095.43 mg/g at pH ~6) dyes. Beyond water treatment, green-synthesized nanoparticles have been further investigated for biomedical applications including contrast imaging, magnetic hyperthermia therapy, and targeted drug delivery [165]. In summary, adopting green synthesis strategies for the development of bioadsorbent materials not only enhances water purification performance but also supports the overarching goal of global environmental sustainability.

2.4. Hybrid biochar architectures incorporating MOFs and MXenes

In recent years, hybrid biochar architectures combined with metal-organic frameworks (MOFs) and MXenes have attracted great attention in the materials science community due to their ability to significantly improve the adsorption performance of organic pollutants,

View Article Online
DOI: 10.1039/D5MA00872G

especially antibiotics in wastewater. These composite structures take advantage of the unique properties of each component, in which biochar has high adsorption capacity and low cost, MOFs stand out with super large surface area, tunable porosity and high selectivity, and MXenes possess superior conductivity along with strong surface interaction and many active functional groups. MOFs are a diverse group of metal–organic frameworks comprising various substructures such as MILs, ZIFs, and other hybrid systems, which are designed with the outstanding characteristics of large surface areas, tunable porosity, and highly selective interactions with target molecules. Therefore, the integration of MOFs into biochar has opened up a promising approach for wastewater treatment, especially for organic pollutants.

One of the prominent trends is to integrate MOFs onto the biochar surface to effectively utilize both material phases. For example, Hanane Chakhtouna and co-workers successfully synthesized MIL–53(Fe)/biochar adsorbent from date palm rachis and achieved simultaneous elimination of CIP and ofloxacin (OFL) up to 218.29 and 223.89 mg/g [166]. The primary mechanisms were identified as π–π resonance, electrostatic interactions, and hydrogen bond formation, while MIL-53(Fe) increased the density of mesopores for faster molecular diffusion. Similarly, Samar M. Mahgoub and co-workers developed Zn-MOF/biochar composite derived from date palm seeds for the treatment of CIP in polluted water [167]. The data discovered that this material achieved a highest adsorption amount of 194.3 mg/g. A notable breakthrough came in 2020, when Chanaka M. Navarathna's group synthesized a magnetic MIL-53-Fe MOF/biochar composite incorporating magnetite. This innovative material boasted an extensive surface area (~350 m^2/g) and demonstrated exceptional Rhodamine B (RhB) adsorption (55 mg/g at pH 6 and room temperature) [168]. Beyond its high efficiency, the composite exhibited outstanding reusability, retaining over 80 % adsorption capacity after multiple cycles, highlighting its stability and promise for treating dye-laden wastewater. In contrast, Liu et al. developed an innovative lignin-gratfed MIL-101-NH_2(Fe)/Biochar composite for TC adsorption [169]. Remarkably, this material exhibited outstanding adsorption performance across a broad pH range, achieving a maximum amount of 760.36 mg/g at pH 4.19, doubling the adsorption efficiency of Carbon-MIL-101-NH_2. A summary of typical studies on ZIF/biochar and MOF/biochar composite materials for antibiotic adsorption has been presented in detail in **Table 2** to provide a comprehensive view of the potential and development trends of this advanced material line. **Figure 7** illustrates the typical antibiotic adsorption mechanism of MOF/biochar composite materials through the interactions: (1)

hydrogen bond formation between functional groups on the biochar surface and antibiotic molecules, (2) pore adsorption from the MOF structure, (3) ion exchange,... in biochar/MOF.

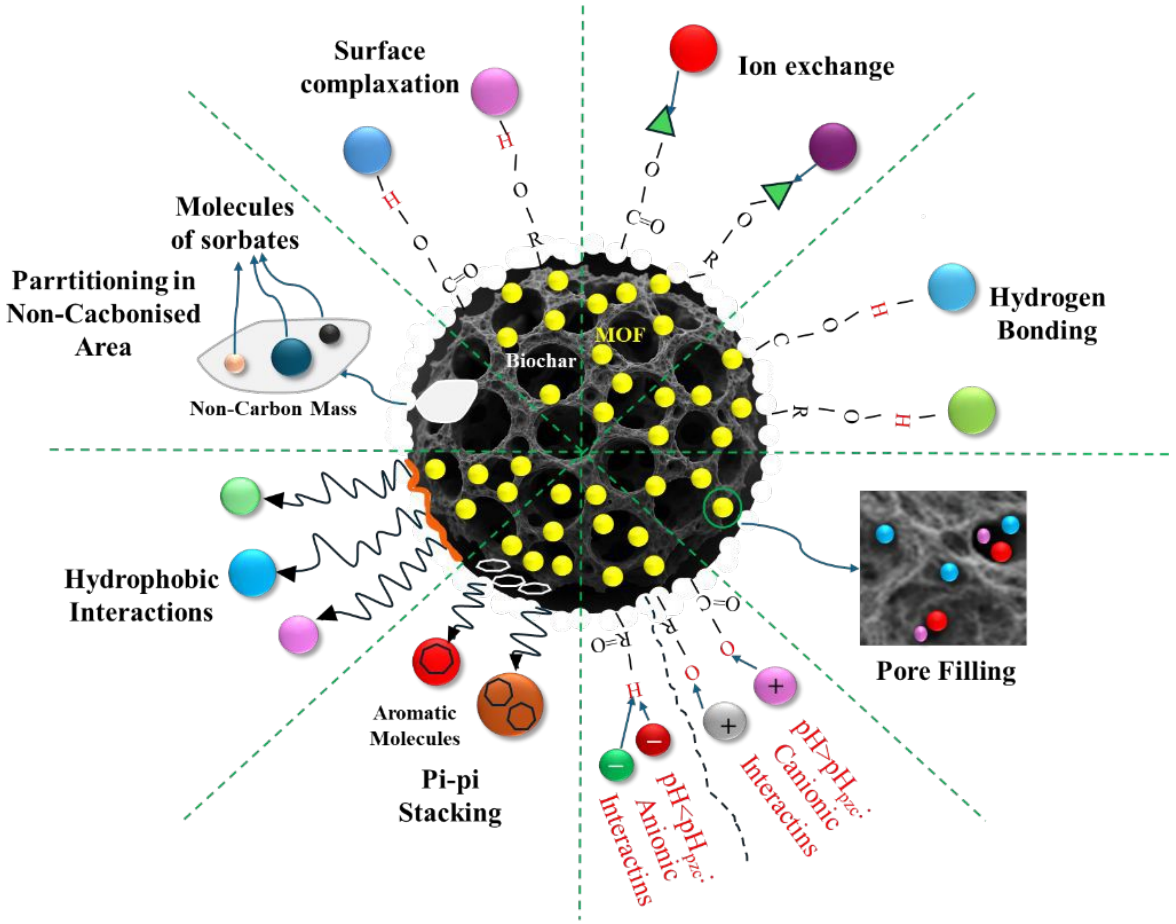

Figure 7. Mechanism of pollutant capture by Biochar/MOF (Reproduced from reference [170] – open access article under CC-BY license).

Table 2. Adsorption of multiple antibiotics using biochar/MOF-based adsorbent

Adsorbent	Antibiotics	Efficiency	Mechanism	Ref.
MIL–53(Fe)/biochar	- CIP - Ofloxacin	-OFL 223.89 mg/g -CIP 218.29 mg/g	π–π resonance, electrostatic interactions, and hydrogen bonding	[151]
Zn-MOF/biochar	- CIP	194.3 mg/g		[152]
Magnetic MIL-53-Fe MOF/biochar	- RhB	55 mg/g		[153]

Lignin-doped Biochar/MIL-101-NH_2(Fe)	- TC	760.36 mg/g		[154]
Fe-Co MOF/$CoFe_2O_4$ modified biochar	- TC	909 mg/g	Chemisorption (non-electrostatic interactions including hydrophobic interactions, hydrogen bond formation, surface coordination mechanisms, and π-π stacking)	[171]
Hybrid (MIL-53(Al)@RH)	- Glyphosate (GLY) - Diclofenac (DCL) - OTC	GLY: 162 mg/g OTC: 139 mg/g DCL: 93 mg/g	Chemical bonding Electrostatic interactions	[172]
HKUST/biochar based adsorbent	- TC	396 mg/g	- Metal-organic complexation - Hydrogen bond formation -Electrostatic force - π-π interaction	[173]
MIL-101(Fe)-PMA-Biochar	- RhB - Methyl Orange (MO)	RhB: 96 % MO: 93 %	- Electrostatic interactions - Hydrogen bonding	[174]
MIL-53(Al)@RH biochar	- GLY	297 mg/g	-π–π stacking interactions - Hydrogen bonding -Complexation	[175]
MPN/NH_2-MIL-101 (Fe)	- TC - 2,4-dichlorophenoxyacetic	- TC: 109 mg/g - 2,4-D: 79 mg/g	- Hydrogen bonding - Electrostatic complexation - π-π mechanisms	[176]

View Article Online
DOI: 10.1039/D5MA00872G

	acid (2,4-D)			
Ti-MOF/TiO_2@WMPB/CTH	DOX	DOX: 95 %	Pseudo-second Order Langmuir isotherm (monolayer adsorption)	[177]
Biochar/ZIF-8	TC	288.85 mg/g	Hydrogen bonding, - π-π interaction	[178]

MXenes constitute an innovative class within the broader field of two-dimensional materials with the general formula $M_{n+1}X_nT_x$, in which M refers to a transition metal (e.g., Ti, V, Nb), X represent nitrogen or carbon, and T_x refers to surface functional groups such as -O, -F, -OH [179]. These substances are generated via the etching of A-layers from the MAX structure (e.g., Ti_3AlC_2), resulting in thin sheets of material with large surface areas, high electrical conductivity, and flexible functionalization [180]. Thanks to these properties, MXenes have been widely explored in fields including sensors, energy storage, and especially water remediation as potential adsorbent materials. The combination of MXene with biochar, a porous carbon material obtained from biomass pyrolysis, has produced composites with superior adsorption capacity due to the synergy between the electrical conductivity and ion exchange capacity of MXene and the functional group-rich active surface of biochar. **Figure 8** shows the fabrication process of Biochar/MXene based adsorbent. A typical envidence is the investigation by Xu et al. (2024), in which the Fe_2O_3/biochar/MXene composite showed high adsorption efficiency for lead ions (Pb^{2+}) and MB dye, reaching more than 99 % removal of Pb^{2+} and MB [181]. The adsorption mechanism is believed to be owing to the combination of functional groups including O^-, OH^-, and F^- from MXene and CO, CN, and OH groups from biochar, creating many adsorption sites for metal ions and dye molecules [181].

Another work discovered by Liu et al. (2023) successfully developed a biochar/MXene composite material using coconut shell as a raw material, which combined with polydopamine (PDA) and polyethyleneimine (PEI) coating that forms $Ti_3C_2T_x$@biochar-PDA/PEI material through the charge self-assembly method [182]. The results showed that this material possesses a porous structure with many active functional groups including –OH, $–NH_2$, and Ti–OH, which enhances the adsorption capacity of radioactive ions U(VI) and Cs(I). Batch sorption

View Article Online
DOI: 10.1039/D5MA00872G

experiments showed that the elimination performance of U(VI)/Cs(I) followed second-order kinetics and Langmuir isothermal, discovering a monolayer sorption mechanism controlled by chemisorption. In particular, this material achieved extremely high adsorption efficiency, with a maximum removal capacity of up to 239.7 mg/g for U(VI) and 40.3 mg/g for Cs(I) [182]. Even in an environment containing many competing ions, the material still maintained its superior adsorption efficiency, demonstrating the good selectivity of this composite. In addition, the reusability of the adsorbent was also examined and after three adsorption-desorption cycles, the material still maintained more than 80 % of its initial efficiency. Mechanism analysis through FTIR spectroscopy, XPS, and DFT simulations discovered that the main mechanisms include ion exchange, electrostatic forces, and chelate complexation between functional groups on the material surface and the target metal ion.

Complementing the above results, the study by Kumar et al. (2025) successfully synthesized $Ti_3C_2T_x$ MXene@biochar (MB) composite materials via an ultrasonic self-assembly method with different ratios between MXene and biochar (1:9, 3:7, and 5:5), aiming to simultaneously treat inorganic pollutants coexisting in wastewater including metal species (Cd, Cu, Cr, Fb), ammonium (NH_4^+), and phosphate (PO_4^{3-}) [183]. The results showed high adsorption efficiencies for Cu, Pb, and Fe when all reached >98 % under optimal conditions. Notably, the MB-1:9 material (high biochar ratio) exhibited Cu removal efficiency of up to 99.89 % at a dose of 12 mg while MB-3:7 was more suitable for NH_4^+ adsorption, achieving an efficiency of 97.83 %. The biosorption models were accurately depicted by the Freundlich model, revealing the possibility of multilayer uptake on the heterogeneous interface. Meanwhile, the kinetics followed a second-order kinetic, indicating the crucial role of the chemical sorption mechanism. The adsorption mechanism was determined to be a combination of several interactions such as electrostatic forces that occurrs between metal species and MXene surface's functional groups (–OH, –O, –F), ion exchange via Ti–OH groups, chelation complexation via –COOH groups as well as physical adsorption in the porous structure of biochar. Furthermore, thermodynamic studies confirmed that the uptake process was endothermic ($\Delta H > 0$) and spontaneous ($\Delta G < 0$) with Zn adsorption exhibiting a strong temperature dependence (ΔH up to 61.7 kJ/mol for MB-5:5) [183]. The MB material also demonstrated good reusability after multiple adsorption-desorption cycles, especially for heavy metals and PO_4^{3-}, showing great potential in practical applications. In addition, MXene/biochar composites have also been tested in the field of wastewater decontamination and energy recovery [184]. A recent work by Liao et al. (2024) discovered that this material has the ability

to effectively eliminate organic pollutants in food wastewater while improving the efficiency of hydrogen recovery from wastewater thanks to the good catalytic and electron transfer properties of MXene.

However, it is worthnoting that up to now, there has been no published study on the direct application of biochar/MXene composite materials in the adsorption of antibiotics, an emerging group of pollutants that are causing concern in the aquatic environment. This creates an important research gap as the ideal properties of MXene (electrostatic interactions, flexible functional groups) and biochar (diversified adsorption capacity, stability) can be combined to effectively treat antibiotic molecules such as CIP, TC, or SMX, which have been successfully treated by individual biochar or MXene forms. Therefore, future research can be directed toward the synthesis and optimization of biochar/MXene composite materials specifically for antibiotic adsorption, while studying the molecular interaction mechanism between the materials and specific antibiotic groups. The development of this new material line not only fills the current gap but also promises to bring sustainable solutions for the treatment of medical and agricultural wastewater, where antibiotic residues are an urgent problem.

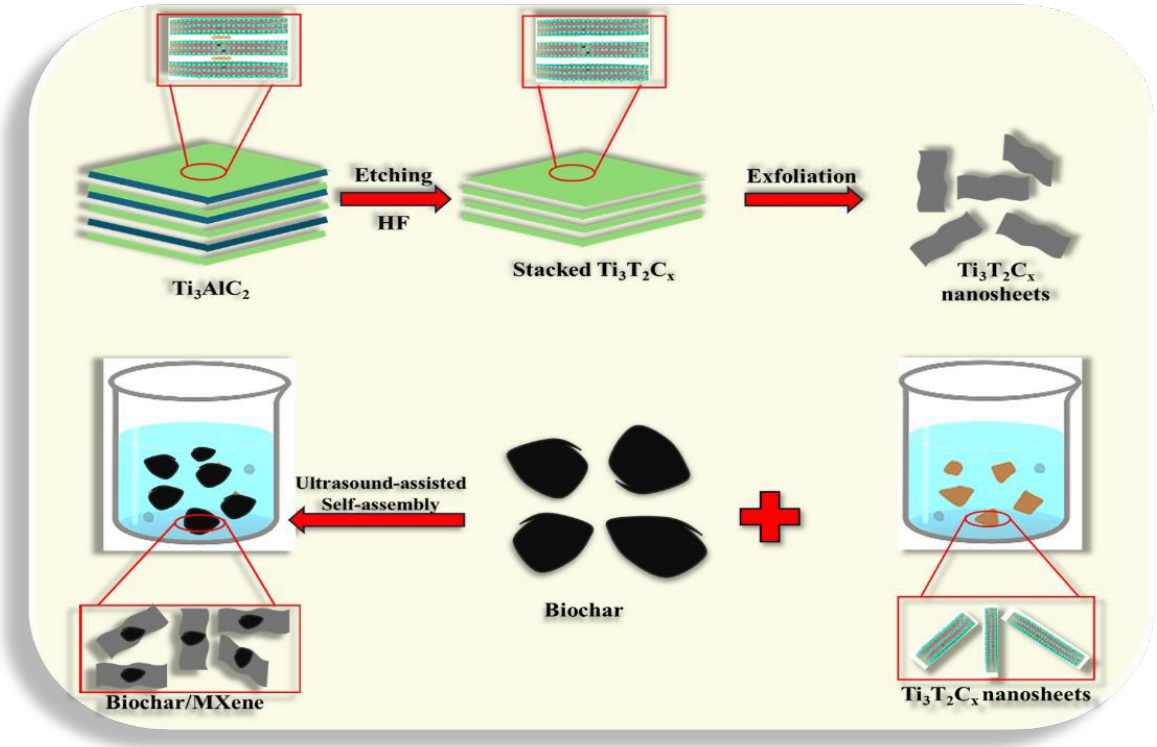

Figure 8. Biochar/MXenes fabrication strategy.

View Article Online
DOI: 10.1039/D5MA00872G

2.6. Techniques for characterizing biochar

The ability of biochar to eliminate substances is improved by chemical, thermal, and mechanical modifications which provide significant benefits to this material. The changes in the structure and biochar's properties depend on various factors including pyrolysis temperature, precursor type, particle size, and modification agent. These changes can be evaluated by various characterization techniques. In many experimental studies, the adsorption properties and efficiencies of modified biochar are further characterized through qualitative methods. Further modified forms of biochar including nano-sized adsorbents, magnetic materials, and other complex derivatives are often characterized by a variety of modern instruments such as TEM, SEM, XPS, EDS, VSM, ICP, FT-IR, and particle size analyzers [152]. Specifically, TEM and SEM are commonly employed to analysis the structure of nano-materials while EDS supports the confirmation of atomic composition. The magnetic characteristics of the biochar are evaluated by measuring the vibrational magnetic moment using a VSM. In addition, particle size analysis allows determining the influence of mechanical modification. SEM and TEM demonstrate the effect of thermal modification while EDX and FTIR techniques mainly serve to evaluate the effectiveness of chemical modification. Compared to raw biochar, the efficiency of modification or activation is better demonstrated through additional analytical methods. These methods are specifically illustrated in the following sections.

3. Biochar for adsorption of antibiotics

3.1. Key variables impacting biochar adsorption performance

In heterogeneous adsorption systems, pollutant removal efficiency depends not only on the properties of the material but also on environmental conditions and operating parameters. Factors such as solution pH, initial contaminant amount, temperature, duration time and material content influence more than just the adsorption kinetics or equilibrium; they also play a crucial role in governing interaction mechanisms at the molecular level. For instance, pH exerts a dual effect: it controls the ionization state and charge distribution of functional groups on the biochar interface while simultaneously influencing the chemical form and electronic activity of the pollutant in solution. These changes directly impact the generation of electrostatic attractions, hydrogen bonding and EDA complexes. Meanwhile, the initial concentration and temperature relate to the thermodynamic driving force, the ability to overcome energy barriers and the surface selectivity of the composite. Thus, understanding the role of each variable provides not only deeper insight into the adsorption process but also a

View Article Online
DOI: 10.1039/D5MA00872G

rational basis for optimizing performance and designing biochar materials in a mechanism-driven framework.

3.1.1. pH

During the biochar treatment of antibiotics, the pH of the reaction working plays an important role because it influences both the surface charge of the adsorbent and the electrochemical structure of the antibiotic molecule [56, 185-187]. This is particularly important for acid-base dissociating molecules such as TC, where pH changes lead to different ionization states that determine both the molecular form and its ability to interact with the adsorbent. A typical example is TC, an antibiotic with three acid dissociation constants, recorded with logKa values of approximately –9.7, –7.7, and –3.3 [188]. These values divide the pH range into four distinct regions, each dominated by a specific ionic form. At high pH levels, well above the first dissociation constant, the HTC_2^- form becomes dominant with a strong negative charge. At low pH and below the third dissociation constant, the molecule exists mainly as the positively charged H_4TC^+ form. Between these extremes, the molecule gradually transitions from H_2TC^- to neutral H_3TC depending on the acidity or alkalinity of the medium. Each ionic form has unique electrochemical characteristics, leading to significant differences in its interaction with the adsorbent surface, especially when that surface contains polarized groups or regions with delocalized electrons [189]. In addition to altering the structure of the antibiotic molecule, pH directly affects the biochar's surface charge through protonation and deprotonation. Once the environmental pH is lower compared to the material's pH_{pzc}, the carbon surface tends to carry a positive charge, promoting attraction with negatively charged ions. In contrast, as the pH exceeds pH_{pzc}, the surface becomes negatively charged, which can lead to electrostatic repulsion with antibiotic anions [190]. Experimental results show that under neutral to slightly acidic conditions and typically between pH 2 and 7, the removal efficiency of antibiotics is significantly higher compared to alkaline conditions [191, 192]. In basic environments, strong deprotonation reduces adsorption due to increased repulsion and weaker hydrogen bonding. Furthermore, pH regulates the charge density and polarity of surface functional groups such as OH, COOH, and NH_2 [193]. These factors influence the formation of hydrogen bonds, electron donor–acceptor complexes, and π–π interactions. However, such interactions tend to weaken when the pH becomes too alkaline, as protonation decreases and changes occur in the energy levels of the involved molecular orbitals. From the above discussion, it is clear that maintaining pH within an optimal range not

View Article Online
DOI: 10.1039/D5MA00872G

only preserves effective adsorption but also improves selectivity for different antibiotics, thereby enhancing both the accuracy and overall efficiency of water treatment using biochar.

In addition to the aforementioned factors, pH is also influenced by the intrinsic characteristics of the biochar, which are ascertained by the input materials and the pyrolysis conditions used during its production. Higher pyrolysis temperatures tend to rise the ash amount, thereby enhancing the alkalinity and elevating the surface pH of the biochar, which directly impacts its interaction with various charge carriers [194]. Variations in pH also influence the suspension properties of the system, including colloidal stability and dispersion, thus regulating adsorption efficiency under real environmental conditions [195]. Moreover, several studies have discovered that the antibiotic removal efficiency of biochar typically fluctuates with the pH of the solution often increasing from acidic to neutral conditions and then declining as the pH becomes more alkaline [196]. This trend is attributed to shifts in the relative charges between the biochar surface and the antibiotic molecules, leading to changes in electrostatic interactions as well as the potential for hydrogen bonding or ion exchange mechanisms.

3.1.2. Duration time

In wastewater treatment using adsorption, the duration time between the material and the contaminant such as biochar, plays a crucial role in determining removal efficiency [197]. Unlike instantaneous reactions, adsorption follows a complex kinetic pathway where antibiotic molecules require sufficient time to migrate and bind to the vacant sites on the material's interface. As this interaction progresses, it gradually leads to a phase of equilibrium when the rate of uptake equals the rate of desorption. In wastewater environments with high levels of organic matter, pollutant concentrations typically decrease over time until this steady state, known as adsorption equilibrium is reached [198]. Accurately determining the time required to reach equilibrium is essential for effective system design and operation. If the contact time is too short, the adsorption process remains incomplete but too long can lead to unnecessary energy and resource consumption. This parameter is strongly effected by the microstructural and chemical characteristics of the biochar, which include porosity, pore size, specific surface area, and surface functional groups. It is also influenced by operating levels including pH, the initial concentration of pollutants, and temperature [199]. An illustrative example of the importance of contact time can be found in a study by Fan and colleagues, who investigated MB adsorption using two types of biochar. One was derived from municipal sewage sludge, while the other was produced from a combination of sewage sludge and tea waste. Their results

View Article Online
DOI: 10.1039/D5MA00872G

revealed a substantial difference in the time needed to reach equilibrium when the first biochar required 24 h [200], whereas the second attained equilibrium in as little as 8 h [201]. This outcome indicates that the origin and structural properties of the biochar have a direct impact on the adsorption kinetics. To gain deeper insight into the influence of duration time and other influencing factors, the researchers employed Design Expert software along with the Box-Behnken response surface methodology to optimize the process. Simulation results demonstrated that, under optimal conditions, the pollutant removal efficiency could reach 99.9 %, underscoring the critical role of operational parameters, including contact time, in overall treatment performance [202]. Additionally, physical characteristics such as material permeability and electrostatic interactions that occurrs between the material and pollutant molecules are acknowledged as major contributors to the uptake rate and the underlying mechanism throughout the process [198]. Therefore, precise control of the contact time is not only vital for maximizing treatment efficiency but also serves as an important indicator for evaluating the practical feasibility of biochar-based systems in the removal of antibiotics from wastewater.

3.1.3. Biochar dosage

Biochar dosage is an important factor that directly effects the adsorption efficiency of pollutants, particularly antibiotics. Once the amount of biochar in the medium increases, the number of available vacant sites on the sorbent's surface also increases, improving the sorbent's capacity to isolate and remove pollutant molecules [203, 204]. For instance, David Adu-Poku et al. (2024) observed that TC removal efficiency improved from 90 to 98.9 % as the mass of biochar rised from 0.05 to 0.1 g [205]. However, this efficiency does not rise indefinitely but instead reaches an optimal threshold. Beyond this point, biochar particles may begin to overlap, causing adsorption layers to merge and obscuring active sites, which reduces overall treatment efficiency [196]. Similarly, one study demonstrated that a biochar dosage of 1 g/L could remove over 70 % and even achieve 100 % removal for TC, erythromycin, and clarithromycin [206]. Yet excessive dosage can diminish adsorption efficiency due to overlapping adsorption layers and active site saturation. Duc Thang Nguyen et al. (2025) found that improving amount of biochar from 0.1 to 0.25 g raised CIP elimination efficiency from 40 to ~ 95 % before reaching saturation [207]. Additionally, if the adsorbent quantity is too high relative to the initial pollutant concentration, insufficient antibiotic molecules remain to occupy all empty sites, which leads to a relative decline in adsorption efficiency [195]. Conversely, well-controlled dosage conditions can significantly accelerate the initial adsorption rate by

View Article Online
DOI: 10.1039/D5MA00872G

enhancing the number of empty sites on the material surface [208]. This also shortens the time required to achieve equilibrium in the treatment system [209]. Thus, determining the optimal biochar dosage is vital to ensure both high removal efficiency and cost-effectiveness for large-scale wastewater treatment. An appropriate dosage maximizes resource utilization, prevents material waste, and reduces production costs in potential industrial biochar applications.

3.1.4. Contaminant concentrations

Initial levels of antibiotics are recognized as a critical factor influencing the adsorption efficiency in treatment systems that use biochar or composite materials. At the beginning, the concentration difference between the solution and the adsorption interface promotes rapid diffusion and strong interactions between antibiotic molecules and the active sites on the material. However, as the concentration continues to rise, the adsorption sites become progressively occupied, resulting in a decline in elimination performance owing to surface saturation. Experimental evidence from various studies supports this pattern. Yan et al. (2020) [210] reported that TC molecules quickly bonded to Zn-modified biochar (ZnBC) at the early stage. Yet, when the TC concentration exceeded 80 mg/L, the adsorption efficiency showed no further significant increase, suggesting the material had reached saturation. Sayin et al. [211] also observed that CIP removal efficiency dropped from 99.9 to 97.3 % as the amount of sorbate increased from 50 to 150 mg/L and fell sharply to 48.2 % at 500 mg/L. This indicates that when the antibiotic concentration surpasses the capacity of the adsorption sites, treatment performance is substantially reduced. Fu et al. [212] further found a rising trend in DNA adsorption with increasing initial concentration when using biochar modified with quaternary phosphonium salts, but the trend plateaued beyond a certain point. Simultaneously, Wu et al. [213] observed that the uptake rate declined as the amount of initial antibiotic rose, which reflected competition among target molecules for the remaining active sites. Recent studies have reported similar findings. Zheng et al. (2021) [214] demonstrated that iron-doped biochar made from agricultural waste increased sulfamethylimidine adsorption capacity from 0.3 to over 4.0 mg/g as the concentration grew from 2 to 35 mg/L, though the efficiency eventually stabilized and no longer increased proportionally. Likewise, a study by Ouyang et al. (2024) [215] using bamboo biochar showed that elimination capacities for MFX, CIP, and OFLX enhanced notably from 30.71, 35.20, and 36.80 mg/g at 10 mg/L to 83.58, 102.91, and 102.77 mg/g at 50 mg/L but the efficiency declined once the concentration surpassed the optimal level. These findings suggest that although raising the initial antibiotic concentration can enhance the uptake amount of biochar up to a point, exceeding that threshold may reduce efficiency due to

View Article Online
DOI: 10.1039/D5MA00872G

active site saturation. Therefore, identifying an appropriate initial antibiotic concentration is essential to optimize the wastewater treatment process using biochar.

3.1.5. Temperature

Temperature variation during adsorption can significantly affect the removal efficiency of pollutants, especially antibiotics. This is because temperature influences both the reaction rate and the interactions that occurrs between the interface of material and pollutant molecules. Most water treatment studies conduct experiments at around 25 °C to simulate typical environmental conditions [216]. However, many results show that temperature changes can cause significant differences in antibiotic removal efficiency, depending on the adsorbent characteristics and pollutant type. For example, when removing TC using biochar from grapefruit peel, rising the temperature from 25 to 40 °C raised the isolation efficiency from 9.89 to 26.27 %. This increase occurred because higher molecular kinetic energy improved the diffusion of TC to adsorption sites [217]. The same tendency was discovered by Cheng et al. [218], in which isolation performance enhanced with a temperature rise from 15 to 35 °C. The above effect is explained by the endothermic nature of the adsorption [219]. In addition, higher temperatures can raise the collision frequency between reactive molecules and SMX, promoting more efficient adsorption [220]. Liu et al. [221] reported a similar trend for p-nitrophenol removal utilizing pine sawdust biochar, as did Lonappan et al. [222] with diclofenac on pine wood biochar. In both cases, adsorption increased with temperature. The observed phenomenon may relate to increased molecular motion, which raises the chance of contact between antibiotics and active sites. It may also result from improvements in the biochar surface structure, owing to the development of aromatic carbon phases that enhance adsorption interactions [223]. However, it should be noted that not all adsorption processes are endothermic. In exothermic systems, higher temperature may reduce efficiency because it reduces the interaction strength between the pollutant and the sorbent.

3.1.6. Effect of other pollutants

In natural water and wastewater environments, the presence of inorganic salts is unavoidable, and they can influence the antibiotic adsorption efficiency of biochar. Liang et al. [224] reported that a certain concentration of sodium can enhance antibiotic adsorption on the surface of treated biochar. However, other studies have presented contrasting findings. Tang et al. [225] and Nguyen et al. [226] observed that the presence of cations in solution reduces adsorption efficiency because of their competition with antibiotic molecules for active sites.

View Article Online
DOI: 10.1039/D5MA00872G

Nguyen et al. [226] further emphasized that both cations and anions contribute to the inhibition of the adsorption process. Apart from monovalent ions, the impact of divalent ions on the antibiotic removal capacity of biochar has also attracted attention and remains a subject of debate. Tan et al. [227] found that Mg^{2+} ions exert a stronger inhibitory effect than Na^{+} ions. Nevertheless, some studies have highlighted potential benefits associated with divalent ions. Nguyen et al. [226], for instance, found that Ca^{2+} can form complexes with antibiotic molecules such as TC, thereby improving the removal efficiency of TC from solution. As a Lewis base, TC can bond with cations like Ca^{2+} and Mg^{2+}, which act as Lewis acids, forming stable complexes that support the adsorption process (Eqs. 4 to 8). In contrast, other studies including Hu et al. [188] and Liang et al. [224] suggested that divalent cations generally reduce adsorption efficiency due to stronger competition at the material surface.

$$Mg^{2+} + HTC^{-} \rightarrow MgHTC^{+} \quad (1)$$

$$Mg^{2+} + TC^{2-} \rightarrow MgTC \quad (2)$$

$$Ca^{2+} + HTC^{-} \rightarrow CaHTC^{+} \quad (3)$$

$$Ca^{2+} + TC^{2-} \rightarrow CaTC \quad (4)$$

The presence of cations in solution can influence the adsorption efficiency of negatively charged antibiotic molecules onto the surface of biochar. The extent of this effect depends significantly on the type of ion. For example, Fu et al. (2021) found that divalent ions tend to enhance the adsorption efficiency of antibiotics more effectively than monovalent ions, owing to their higher surface charge density and stronger interactions with biochar. Calderón-Franco et al. [228] investigated the effects of Na^{+}, Ca^{2+}, and Mg^{2+} on the adsorption of several common antibiotics. The results indicated that Mg^{2+} improved adsorption efficiency by approximately 33 %, whereas Na^{+} and Ca^{2+} did not cause any significant changes. These findings contrast somewhat with those of Wang et al. [229], who demonstrated that Ca^{2+} can form stronger ionic bridges than Mg^{2+} and may also create complexes with the functional groups of antibiotics, resulting in more compact molecular structures that fit more effectively into the micropores of biochar. Humic acids (HA) have also been shown to play an important role in promoting antibiotic adsorption. Calderón-Franco et al. [228] reported that HA not only directly adsorbs antibiotics but also adheres to the biochar surface, acting as an intermediate bridge layer that facilitates adsorption. Beyond these studies, several recent works have provided further insights into the role and mechanisms of cations in the adsorption process. Qiong Lu et al. [230], for

View Article Online
DOI: 10.1039/D5MA00872G

instance, emphasized that alkaline earth metal ions such as Mg^{2+} and Ca^{2+} not only enhance charge coupling between biochar and antibiotic molecules but also contribute to the structural stability of the material under variable pH conditions, particularly in neutral to alkaline environments. The adsorption mechanism involves more than just ionic bridging. It also includes π–π interactions, hydrogen bonding, and electrostatic forces, all of which are influenced by the type of cations present in the solution [231]. Notably, some studies have shown that incorporating metal oxides like $MgFe_2O_4$ into biochar can improve the adsorption efficiency of SMX and TC by combining several mechanisms including π–π interactions, Ca^{2+} ion bridging, and surface-mediated functional group binding [232]. In parallel, research on seaweed-derived biochar has demonstrated high antibiotic adsorption efficiency at elevated temperatures. This is primarily achieved through π–π interactions, pore filling, and hydrogen bonding, suggesting effective strategies for optimizing adsorbent materials under favorable thermodynamic conditions. Finally, the effects of aged biochar have also been documented. In the presence of Na_+ and Ca^{2+} ions, aged biochar exhibited reduced adsorption capacity for NOR [230]. In contrast, humic acid enhanced adsorption at acidic pH but had a diminishing effect at neutral pH. These observations underscore the importance of considering coexisting substances in the environment when assessing the performance of biochar in antibiotic removal.

3.2. Quantum chemical insights via density functional theory (DFT) calculations

Density Functional Theory (DFT) has emerged as a pivotal tool for investigating the sorption mechanisms of organic pollutants on carbon-based adsorbents particularly biochar. This computational approach enables detailed examination of interactions between antibiotic molecules and biochar surfaces at the electronic level providing insights into fundamental processes such as π-π interactions hydrogen bond formation and chemical bonding while offering valuable guidance for designing biochar with optimized structures. Current applications of DFT in simulating antibiotic adsorption predominantly employ computational software packages such as Gaussian Materials Studio or $Dmol^3$ utilizing exchange-correlation functionals like B3LYP PBE or ωB97X-D combined with basis sets such as 6-31++G(d,p) and DNP. In recent years, many studies have expanded this approach by integrating experimental methods with DFT to elucidate the mechanism of antibiotic adsorption on biochar at the electronic level. Representative examples include the work of Badshah et al. (2024) [233], which investigated the stepwise mechanism of antibiotic removal using activated carbon, Zhang et al. (2024) [234], who standardized and analyzed the micromechanism of tetracycline adsorption on biochar, and Bai et al. (2023) [235], who employed magnetite-functionalized

View Article Online
DOI: 10.1039/D5MA00872G

biochar to clarify the adsorption mechanism of four sulfonamide antibiotics. More recent contributions include Ezzahi et al. (2025) [236], who examined activated biochar derived from lignocellulosic biomass for fluoroquinolone removal, Ren et al. (2025) [237], who validated the adsorption mechanism of metronidazole on CO_2-activated biochar, and Jiang and Hu (2025) [238], who analyzed the synergistic effect between biochar and microplastics in tetracycline adsorption. Collectively, these studies demonstrate that combining experimental data with DFT simulations provides valuable insights into the roles of surface functional groups, metal ion bridging, π–π interactions, and pore filling. Such advances highlight the ongoing shift from purely experimental investigations to quantitative analyses at the electronic level and contribute to establishing a stronger scientific foundation for the design of next-generation biochar materials. This section comprehensively reviews representative studies that employed DFT to analyze antibiotic adsorption on biochar representing a significant advancement from purely experimental investigations to quantum mechanical and electron-level understanding.

Among the pioneering works, Chen et al. [239] conducted a combined experimental and DFT modeling study examining sulfamethazine (SMT) adsorption onto porous cellulose biochar (MCB). Their computational approach utilized Materials Studio 2017 R2 software implementing the GGA-PBE exchange-correlation functional with DNP 4.4 basis set and incorporating Van der Waals corrections through Grimme's DFT-D method. The biochar model was constructed as a planar graphene sheet comprising seven aromatic rings with a 20 Å vacuum layer along the z-axis and employing a 4×4×1 k-point grid. Simulations were performed at 298 K in an aqueous environment simulated using the COSMO model (ε = 78.54). Following geometric optimization the SMT molecule was positioned on the biochar surface in multiple configurations. The adsorption energy (E_{ads}) was calculated using the standard expression:

$$E_{ads} = E_{complex} - (E_{biochar} + E_{SMT}) \quad (5)$$

where $E_{complex}$ represents the total system energy, $E_{biochar}$ denotes the energy of the biochar model and E_{SMT} corresponds to the energy of the antibiotic molecule. Results (in **Figure 9**) demonstrated that the most thermodynamically favorable adsorption configuration occurred when SMT adopted a parallel orientation relative to the graphene surface facilitating π-π stacking and electron donor-acceptor (EDA) interactions particularly at pyrrole group sites characterized by high π-electron density.

View Article Online
DOI: 10.1039/D5MA00872G

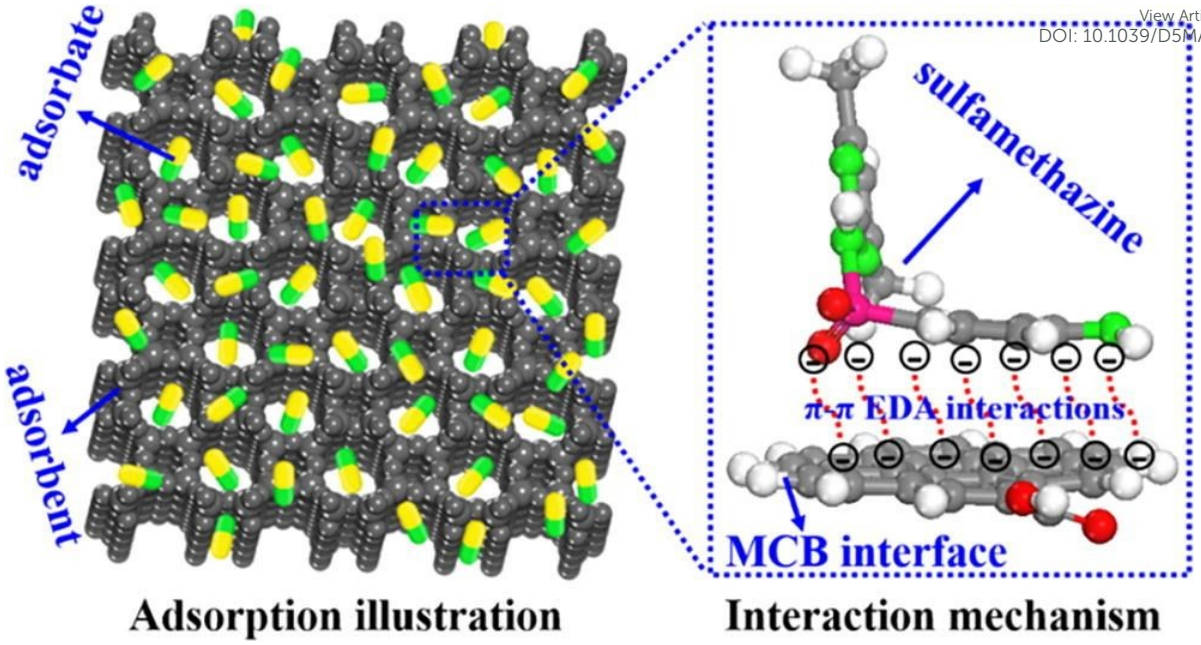

Figure 9. Illustration of the interaction between adsorbent and antibiotic (Reproduced from reference [239] with permission from Elsevier, copyright 2019).

Complemented by in-depth analysis using DFT simulations, the projected density of states (PDOS) and charge density distribution calculations clearly demonstrate that the adsorption of SMT onto biochar occurs through π–π interactions, accompanied by strong electron transfer between molecular orbital regions (**Figure 10**). The most stable adsorption configuration is observed when SMT adopts a V-shaped conformation, which optimizes the overlap between the π orbitals of the aromatic rings in SMT and those on the biochar surface. Moreover, the PDOS spectrum reveals a significant redistribution of the electronic density of states after adsorption, particularly in the region near the Fermi level. A notable enhance in both the number and intensity of peaks in the p-orbital spectrum, compared to the s-orbital, confirms the dominant role of p electrons in the interaction process.

View Article Online
DOI: 10.1039/D5MA00872G

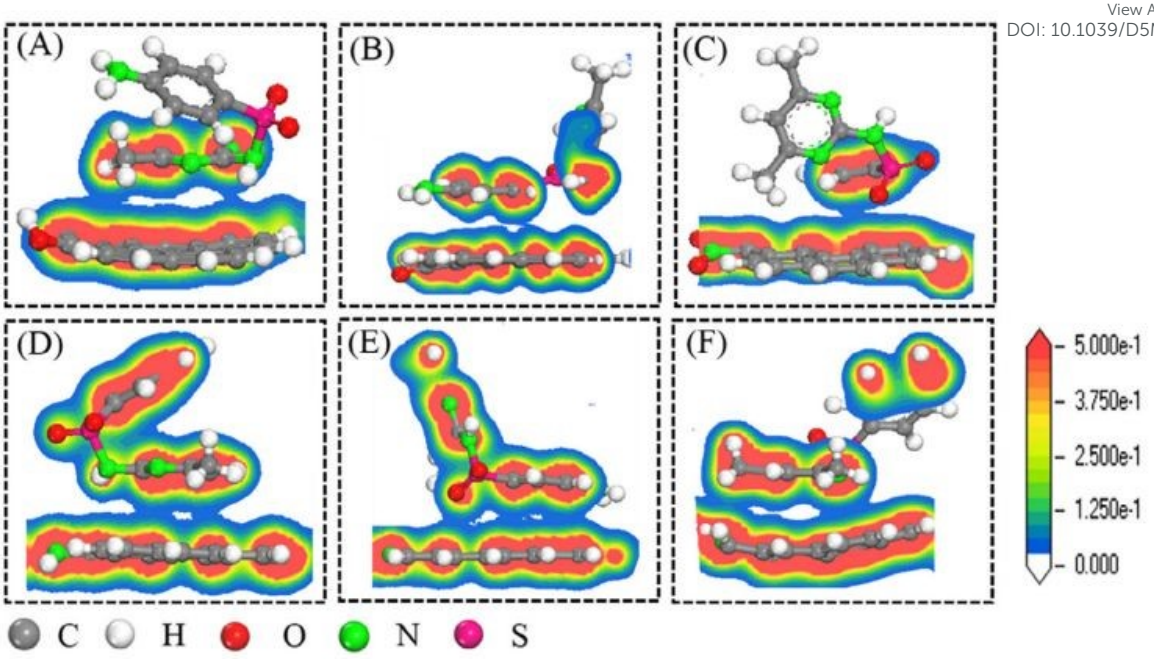

Figure 10. Charge density images showing SMT adsorption on functionalized MCB surfaces: (A) MCB-OH, (B) MCB-COOH, (C) MCB-NO_2, (D) MCB-NH_2, (E) C_5H_5N-MCB, and (F) C_4H_5N-MCB (Reproduced from reference [239] with permission from Elsevier, copyright 2019).

In systems such as OH-substituted MCB, NH_2-substituted MCB, and pyrrole-substituted MCB, the PDOS peaks originally located in the high-energy region corresponding to the HOMO were attenuated and reappeared at lower energy levels after adsorption, indicating electron transfer from the biochar to SMT. In contrast, for systems containing strong electron-withdrawing groups including NO_2 and COOH, several characteristic SMT peaks that appeared in the negative energy range before adsorption (from –3 to 0 eV) shifted into the positive energy range (from 1.5 to 4.5 eV) after adsorption, reflecting a reverse electron transfer direction from SMT to biochar. These findings align with the π–π electron donor–acceptor (EDA) interaction model, where both the direction and magnitude of electron transfer are governed by the polarity of the functional group. Among all functional groups studied, the pyrrole group had the most pronounced effect. It significantly increased the electronic density of states, created a distinct overlap between the PDOS peaks of SMT and biochar after adsorption, resulted in the most negative adsorption energy value. This highlights the critical role of pyrrole in enhancing the π–π EDA interaction and improving the selective uptake efficiency of SMT. Additional analyses including electrostatic potential (ESP) mapping and density of states (DOS) calculations revealed significant electron redistribution upon adsorption confirming the

View Article Online
DOI: 10.1039/D5MA00872G

chemical nature of these interactions. The authors concluded that strategic enhancement of π-donor functional groups such as pyrrole moieties on biochar surfaces represents a promising approach for developing materials with superior selective adsorption capabilities.

Expanding upon the π-rich adsorption mechanism identified in the aforementioned study Liu et al. [240] implemented a more sophisticated electronic analysis approach using biochar derived from durian peel and activated with KOH (KBC) for CIP adsorption. Their DFT simulations performed with Gaussian 09 software employed the hybrid B3LYP functional and 6-31++G(d,p) basis set enabling simultaneous investigation of π-π stacking interactions hydrogen bonding effects and functional group influences. Following geometric optimization of the CIP molecule the researchers calculated frontier molecular orbital energies including HOMO (-5.83 eV) LUMO (-1.41 eV) and the resulting band gap (ΔE = 4.42 eV) which collectively indicated pronounced electron-accepting characteristics. Electrostatic potential (ESP) mapping and molecular orbital calculations revealed that the oxygen-containing functional groups on the biochar surface, particularly the carboxyl and carbonyl groups with strong negative charge distributions, serve as preferential vacant sites for interactions with the locally positively charged regions of the CIP molecule **(Figure 11)**. The optimized adsorption profiles indicated that CIP can bind strongly to the biochar surface through both hydrogen bond formation and coplanar π–π interactions. Notably, adsorption energy analysis for each functional group highlighted the dominant role of the carboxyl (−8.06 eV) and carbonyl (−7.89 eV) groups, in contrast to the lower activity of groups like C=C (−4.08 eV) and OH (−2.72 eV). These findings confirm that oxygen-containing groups not only enhance hydrogen bonding but also function as key π donors in electron donor–acceptor π–π interactions. In addition, the relatively small HOMO–LUMO energy gap of CIP (4.42 eV) suggests a strong electron-accepting ability, which supports the formation of stable donor–acceptor complexes with the electron-rich biochar surface.

View Article Online
DOI: 10.1039/D5MA00872G

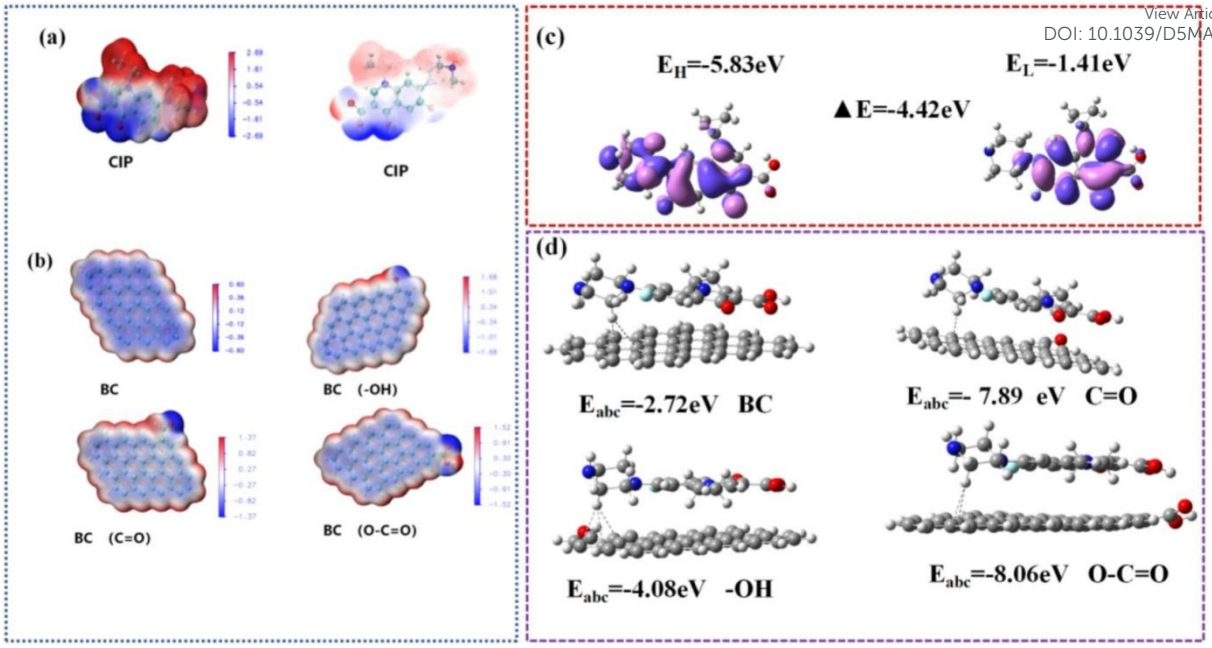

Figure 11. (a) ESP distribution of CIP, (b) ESP distributions of BC and its functionalized forms (–OH, C=O, O–C=O), (c) HOMO and LUMO frontier molecular orbitals, and (d) optimized sorption energies and configurations of CIP on biochar with varying oxygen-containing groups (Reproduced from reference [240] with permission from Elsevier, copyright 2025).

Surface charge distribution analysis was conducted using VMD software identified regions of strong negative charge localization particularly at -O-C=O and -C=O functional groups. Systematic calculations of adsorption energies across different functional group sites employing the conventional energy difference formula revealed the following trend: -O-C=O (-8.06 eV) > C=O (-7.89 eV) > C=C (-4.08 eV) > -OH (-2.72 eV). These findings not only established the predominance of oxygen-containing functional groups in uptake processes but also validated the predictive utility of ESP analysis for identifying preferential adsorption sites. Consequently the research team proposed that biochar materials enriched with carboxyl and carbonyl groups would represent an optimal design strategy for efficient fluoroquinolone (FQ) removal.

Although Liu et al. [240] provided comprehensive insights into the role of electron-rich functional groups in enhancing antibiotic removal via hydrogen bond formation and π-π stacking interactions their investigation primarily focused on specific molecular systems and highly tailored material models. This limitation prompted an important scientific question regarding the existence of generalizable principles governing interactions between polycyclic

aromatic antibiotics and carbonaceous materials such as biochar or graphene. To address this fundamental question Peng et al. [241] developed an innovative combined experimental and DFT simulation approach specifically designed to evaluate the influence of aromatic ring count in antibiotic structures on their adsorption behavior toward π-rich materials including graphene and biochar. In their investigation, the authors employed DFT modeling to systematically evaluate adsorption energies for a series of π-ring compounds with progressively increasing aromatic ring counts (ranging from benzene to pentacene) on graphene flake surfaces. The computational simulations utilized Gaussian 09 software with the ωB97X-D exchange-correlation functional - a hybrid functional incorporating Van der Waals dispersion corrections - paired with the 6-31+G(d,p) basis set, which offers superior accuracy for modeling π-conjugated systems. Following ground-state optimization of all molecular structures, adsorption energies (E_{ads}) were determined using the conventional formula:

$$E_{ads} = E_{system} - (E_{adsorbent} + E_{adsorbate}) \quad (6)$$

where E_{system} represents the total post-adsorption energy, $E_{adsorbent}$ denotes the graphene energy, and $E_{adsorbate}$ corresponds to the isolated π-ring molecule energy. Computational results demonstrated a progressive enhancement in E_{ads} values with increasing aromatic ring count: from -14.97 kcal/mol for benzene to -49.69 kcal/mol for pentacene. These elevated E_{ads} values signify stronger, more stable adsorption bonds, unequivocally demonstrating the direct proportionality between aromatic ring number and adsorption capacity on π-electron-rich surfaces, thereby highlighting the fundamental importance of π-π stacking interactions. Notably, the benzene E_{ads} value equates to approximately 25 kBT at 300 K (roughly triple the hydrogen bond energy between water molecules), confirming that even in the simplest aromatic system, π-π interactions provide sufficient strength to maintain stable adsorption structures under ambient conditions.

Complementing the theoretical modeling, the study conducted parallel experimental adsorption tests using seven antibiotics featuring varying aromatic ring counts (TC, OFL, AMX, SMZ, SDZ, CIP, and SMX). Experimental observations revealed TC and OFL (both containing four aromatic rings) exhibited the most rapid adsorption kinetics, while SMX and CIP (each with one aromatic ring) showed the slowest uptake rates - findings that precisely mirrored the trends predicted by DFT simulations. Additional confirmation came from fluorescence microscopy imaging, which demonstrated nearly complete FITC model compound quenching on graphene surfaces within 30 min, further corroborating the

View Article Online
DOI: 10.1039/D5MA00872G

predominance of π-π adsorption mechanisms. A particularly significant discovery involved the adsorption strength being sufficient to induce localized "dehydration" effects, whereby aromatic rings could effectively displace weakly bound water molecules, thereby enhancing both adsorption selectivity and stability in aqueous environments. Through comprehensive analysis of both experimental data and theoretical calculations, the study established that adsorption efficiency depends not only on antibiotic aromatic ring density but also critically on carbon material surface characteristics. High-temperature carbonized biochar (e.g., processed at 1000 °C) with greater aromatic ring density demonstrated markedly enhanced π-π interaction capabilities. Consequently, strategic optimization of pyrolysis temperature and precise control over graphitization degree emerge as crucial parameters for designing biochars with superior selectivity toward conjugated antibiotics. This research exemplifies how DFT modeling can transcend single-interaction simulations to establish quantitative structure-activity relationships between molecular architecture and adsorption performance - achievements that remain challenging to accomplish through purely experimental approaches.

In contrast to the theoretical clarity achieved with ideal materials like graphene, real-world biochars exhibit far greater structural complexity, frequently featuring abundant surface defects, mixed functionalities, and potential for chemical transformation. To bridge the gap between modeling assumptions and actual material behavior, Hu et al. [242] explored a more application-relevant system: iron-activated beechwood biochar (Fe-BC-800) for adsorbing sulfonamide antibiotics such as sulfamethazine (SMZ) and sulfamerazine (SMR). Their computational approach employed Materials Studio with the Dmol^3 module, an all-electron quantum simulator particularly suitable for inorganic materials and metal-doped carbon surfaces. The simulations used the GGA-PBE exchange-correlation functional with DNP basis set and incorporated spin-polarized settings to accurately model unpaired electron states at iron sites. A 20 Å vacuum layer along the z-axis eliminated interlayer interactions in the vacuum-state system. After optimizing SMZ and SMR structures via the BFGS algorithm, the researchers evaluated adsorption energies using the equation:

$$E_{ads} = E_{SMZ@biochar} - (E_{biochar} + E_{SMZ}) \quad (7)$$

where $E_{SMZ@biochar}$ represents the total adsorption energy, $E_{biochar}$ denotes functionalized biochar energy, and E_{SMZ} corresponds to optimized antibiotic energy. Results revealed maximum adsorption energies at -Fe-O (-35.8 kcal/mol) and -OH (-32.1 kcal/mol) sites, where SMZ/SMR amino groups acted as proton acceptors forming strong hydrogen bonds with oxygen atoms

View Article Online
DOI: 10.1039/D5MA00872G

while aromatic rings maintained parallel orientation to biochar's π-plane, establishing π-π stacking interactions. The study's key innovation involved density of states (DOS) calculations showing new energy levels near the HOMO region post-adsorption, confirming electron redistribution and chemisorption characteristics. Electrostatic potential (ESP) mapping further identified electron-rich regions at oxygen and iron functional groups, which served as electron traps for positively charged antibiotic moieties. These analyses demonstrated iron's dual role as both oxidation catalyst and surface polarization enhancer, strengthening biochar's interaction with charged antibiotic functional groups. Beyond proving Fe-functionalized biochar's efficacy for sulfonamide adsorption, this work established DFT's utility for simulating electron density changes at functionalized sites - a crucial factor determining real-world material performance. This approach proves particularly valuable for complex wastewater treatment scenarios where adsorption mechanisms transition from purely physical to electronically activated processes requiring quantum-level understanding.

While existing research has demonstrated the potential of designed and functionalized biochar for optimizing aromatic antibiotic adsorption through hydrogen bond formation and π-π stacking mechanisms, a critical gap remains in understanding how environmental conditions - particularly pH - influence the electronic nature of adsorption processes. In real wastewater systems, pH variations simultaneously alter antibiotic ionization states and biochar surface protonation levels, dramatically modifying electronic interaction capacities. Addressing this knowledge gap, Li et al. [243] employed DFT modeling to examine how different functional groups (-COOH, -OH, π-ring) on corncob biochar influence SMX adsorption under alkaline conditions where SMX primarily exists in anionic form, favoring ionic/π-bond formation with electropositive surface sites (**Figure 12**). Their simplified yet chemically representative model featured common functional groups on a monolayer graphene substrate. Calculations were performed using Gaussian 09 with the B3LYP functional and 6-31+G(d,p) basis set. Following geometric optimization of SMX-biochar interaction structures, adsorption energies were measured utilizing standard formulations:

$$E_{ads} = E_{SMX@biochar} - (E_{biochar} + E_{SMX}) \quad (8)$$

View Article Online
DOI: 10.1039/D5MA00872G

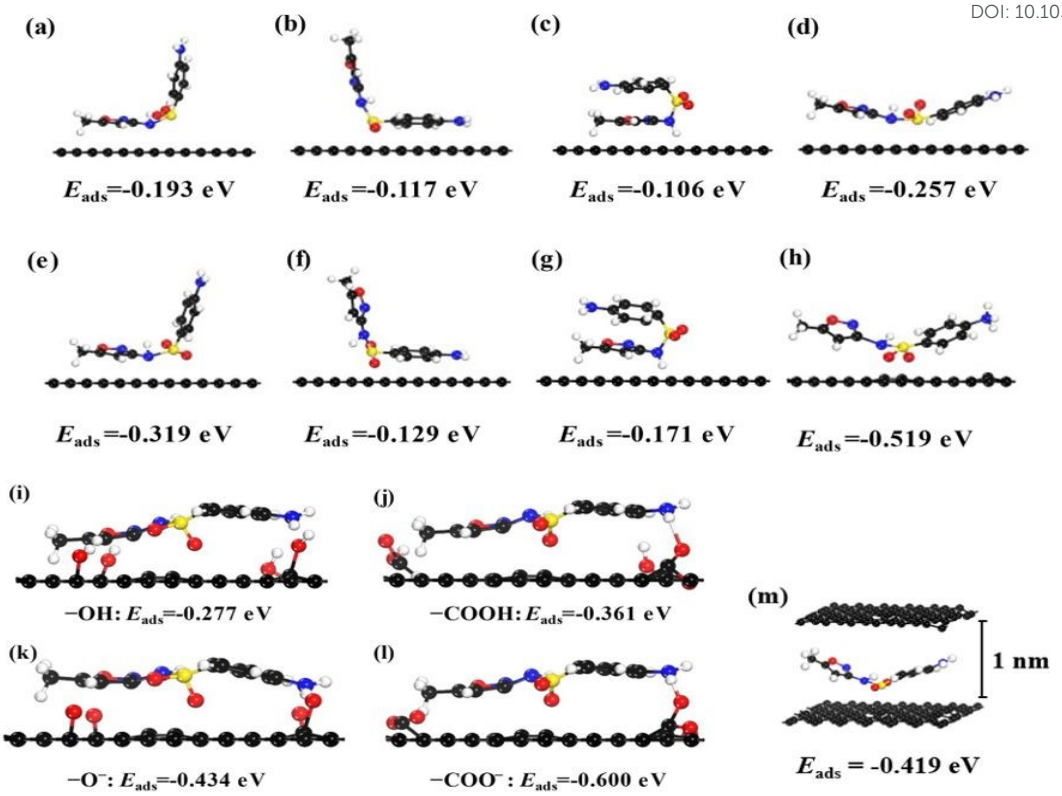

Figure 12. Equilibrium adsorption structures and corresponding elimination energies of SMX on biochar. (a)–(d): different adsorption configurations between neutral SMX and biochar; (e)–(h): various binding modes of the protonated SMX^+ with biochar; (i)–(l): interactions of deprotonated SMX^- with –OH/–COOH functionalized biochar; (m): a sandwich-like configuration involving biochar–SMX–biochar assembly (Reproduced from reference [243] with permission from Elsevier, copyright 2023).

Results revealed that at pH ~9.5, the -COO^- group exhibited the strongest adsorption influence (-34.2 kcal/mol), significantly outperforming -OH (-18.6 kcal/mol) and neutral π-ring (-21.9 kcal/mol) groups. This phenomenon stems from dual proton loss: SMX loses sulfonamide amine protons to become anionic while biochar's -COOH groups deprotonate to form -COO^-, increasing surface negative charge density. The DFT results further support the above finding, showing that the uptake energy (E_{ads}) of –COO^- reaches –0.600 eV, significantly higher than that of –OH (–0.277 eV) or –COOH (–0.361 eV). This indicates that the –COO^- group not only acts as a strong negative charge center but also forms strong coordination hydrogen bonds with electron-rich regions on SMX, particularly the isoxazole cyclic amine group. Remarkably, adsorption still proceeds via coordinated electronic mechanisms, primarily via π-π EDA interactions and hydrogen bond formation at biochar's

View Article Online
DOI: 10.1039/D5MA00872G

electron-rich regions. Multiwfn-generated electrostatic surface potential (ESP) maps clearly visualized this charge redistribution, showing strong polarization at -COO^- and π-electron regions that serve as dominant adsorption sites for SMX's positively charged moieties, particularly the isoxazole ring amine group. The differential charge density map in the DFT simulation further elucidates the electron donor–acceptor forces that occurrs between SMX and biochar. Yellow regions on SMX indicate electron-accepting sites, whereas blue regions on biochar correspond to electron-donating areas, underscoring the critical role of π–π EDA interactions in the elimination process. Notably, among the tested configurations, the planar arrangement of SMX where the two aromatic rings are aligned, exhibits significantly higher adsorption energy compared to orthogonal or V-shaped configurations. Specifically, the planar configuration yields an Eads value of –0.257 eV, demonstrating that optimal alignment for π–π interactions is the key determinant of adsorption efficiency. The study further demonstrated pH's profound impact on the system's frontier molecular orbitals. Under acidic conditions, a large HOMO-LUMO gap between SMX and biochar corresponded to weak interactions. Alkaline conditions caused SMX's HOMO to shift upward and biochar's LUMO downward, reducing ΔE and enhancing electron donor-acceptor capabilities - the key driver of improved EDA-mediated adsorption. The theoretical basis also demonstrates that at high pH levels, the anionic state of SMX and biochar leads to an improve in the HOMO of SMX and a decline in the LUMO of biochar. This arrangement reduces ΔE and enhances the likelihood of electron exchange, explaining why adsorption is more effective under alkaline conditions. This pH-dependent electronic structure modulation suggests wastewater treatment optimization could be achieved through operational pH adjustment rather than relying solely on material properties. These DFT-derived insights not only elucidate biochar functional group roles but also establish that electronic interaction capacities are environmentally dependent, particularly on pH. Moreover, a slit-like pore biochar model composed of two parallel graphene layers (~1 nm spacing) was employed to simulate the 'pore-filling' effect. The model exhibited an adsorption energy of –0.419 eV, surpassing that of neutral π–π interactions but remaining weaker than π^+–π or (C)AHB interactions. These findings highlight the significant role of pores in the adsorption mechanism, particularly under neutral pH conditions or in systems with limited active functional groups. Consequently, optimal antibiotic adsorption requires simultaneous consideration of material design and physicochemical operating conditions - significantly expanding practical application potential. This work powerfully illustrates DFT's dual utility as both a fundamental interaction probe and a predictive tool for adsorption

View Article Online
DOI: 10.1039/D5MA00872G

behavior under variable conditions, offering insights beyond the reach of purely experimental approaches.

Research by Li et al. demonstrates that environmental factors such as pH can alter charge redistribution during antibiotic adsorption on biochar. However, real-world wastewater from hospitals, agriculture, and industry presents a more complex challenge, as it typically contains mixtures of antibiotics, heavy metals, and other pollutants. These complex systems can alter pollutant molecular structures through ligand effects and also affect the electronic characteristics of the material. Within this framework, the study by Zhao et al. [244] provides a critical connection between single-compound adsorption research and real-world environments by using DFT modeling to investigate the simultaneous adsorption of antibiotics such as oxytetracycline, sulfamethazine and amoxicillin with metal ions like Zn^{2+} and Cu^{2+} on biochar derived from rice straw activated at 700 to 800 °C. The authors used DFT to examine the role of functional groups with oxygen atoms on biochar including carboxyl, carbonyl, and hdroxyl groups, in forming ligand bonds with both antibiotic and metal species (**Figure 13**). Calculations were carried out in Gaussian 16 software using the B3LYP functional, which offers a balance between accuracy and computational cost, along with the 6-31+G(d,p) basis set for light atoms and LANL2DZ for metals. The model system consisted of a biochar cluster bearing optimized functional groups, which were allowed to interact with antibiotics in the presence or absence of metal ions. Adsorption energy was determined using the extended equation for a three-component system:

$$E_{ads} = E_{complex} - (E_{biochar} + E_{antibiotic} + E_{metal\ ion}) \quad (9)$$

where Ecomplex is the total energy of the combined system and the other terms represent individual component energies. The results indicated that adding Zn^{2+} or Cu^{2+} significantly enhanced adsorption energy compared to metal-free systems. For example, the adsorption energy of sulfamethazine on –COOH modified biochar was –28.4 kcal/mol, and increased to 42.7 kcal/mol in the presence of Cu^{2+}. This enhancement is attributed to a dual-site ligand mechanism in which the metal ion bridges the carboxyl group on biochar and the amino or phenolic site on the antibiotic, forming a stable five or six-membered chelate ring. Additionally, HOMO and LUMO simulations revealed that the HOMO energy level of the antibiotic shifted closer to the LUMO of biochar after ligand formation, suggesting favorable electron transfer from the antibiotic to the adsorbent.

View Article Online
DOI: 10.1039/D5MA00872G

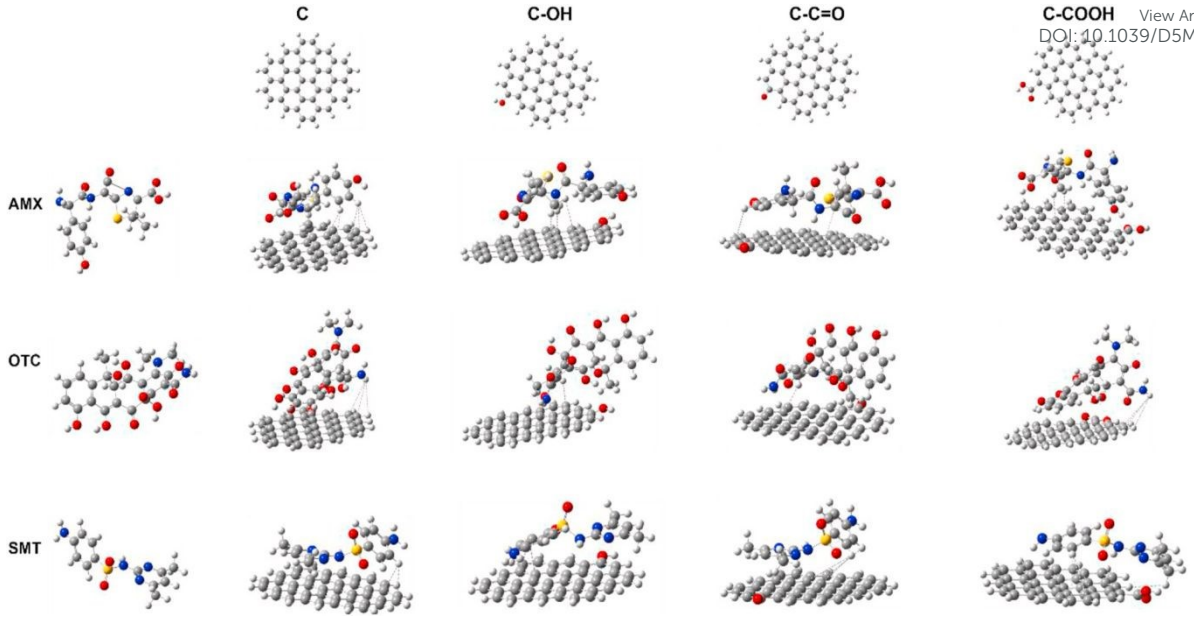

Figure 13. The interaction geometries between antibiotics (such as AMX, OTC, and SMT) and biochar (Reproduced from reference [244] with permission from Elsevier, copyright 2023).

When metal ions were introduced, the LUMO level of the system decreased further, reflecting enhanced electron-accepting capacity consistent with the role of Zn^{2+} and Cu^{2+} as central acceptors in coordinate bonding. The electrostatic potential map showed negative charge localization around carboxylate and carbonyl oxygen atoms on biochar while Zn^{2+} held positive charge at the center, which strengthened electrostatic attraction and ligand coordination. One important result of this investigation is the comparison of different functional groups on biochar. DFT results demonstrated that the carboxyl group formed the strongest interaction with both antibiotic and metal ion, followed by hydroxyl and then non-activated carbonyl groups. These theoretical results align with experimental data obtained from XPS and FTIR, confirming the dominant role of the carboxyl center in resonance-based adsorption. Moreover, all adsorption energies in the biochar–antibiotic–metal ion complexes exceeded –40 kcal/mol, surpassing the threshold for physical adsorption and indicating a stable chemisorption process. Ding et al.'s study advances the understanding of multicomponent pollutant systems and shows that interactions between antibiotics and metal ions can enhance overall adsorption performance, a phenomenon often difficult to isolate through conventional experiments. DFT proves essential in modeling electron states and ligand structures as well as in quantifying binding energies, thereby offering insights with real-world significance. Therefore, DFT is no longer just a complementary method but serves as a central tool in the

View Article Online
DOI: 10.1039/D5MA00872G

design and evaluation of biochar adsorbents for environmental decontamination where adsorption processes are increasingly complex.

3.3. Mechanism

Antibiotic contaminants in water attach to surfaces via chemical or physical interaction processes. Physical adsorption which occurs less frequently, takes place when less polar antibiotics associate with nonpolar sorbents including carbon nanotubes or minerals. The performance of this technique depends on the adsorbent's surface area [245]. Chemical or interactive adsorption is more common because antibiotics have vacant sites including functional groups and electrostatic regions containing atoms like nitrogen, sulfur, or oxygen [246]. Several interactions including van der hydrogen bond formation, Waals forces, and electrostatic attraction contribute to the isolation of these substances [247]. Biochar facilitates the adsorption of antibiotics through mechanisms like surface complexation, hydrophobic effects, pore filling, π-π interactions, electrostatic forces, hydrogen bond formation, and ion pair formation [248, 249]. Recent studies have pointed out that these mechanisms often act concurrently and are largely dependent on the type of biomass used, the pyrolysis conditions, and subsequent surface functionalization [250, 251]. Notably, the combined contributions of pore filling, electrostatic attraction, and π–π interactions have been identified as the principal routes governing antibiotic adsorption onto biochar [252].

3.3.1. Surface complexation

Antibiotics and DNA can form complexes with metal species both in solution and on the biochar's interface, which promotes uptake capacity and is considered a form of ligand exchange [253]. Multiple investigations have shown that the occurrence of metal species in solution enhances the removal of TC by forming metal ion-TC complexes [227]. In addition, metal species can bind with phosphate groups in DNA to form inner sphere complexes, which reduce electrostatic repulsive forces between DNA and make them easier to adsorb onto the surface or into the pores of biochar as compact structures [229]. Many recent studies have shown that oxygen-containing functional groups, such as carboxyl (–COOH) and hydroxyl (–OH) groups, on the biochar surface can coordinate with soluble cations (e.g., Fe^{2+}, Ca^{2+}, or Zn^{2+}) [254-256]. This coordination facilitates the formation of stable intragranular complexes with antibiotic molecules. For instance, Li et al. (2022) demonstrated that Ca^{2+} can act as a cation bridge between tetracycline molecules and the carboxyl groups of biochar, which significantly enhances adsorption efficiency through a complexation mechanism [257]. Recent reviews underscore that biochar modified with metal ions or rich in iron oxides often

View Article Online
DOI: 10.1039/D5MA00872G

demonstrates enhanced antibiotic adsorption efficiency. This is primarily attributed to a strengthened complexation mechanism, which is particularly effective in slightly acidic environments where complexation with antibiotic functional groups is favored [258]. Complexation occurring on the material surface plays an important role in this process, particularly for modified biochar. Wei et al. [259] showed that iron-containing phases such as Fe-O and Fe-OOH in sludge-derived biochar can form complexes with TC, thereby improving treatment efficiency.

3.3.2. Electrostatic forces and charge regulation

The ionization of pollutants such as antibiotics in solution is strongly influenced by pH and the electrostatic repulsive forces between them and the material's surface. This also affects the interface properties of the material [210, 260]. The pH zero charge point (pH_{pzc}) values of two biochars introducted by Qing Ge et al. [261] and Alsaiari et al. [262] including KOH modified bamboo biochar and MOF grafted magnetic biochar, were 6.68 and 5.76, respectively. In cases where the environment has a pH value less than the pH_{pzc}, the surface of APB and PB is positively charged, which facilitates the elimination of negatively charged pollutants. For example, the CIP molecule exists primarily as a cation at pH less than 6.16, an amphoteric form between pH 6.16 and 8.74, and an anion at pH greater than 8.74 [263]. DNA could also be sorbed onto biochar via electrostatic repulsive forces, as discovered by Wu et al. (2022a) [213] and Lian et al. (2020) [264]. DNA has an isoelectric point at around pH 5.0. At pH values below this point, the functional groups on DNA are protonated, making it positively charged. In contrast, the biochar surface is generally negatively charged at pH values above 3.0. Therefore, at pH around 4.0, both DNA and biochar have a lower negative charge, reducing electrostatic repulsion and enhancing adsorption capacity [229, 265].

In addition, the formation of salt bridges via cations such as metal cations can act as a bridge between biochar and antibiotics. The biochar's surface features negatively charged OH and COOH groups, while the sulfonic acid groups on antibiotics are also negatively charged, resulting in electrostatic repulsion [266]. However, cations in solution can reduce this repulsion and enhance the adsorption interaction by acting as salt bridge mediators. Li et al. (2025) demonstrated that the presence of dissolved cations (Ca^{2+}, Zn^{2+}) can act as a cation bridge, which mitigates electrostatic repulsion and thus enhances the adsorption capacity [267]. Zhang et al. (2023) also pointed out that the formation of salt bridge between the sulfonic group of antibiotics and the –COOH/–OH group on biochar via metal ions is an important factor in stabilizing the adsorption complex [268]. Fang et al. [265] demonstrated this using zeta

View Article Online
DOI: 10.1039/D5MA00872G

potential and FTIR spectra. As the cation concentration increased, the zeta potential of biochar decreased significantly, reflecting the weakening of electrostatic repulsion. Simultaneously, the FTIR analysis revealed that the absorption band related to the C-OH group of biochar became broader in the presence of metal cation, confirming the formation of a salt bridge between metal cation and polar functional groups of antibiotics.

3.3.3. Ion exchange

The ion exchange mechanism in the attachment of antibiotics onto biochar and its decorated variants is a key process that contributes to enhancing the efficiency of removing trace pollutants from aquatic environments, particularly antibiotics [269, 270]. Biochar materials which generated via the pyrolysis of organic biomass under anaerobic conditions, typically contain inorganic cations such as potassium, magnesium, sodium, and calcium as well as sometimes anions such as chloride, nitrate, or phosphate, depending on the feedstock and pyrolysis conditions [271]. These ions are mainly present as loosely bound species on the material surface or embedded within the pore network and capillary structure of the biochar, enabling them to exchange readily with other ions in the solution, including ionizable functional groups from antibiotic molecules. In modified biochar, which is functionalized with acids such as H_2SO_4 or HCl, bases such as KOH or NaOH or with materials containing specific functional groups like carboxyl, hydroxyl, sulfonic, or amine groups, the ion exchange capacity is significantly improved due to the introduction of more active sites with higher charge density and increased structural flexibility [272]. Experimental studies have confirmed this mechanism. For instance, Premarathna et al. [273] utilized clay minerals to decorate biochar and observed that cations located between clay layers could be readily exchanged with positively charged ions in solution, thereby enhancing the adsorption process. Likewise, Guo et al. [272] found that under acidic conditions, tylosin, a positively charged antibiotic molecule at pH below 7, was effectively adsorbed onto biochar modified with goethite through both cation exchange and electrostatic interactions. Another work by Li et al. [274] demonstrated that the positively charged piperazine rings of CIP interacted with ion exchange sites on the biochar surface, confirming the contribution of ion exchange under neutral to mildly acidic pH conditions. This ion exchange mechanism depends not only on the charge characteristics of the antibiotic and the environmental pH, but also on the buffering capacity, ionic strength, the occurrence of competing ions, and the molecular structure of both the sorbate and the adsorbent. Thus, understanding the ionic composition of biochar and the nature of charge interactions between its antibiotic molecules and functional groups provides an essential

scientific foundation for designing highly efficient adsorbent materials and optimizing operating conditions for the treatment of antibiotic-contaminated water [275].

3.3.4. Pore confinement and diffusion mechanisms

The pore confinement and diffusion mechanisms in the attachment of antibiotics onto biochar and its decorated variants are essential physical processes that control the accessibility, transport, and ultimate retention of antibiotic molecules in the pore network of the adsorbent. Biochar typically possesses a hierarchical pore structure consisting of mesopores (between 2 and 50 nm), macropores (greater than 50 nm), and micropores (less than 2 nm) [276], which are formed during the pyrolysis of organic biomass under anaerobic or hypoxic environment. The distribution, volume, and connectivity of this pore system are strongly influenced by the composition of the precursor, the temperature of pyrolysis, and the post-treatment modification methods [277]. In addition, metal ions (Ca^{2+}, Mg^{2+}) or charged functional groups (COO^{-}, NH_3^{+}) on the porous interface of biochar facilitate the combination of electrostatic forces and confined steric interactions, thereby enhancing the retention of appropriately sized antibiotic molecules [278]. Antibiotic molecules, depending on their size, shape, and hydration radius, can penetrate into various types of capillaries to different extents. Among these, micropores play a key role in providing large surface areas and high-energy adsorption sites, while mesopores and macropores facilitate the transport of molecules by reducing diffusion resistance and shortening the time required to reach the active sites [279]. Modified biochars, especially those that are chemically or physically activated, often exhibit larger surface areas, increased capillary volumes, and more favorable pore size distributions, which enhance the accessibility of antibiotic molecules to adsorption sites.

Molecular entrapment occurs when antibiotic molecules become confined within narrow capillaries, thereby strengthening physical interactions including hydrogen bond formation, van der Waals forces or pi-pi interactions due to the close proximity between the capillary walls and the molecules. This spatial confinement extends the retention time of antibiotics within the pore structure, thus improving the adsorption efficiency. For example, Guo et al. [279] discovered that CIP molecules could enter the mesoporous system of biochar derived from fish scales and were stabilized through multiple simultaneous interactions within the confined capillary space, significantly enhancing adsorption efficiency. Similarly, Feng et al. [280] reported that NOR was effectively adsorbed in the microporous region of loofah-derived biochar, where geometric constraints and limited diffusion played a critical role in increasing both selectivity and retention of antibiotic molecules. Furthermore, the diffusion process of

View Article Online
DOI: 10.1039/D5MA00872G

antibiotics into the biochar structure comprises several stages, including diffusion across the external film of the adsorbent, internal particle diffusion, and diffusion within the capillary system, all of which are affected by the physicochemical characteristics of both the material and the antibiotics. The interaction between pore-based molecular confinement and diffusion mechanisms becomes particularly significant at low pollutant concentrations, where steric effects and slow transport rates enhance apparent adsorption performance. However, at higher concentrations of pollutants or in the presence of competing substances, capillary blockage and limited diffusion can reduce adsorption efficiency. Therefore, understanding the pore architecture and the kinetics of diffusion is fundamental for optimizing the design of biochar-based adsorbents. This knowledge supports the development of materials with tailored pore systems and surface functionalities to maximize transport, retention, and molecular interactions with antibiotics, ultimately improving the treatment of micropolluted water.

3.3.5. π-π electron donor–acceptor interactions

π–π stacking is a non-covalent, weak intermolecular interaction that is of vital importance in the elimination mechanisms of aromatic contaminants, particularly through interactions between electron-rich and electron-deficient aromatic systems. On the surface of biochar, functional moieties such as carboxyl, nitro, and ketone groups frequently function as π-electron acceptors, facilitating π–π electron donor–acceptor (EDA) interactions with aromatic pollutants. For example, in the work by Yan et al. [281], biochar fabricated from barley straw via phosphoric acid impregnation and microwave treatment exhibited distinct π–π and n–π interactions between its surface carboxyl groups and the aromatic rings of NOR. These interactions were evidenced through C and O K-edge X-ray absorption near-edge structure (XANES) spectroscopy, underscoring the pivotal role of EDA mechanisms in the adsorption process. Similarly, Chen et al. [282] demonstrated that TC can be effectively eliminated by 3D PPY/CMC aerogels, where adsorption was primarily governed by π–π EDA interactions in both sandwich and parallel-displaced configurations. This was supported by density functional theory (DFT) calculations and frontier orbital theory, revealing that these interactions contributed to high uptake performance across a broad pH range. Furthermore, Li et al. [283] reported that biochar activated with phosphoric acid exhibited a significant enhancement in the proportion of π–π interactions from 35 to 48 % at pH 2 which accompanied by an increase in oxygenated functional groups (notably –COOH), thereby improving SMX adsorption efficiency. Collectively, these findings highlight the positive correlation between the density of oxygen-containing functional groups on biochar surfaces and the strength of π–π EDA

interactions, which in turn enhances the sorption capacity for aromatic pollutants. Moreover, physicochemical parameters such as pyrolysis temperature, carbonization degree, and surface modification strategies influence the π-electron distribution on the carbon framework. Typically, biochar prepared at temperatures below 500 °C tends to behave as a π-electron acceptor, whereas materials produced above 500 °C often exhibit π-electron donor characteristics due to the formation of more electron-rich conjugated domains [2]. Thus, the optimization of thermal processing conditions and surface chemistry is essential for tailoring the electron-donating or -accepting behavior of biochar, and ultimately for maximizing adsorption performance via π–π electron donor–acceptor mechanisms.

4. Comparison of various biochar-derived adsorbents

The comparison of the adsorption capacity of various biochar types for different antibiotics reveals a significant diversity in efficiency (q_{max}) (**Table 3**), which depends on the origin of the raw material, the modification method, and the surface structure of the biochar. Traditional biochar adsorbents such as those derived from sewage sludge, bagasse, bamboo, banana peel, or wood often exhibit low to medium adsorption capacities, typically ranging from 7.91 to 120 mg/g. For instance, biochar from sewage sludge adsorbed only 8.69 mg/g of NOR [258], while biochar produced from bagasse reached 105 mg/g for CIP [269]. Some chemically activated or specially modified biochars such as those made from cow dung, rice husks, or sunflower seed husks, revealed a clear improvement in uptake capability. As an example, H_3PO_4-activated sunflower seed husk biochar achieved an uptake amount of 429.3 mg/g for TC [277].

A key highlight of this review is the superior performance of highly modified biochars, especially those doped with heteroatoms or nanomaterials. For example, $MnCl_2$-impregnated biochar reached 534 mg/g [279], while N,S co-doped biochar achieved an outstanding 1490.10 mg/g for TC [286]. These results suggest that the incorporation of heteroatoms such as nitrogen, sulfur, or transition metals can create highly active surface sites, while also altering the electronic structure, surface area, and functional group density, all of which play essential roles in the adsorption mechanism. Particularly, graphitic biochars such as porous graphitic biochar (1122.20 mg/g) [283] and N-doped graphitic biochar (1377.83 mg/g for SMX, 1070.40 mg/g for CIP) [284] exhibit far greater adsorption efficiencies compared to conventional biochars due to their enhanced conductivity, high porosity, and strong π–π interactions with the aromatic structures of antibiotics.

Current research trends focus on developing hybrid or advanced functionalized adsorbents, including metal-doped biochars (Fe/N, Mg/Fe, K-FeO_4), biochars combined with nanomaterials (such as g-MoS_2 or hydroxyapatite), and biochars derived from unique organic sources like traditional Chinese medicine residues, dye waste, or agricultural by-products rich in functional groups. These materials not only enhance adsorption performance but also offer promising potential for reuse and practical application. For example, biochars derived from dyeing sludge or other functionalized sources can reach adsorption capacities exceeding 1000 mg/g [282, 281], making them highly attractive for treating heavily polluted wastewater.

Table 3. Adsorption capabilities from various biochar-derived adsorbent

Adsorbents	Antobiotics	q_{max} (mg/g)	Ref.
Fe oxide/biochar	Macrolide	7.91	[284]
Sludge-derived Biochar	NOR	8.69	[285]
Chitosan-biochar composite	SMX	14.73	[286]
Ball milled biochar	Sulfapyridine	57.90	[287]
HNO_3-modifitied biochar	Sulfonamides	40.00	[288]
N-doped Magnetic Biochar	SMX	42.90	[289]
Bamboo Biochar	FQ	45.88	[290]
H_3PO_4-activated cow dung biochar	CIP	53.89	[291]
Fe/N grafted biochar	CIP	46.45	[292]
Alkali-modified biochar	BPA	71.43	[260]
B6-upgraded biochar	TC	76.92	[293]
Wood biochar	TCH	84.54	[294]
$MgFe_2O_4$-magnetic biochars	SMX TC	50.75 120.36	[295]
Bagasse biochar	CIP	105	[296]
Metal doped-sewage sludge biochar	AMX TC SMX	109.89 123.35 99.01	[297]
Banana peel -based biochar	Doxycycline (DO)	113.60	[298]
Coffee grounds biochar	TC	113.64	[226]
Co-gadolinium modified biochar	TC	119.05	[188]

Hydroxyapatite modified biochar	Tylosin	135.13	[299]
Herbal medicine residues-based biochar	TC OTC Chlortetracycline	188.70 129.90 200.00	[300]
H_3PO_4 activated-biochar	SMX	191.00	[283]
g-MoS_2 decorated biochar	TCH	245.49	[301]
$NiFe_2O_4$/biochar	TC	420.41	[302]
Rice straw biochar	CIP	131.58	[303]
	DO	432.90	
H_3PO_4-activated sunflower seed husk biochar	CIP Ibuprofen SMX TC	361.6 251.1 251.3 429.3	[304]
K_2FeO_4 modified biochar	CIP	434.78	[305]
$MnCl_2$-impregnated biochar	TC	534.00	[306]
Caulis spatholobi biochar	TC	830.78	[307]
Functionalized-Biochar	TC	835.70	[308]
Dyeing sludge-derived biochar	TC	1081.30	[309]
Porous graphitic biochar	TC	1122.20	[310]
N-doped graphitic biochar	SMX CIP	1377.83 1070.40	[311]
Corncob xylose residue-based biochar	SMX	1429	[312]
N,S co-doped biochar	TC	1480.10	[313]

Based on the summarized data, it becomes obvious that biochar adsorption performance depends closely on three main factors. The first is the type of antibiotic, particularly those with aromatic rings or hydroxyl and amino groups that form hydrogen bonds and π–π interactions. The second involves the structure and composition of the biochar including surface area, functional group content, and the extent of modification. The third relates to the processing and activation techniques such as metal impregnation, heteroatom doping, acid or base treatment, or pyrolysis at high temperatures to increase conductivity and surface area. These insights

View Article Online
DOI: 10.1039/D5MA00872G

suggest that future studies should prioritize designing multifunctional biochars with highly porous architectures, abundant heteroatoms, and regenerative features to meet the increasingly complex demands of real-world wastewater treatment.

5. Challenges and future directions for biochar-based material utilization

While biochar is increasingly recognized as a versatile material in fields ranging from soil remediation and pollution adsorption to advanced technologies, there remain considerable challenges in achieving its large-scale practical application. One major issue lies in the heterogeneity of feedstock sources and pyrolysis conditions, which causes variations in microporous structure, chemical composition, and biomechanical properties [314]. These factors directly influence the adsorption efficiency, electrical conductivity, and mechanical strength of the final material. Recent comprehensive reviews indicate that the absence of standardized indicators for properties such as functional group content, porosity, conductivity, and H/C to O/C ratios has delayed the rational design of biochar for specific uses. Nevertheless, this gap also opens new research opportunities. Scientists are now developing molecular-level models of biochar using computer simulations based on experimental data. These models allow for the creation of materials with controlled porosity and surface chemistry, optimized for applications such as pollutant adsorption, electrical conduction, and structural performance. When integrated with multi-criteria decision analysis (MCDA), these models help identify optimal production conditions tailored for specific sectors, including agriculture, environmental management, construction, and energy. Another critical challenge is the potential presence of residual pollutants such as phenolic compounds, polycyclic aromatic hydrocarbons (PAHs), or metal species [315]. This risk is especially high when using untreated waste feedstocks or operating under low-temperature pyrolysis. To minimize environmental impact, it is necessary to integrate a comprehensive risk assessment process, standardize production protocols in accordance with international frameworks such as IBI, and employ pyrolysis equipment with precise control over temperature and residence time. Another commonly overlooked limitation is that chemical modification methods of biochar such as impregnation with strong acids, bases, or transition metals can enhance surface activity and adsorption capacity, yet also carry the risk of generating toxic and hard-to-manage waste. This underscores the need to develop safer, greener, and more environmentally sustainable modification approaches.

In terms of real-world applications, biochar has demonstrated broad potential (**Figure 14**). It has been used in environmentally friendly concrete and construction materials to

improve mechanical strength, enhance durability, and reduce cement usage. Its multi-porous structure and surface functional groups have also enabled the development of soundproofing and waterproofing solutions, as well as green electronic components like electrodes for supercapacitors and microbial fuel cells. Emerging directions include research into using biochar in CO_2-reducing cores for abandoned oil and gas wells, leveraging its long-term carbon sequestration potential and energy efficiency. Looking ahead, three essential directions should be prioritized:

- Standardization and quality control: Develop a set of key indicators such as porosity, H/C–O/C ratio, particle size, and surface functionality tailored to each biochar application (e.g., water treatment, soil improvement, electrodes, or building materials). Establish systems to assess performance under long-term field conditions.
- Integration of fabrication, modeling, and experimentation: Use molecular simulation and MCDA to design application-specific biochar. Strengthen pilot-scale testing to evaluate real-time adsorption capacity, electrical conductivity, and interactions in systems like concrete, electronic materials or agricultural ecosystems [316].

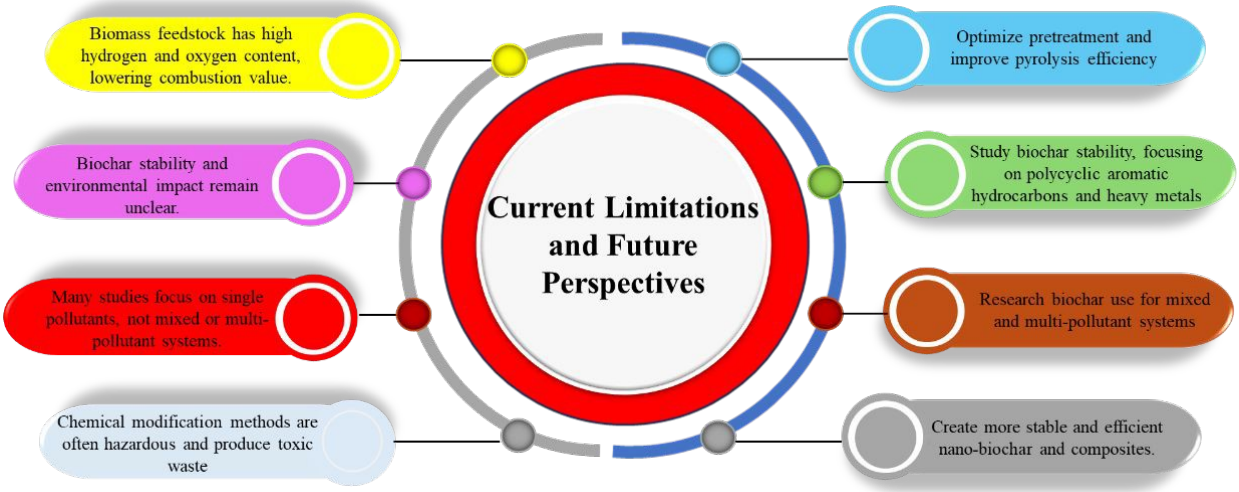

Figure 14. Current limitations and future perspecitves of biochar

- Expansion into non-traditional applications: Transfer biochar technologies into advanced material domains such as energy storage electrodes, biodegradable conveyor systems or corrosion-resistant carbon cores. Special attention should be given to its potential role in the circular economy through recycled composites, bio-based additives or emission-neutralizing systems in heavy industry.

View Article Online
DOI: 10.1039/D5MA00872G

6. Conclusion

In the context of increasingly severe antibiotic pollution and the limitations of conventional treatment methods, biochar has emerged as a promising adsorbent material due to its porous structure, low cost, and environmental compatibility. This review has systematically summarized the advances in biochar research, covering raw material selection, fabrication methods, and modification strategies including chemical activation, electrochemical treatment, plasma processing, and atomic doping. Notably, advanced modification techniques have greatly enhanced the efficiency of antibiotic adsorption by improving surface area, increasing the density of functional groups, and strengthening molecular interactions. The integration of quantum computational tools, particularly density functional theory (DFT), has provided insights into adsorption mechanisms at the atomic level and offered a new approach for designing optimized biochar materials. Furthermore, the combination of biochar with emerging materials such as MOFs and MXenes is identified as a promising direction, especially in improving selectivity and efficiency for the sustainable removal of antibiotic compounds. Despite these developments, several challenges remain including the practical applicability, long-term stability, and environmental safety of the spent adsorbents. Future research should therefore focus on optimizing material structures, expanding the use of quantum mechanical modeling, and conducting pilot-scale experiments to develop more effective and sustainable wastewater treatment solutions.

CRediT authorship contribution statement.

Van Doan Nguyen: Conceptualization (supporting); Formal analysis (Lead); Investigation (equal); Writing—original draft (equal). **The Anh Luu**: Data curation (lead); Formal analysis (equal); Investigation (equal); Writing—original draft (equal). **Guo-Ping Chang-Chien**: Validation (supporting); Writing—review and editing (supporting). **Van Giang Le**: Conceptualization (lead); Funding acquisition (lead); Project administration (Lead); Supervision (lead); Writing—review and editing (lead).

Declaration of competing interest.

The authors declare that they have no known competing financial interests or personal relationships that could have appeared to influence the work reported in this paper.

Acknowledgments.

We are grateful for the insightful comments of Prof. Dr. Ruyean Doong on the manuscript. We also thank the editors and anonymous reviewers for their helpful commentsand suggestions

View Article Online
DOI: 10.1039/D5MA00872G

Declaration of Generative AI and AI-assisted technologies in the writing process

During the preparation of this manuscript, the authors used ChatGPT to polish the English language of the introduction, result and discussion parts of the manuscript, without changing the content. The authors take full responsibility for the content of the publication.

Data availability.

The authors do not have permission to share data.

References

[1] Zhao, Y., X. Li, Y. Li, H. Bao, J. Xing, Y. Zhu, J. Nan, and G. Xu, Biochar Acts as an Emerging Soil Amendment and Its Potential Ecological Risks: A Review. 2023. **16**(1): p. 410.

[2] Dai, Y., N. Zhang, C. Xing, Q. Cui, and Q. Sun, The adsorption, regeneration and engineering applications of biochar for removal organic pollutants: A review. Chemosphere, 2019. **223**: p. 12-27.

[3] Cha, J.S., S.H. Park, S.-C. Jung, C. Ryu, J.-K. Jeon, M.-C. Shin, and Y.-K. Park, Production and utilization of biochar: A review. Journal of Industrial and Engineering Chemistry, 2016. **40**: p. 1-15.

[4] Seow, Y.X., Y.H. Tan, N.M. Mubarak, J. Kansedo, M. Khalid, M.L. Ibrahim, and M. Ghasemi, A review on biochar production from different biomass wastes by recent carbonization technologies and its sustainable applications. Journal of Environmental Chemical Engineering, 2022. **10**(1): p. 107017.

[5] Pang, S., Advances in thermochemical conversion of woody biomass to energy, fuels and chemicals. Biotechnology Advances, 2019. **37**(4): p. 589-597.

[6] Tripathi, M., J.N. Sahu, and P. Ganesan, Effect of process parameters on production of biochar from biomass waste through pyrolysis: A review. Renewable and Sustainable Energy Reviews, 2016. **55**: p. 467-481.

[7] Srivatsav, P., B.S. Bhargav, V. Shanmugasundaram, J. Arun, K.P. Gopinath, and A. Bhatnagar, Biochar as an Eco-Friendly and Economical Adsorbent for the Removal of Colorants (Dyes) from Aqueous Environment: A Review. 2020. **12**(12): p. 3561.

[8] Spokas, K.A., K.B. Cantrell, J.M. Novak, D.W. Archer, J.A. Ippolito, H.P. Collins, A.A. Boateng, I.M. Lima, M.C. Lamb, and A.J. McAloon, Biochar: a synthesis of its agronomic impact beyond carbon sequestration. Journal of environmental quality, 2012. **41**(4): p. 973-989.

[9] Groot, H., K. Fernholz, M. Frank, J. Howe, J. Bowyer, and S. Bratkovich, Biochar 101: An introduction to an ancient product offering modern opportunities. Dovetail Partners INC, 2016. **9**(1): p. 1-6.

[10] Pandey, B., Y.K. Prajapati, and P.N. Sheth, Recent progress in thermochemical techniques to produce hydrogen gas from biomass: A state of the art review. International Journal of Hydrogen Energy, 2019. **44**(47): p. 25384-25415.

[11] Wang, Y., Y.-J. Hu, X. Hao, P. Peng, J.-Y. Shi, F. Peng, and R.-C. Sun, Hydrothermal synthesis and applications of advanced carbonaceous materials from biomass: a review. Advanced Composites and Hybrid Materials, 2020. **3**(3): p. 267-284.

[12] Arellanoa, O., M. Flores, J. Guerra, A. Hidalgo, D. Rojas, and A. Strubinger, Hydrotherma l carbonization (HTC) of corncob and characterization of the obtained hydrochar. Chem Eng, 2016. **50**.

[13] Hoffmann, V., D. Jung, J. Zimmermann, C. Rodriguez Correa, A. Elleuch, K. Halouani, and A. Kruse, Conductive Carbon Materials from the Hydrothermal Carbonization of Vineyard Residues for the Application in Electrochemical Double-Layer Capacitors (EDLCs) and Direct Carbon Fuel Cells (DCFCs). 2019. **12**(10): p. 1703.

[14] Liu, Z., Z. Wang, H. Chen, T. Cai, and Z. Liu, Hydrochar and pyrochar for sorption of pollutants in wastewater and exhaust gas: A critical review. Environmental Pollution, 2021. **268**: p. 115910.

[15] Qian, K., A. Kumar, H. Zhang, D. Bellmer, and R. Huhnke, Recent advances in utilization of biochar. Renewable and Sustainable Energy Reviews, 2015. **42**: p. 1055-1064.

[16] Wang, J. and S. Wang, Preparation, modification and environmental application of biochar: A review. Journal of Cleaner Production, 2019. **227**: p. 1002-1022.

[17] Zhang, Z., Z. Zhu, B. Shen, and L. Liu, Insights into biochar and hydrochar production and applications: A review. Energy, 2019. **171**: p. 581-598.

[18] Pineda Pineda, M.X. and D.C. Flórez Guarín, Evaluación del Hydrochar producido por tratamiento hidrotermal como medio adsorbente de color de un agua residual. 2019.

[19] Navas-Cárdenas, C., M. Caetano, D. Endara, R. Jiménez, A.B. Lozada, L.E. Manangón, A. Navarrete, C. Reinoso, A.E. Sommer-Márquez, and Y. Villasana, The Role of Oxygenated Functional Groups on Cadmium Removal using Pyrochar and Hydrochar Derived from Guadua angustifolia Residues. 2023. **15**(3): p. 525.

[20] Angın, D., E. Altintig, and T.E. Köse, Influence of process parameters on the surface and chemical properties of activated carbon obtained from biochar by chemical activation. Bioresource Technology, 2013. **148**: p. 542-549.

[21] Tong, Y., P.J. McNamara, and B.K. Mayer, Adsorption of organic micropollutants onto biochar: a review of relevant kinetics, mechanisms and equilibrium. Environmental Science: Water Research & Technology, 2019. **5**(5): p. 821-838.

[22] Guo, M., W. Song, and J. Tian, Biochar-facilitated soil remediation: mechanisms and efficacy variations. Frontiers in Environmental Science, 2020. **8**: p. 521512.

[23] Chu, Y., M.A. Khan, S. Zhu, M. Xia, W. Lei, F. Wang, and Y. Xu, Microstructural modification of organo-montmorillonite with Gemini surfactant containing four ammonium cations: molecular dynamics (MD) simulations and adsorption capacity for copper ions. Journal of Chemical Technology Biotechnology, 2019. **94**(11): p. 3585-3594.

[24] Qu, J., Q. Meng, W. Peng, J. Shi, Z. Dong, Z. Li, Q. Hu, G. Zhang, L. Wang, S. Ma, and Y. Zhang, Application of functionalized biochar for adsorption of organic pollutants from environmental media: Synthesis strategies, removal mechanisms and outlook. Journal of Cleaner Production, 2023. **423**: p. 138690.

[25] Gorovtsov, A.V., T.M. Minkina, S.S. Mandzhieva, L.V. Perelomov, G. Soja, I.V. Zamulina, V.D. Rajput, S.N. Sushkova, D. Mohan, and J. Yao, The mechanisms of biochar interactions with microorganisms in soil. Environmental Geochemistry and Health, 2020. **42**(8): p. 2495-2518.

[26] Fabietti, G., M. Biasioli, R. Barberis, and F. Ajmone-Marsan, Soil contamination by organic and inorganic pollutants at the regional scale: the case of Piedmont, Italy. Journal of Soils and Sediments, 2010. **10**(2): p. 290-300.

[27] Lu, Y., K. Gu, Z. Shen, C.-S. Tang, B. Shi, and Q. Zhou, Biochar implications for the engineering properties of soils: A review. Science of The Total Environment, 2023. **888**: p. 164185.

[28] Glaser, B., J. Lehmann, and W. Zech, Ameliorating physical and chemical properties of highly weathered soils in the tropics with charcoal – a review. Biology and Fertility of Soils, 2002. **35**(4): p. 219-230.

[29] Han, M., J. Zhang, L. Zhang, and Z. Wang, Effect of biochar addition on crop yield, water and nitrogen use efficiency: A meta-analysis. Journal of Cleaner Production, 2023. **420**: p. 138425.
[30] Nguyen, T.-B., K. Sherpa, X.-T. Bui, V.-T. Nguyen, T.-D.-H. Vo, H.-T.-T. Ho, C.-W. Chen, and C.-D. Dong, Biochar for soil remediation: A comprehensive review of current research on pollutant removal. Environmental Pollution, 2023. **337**: p. 122571.
[31] Yargicoglu, E.N., B.Y. Sadasivam, K.R. Reddy, and K. Spokas, Physical and chemical characterization of waste wood derived biochars. Waste Management, 2015. **36**: p. 256-268.
[32] Tang, J., W. Zhu, R. Kookana, and A. Katayama, Characteristics of biochar and its application in remediation of contaminated soil. Journal of Bioscience and Bioengineering, 2013. **116**(6): p. 653-659.
[33] Mašek, O., W. Buss, P. Brownsort, M. Rovere, A. Tagliaferro, L. Zhao, X. Cao, and G. Xu, Potassium doping increases biochar carbon sequestration potential by 45%, facilitating decoupling of carbon sequestration from soil improvement. Scientific Reports, 2019. **9**(1): p. 5514.
[34] Samanta, M. and D. Mitra, *Treatment of Petroleum Hydrocarbon Pollutants in Water*, in *Water Pollution and Remediation: Organic Pollutants*, Inamuddin, M.I. Ahamed, and E. Lichtfouse, Editors. 2021, Springer International Publishing: Cham. p. 229-275.
[35] Lou, Y., S. Joseph, L. Li, E.R. Graber, X. Liu, and G. Pan, Water extract from straw biochar used for plant growth promotion: an initial test. BioResources, 2016. **11**(1): p. 249-266.
[36] Xiang, W., X. Zhang, J. Chen, W. Zou, F. He, X. Hu, D.C.W. Tsang, Y.S. Ok, and B. Gao, Biochar technology in wastewater treatment: A critical review. Chemosphere, 2020. **252**: p. 126539.
[37] Présiga-López, D., A. Rubio-Clemente, and J.F. Pérez, Uso del biocarbón como material alternativo para el tratamiento de aguas residuales contaminadas. Revista UIS Ingenierías, 2021. **20**(1): p. 121-134.
[38] Klaunig, J.E., L.M. Kamendulis, and B.A. Hocevar, Oxidative stress and oxidative damage in carcinogenesis. Toxicologic pathology, 2010. **38**(1): p. 96-109.
[39] Ho, S., Low-Cost Adsorbents for the Removal of Phenol/Phenolics, Pesticides, and Dyes from Wastewater Systems: A Review. 2022. **14**(20): p. 3203.
[40] Jiménez-Oyola, S., M.-J. García-Martínez, M.F. Ortega, E. Chavez, P. Romero, I. García-Garizabal, and D. Bolonio, Ecological and probabilistic human health risk assessment of heavy metal(loid)s in river sediments affected by mining activities in Ecuador. Environmental Geochemistry and Health, 2021. **43**(11): p. 4459-4474.
[41] Doan, N.V., V.T. Cuong, T.H. Nguyen, T.X. Do, and A.-T. Vu, Preparation of novel CS/SiO_2-EDTA nanocomposite from ash of rice straw pellets for enhanced removal efficiency of heavy metal ions in aqueous medium. Journal of Water Process Engineering, 2024. **60**: p. 105175.
[42] Tan, V.T., L.T. Vinh, N.H. Tuan, N.V. Doan, T.T. Diep, and P.V. Tuan, Synthesis of α-Al_2O_3 nanosize by combustion reaction using sucrose and graphene oxide as fuel precursors. Journal of Crystal Growth, 2025. **652**: p. 128048.
[43] Li, J., K. Zhang, and H. Zhang, Adsorption of antibiotics on microplastics. Environmental Pollution, 2018. **237**: p. 460-467.
[44] de Sousa, D.N.R., S. Insa, A.A. Mozeto, M. Petrovic, T.F. Chaves, and P.S. Fadini, Equilibrium and kinetic studies of the adsorption of antibiotics from aqueous solutions onto powdered zeolites. Chemosphere, 2018. **205**: p. 137-146.

[45] Ahmed, M.B., J.L. Zhou, H.H. Ngo, and W. Guo, Adsorptive removal of antibiotics from water and wastewater: Progress and challenges. Science of The Total Environment, 2015. **532**: p. 112-126.

[46] Obi, C.C., M.N. Abonyi, P.E. Ohale, C.E. Onu, J.T. Nwabanne, C.A. Igwegbe, T.T. Kamuche, and I.H. Ozofor, Adsorption of antibiotics from aqueous media using nanocomposites: Insight into the current status and future perspectives. Chemical Engineering Journal, 2024. **497**: p. 154767.

[47] Li, H., D. Zhang, X. Han, and B. Xing, Adsorption of antibiotic ciprofloxacin on carbon nanotubes: pH dependence and thermodynamics. Chemosphere, 2014. **95**: p. 150-155.

[48] Kim, H., Y.S. Hwang, and V.K. Sharma, Adsorption of antibiotics and iopromide onto single-walled and multi-walled carbon nanotubes. Chemical Engineering Journal, 2014. **255**: p. 23-27.

[49] Gangar, T. and S. Patra, Antibiotic persistence and its impact on the environment. 3 Biotech, 2023. **13**(12): p. 401.

[50] Hamad, M.T.M.H. and M.E. El-Sesy, Adsorptive removal of levofloxacin and antibiotic resistance genes from hospital wastewater by nano-zero-valent iron and nano-copper using kinetic studies and response surface methodology. Bioresources and Bioprocessing, 2023. **10**(1): p. 1.

[51] Thai-Hoang, L., T. Thong, H.T. Loc, P.T.T. Van, P.T.P. Thuy, and T.L. Thuoc, Influences of anthropogenic activities on water quality in the Saigon River, Ho Chi Minh City. Journal of Water and Health, 2022. **20**(3): p. 491-504.

[52] Schuster, D., K. Axtmann, N. Holstein, C. Felder, A. Voigt, H. Färber, P. Ciorba, C. Szekat, A. Schallenberg, and M. Böckmann, Antibiotic concentrations in raw hospital wastewater surpass minimal selective and minimum inhibitory concentrations of resistant Acinetobacter baylyi strains. Environmental microbiology, 2022. **24**(12): p. 5721-5733.

[53] Oncel, M., A. Muhcu, E. Demirbas, and M. Kobya, A comparative study of chemical precipitation and electrocoagulation for treatment of coal acid drainage wastewater. Journal of Environmental Chemical Engineering, 2013. **1**(4): p. 989-995.

[54] Charerntanyarak, L., Heavy metals removal by chemical coagulation and precipitation. Water Science Technology, 1999. **39**(10-11): p. 135-138.

[55] Nguyen, V.D. and A.-T. Vu, Synthesis of novel EDTA-modified Aluminum Oxide for Improved Removal of Heavy Metal in Contaminated Water. Materials Research Bulletin, 2025: p. 113578.

[56] Ho, T.A., V.D. Nguyen, N.B. Van, K.T. Vu, T.D. Dinh, A.T. Nguyen Duc, T.D. Do, M.K. Nguyen, S.T. Le, D.T. Le, Q.M. Pham, and A.-T. Vu, Preparation of novel DTPA-Modified silica aerogel from rice husk for effective removal of Pb2+ ions from water. Inorganic Chemistry Communications, 2025. **179**: p. 114768.

[57] Aigbe, U.O., K.E. Ukhurebor, R.B. Onyancha, O.A. Osibote, H. Darmokoesoemo, and H.S. Kusuma, Fly ash-based adsorbent for adsorption of heavy metals and dyes from aqueous solution: a review. Journal of Materials Research and Technology, 2021. **14**: p. 2751-2774.

[58] Nguyen, V.D., T.P. Nguyen, and A.-T. Vu, Chemical modification of lettuce leaves using NaOH and EDTA: A brilliant biosorbent for the adsorption of heavy metal ions from aqueous solution. Journal of Water Process Engineering, 2025. **71**: p. 107202.

[59] Nguyen, V.D., M.T. Nguyen, and A.-T. Vu, Production of green biosorbent from chemically modified moringa leaves for enhanced removal of heavy metal in aqueous environment. Biomass Conversion and Biorefinery, 2024.

[60] Ajiboye, T.O., O.A. Oyewo, and D.C. Onwudiwe, Simultaneous removal of organics and heavy metals from industrial wastewater: A review. Chemosphere, 2021. **262**: p. 128379.
[61] Zhuang, S. and J. Wang, Cesium removal from radioactive wastewater by adsorption and membrane technology. Frontiers of Environmental Science & Engineering, 2023. **18**(3): p. 38.
[62] Nguyen, V.D., A.-T. Vu, and T.V. La, Fabrication of high-purity alumina particles by spray drying and surface modification with SDS for methylene blue removal. Particuology, 2025.
[63] Kasera, N., P. Kolar, and S.G. Hall, Nitrogen-doped biochars as adsorbents for mitigation of heavy metals and organics from water: a review. Biochar, 2022. **4**(1): p. 17.
[64] Tian, X., S. Chu, Y. Hu, L. Luo, X. Lin, and H. Wang, Removal of heavy metals from single- and multi-metal solution by magnetic microalgae-derived biochar. Journal of Water Process Engineering, 2025. **69**: p. 106622.
[65] Yang, M., S. An, H. Gao, Z. Du, X. Zhang, L.D. Nghiem, and Q. Liu, Selective adsorption of copper by amidoxime modified low-temperature biochar: Performance and mechanism. Science of The Total Environment, 2025. **958**: p. 178072.
[66] Madzin, Z., I. Zahidi, A. Talei, M.E. Raghunandan, A.A. Hermawan, and D.S. Karam, Optimising spent mushroom compost biochar for heavy metal removal: Mechanisms and kinetics in mine water treatment. Journal of Water Process Engineering, 2025. **69**: p. 106829.
[67] Sun, Y., Q. Yu, T. Yang, R. Li, and S. Zhao, Preparation and electrochemical properties of modified biochar. Biomass and Bioenergy, 2025. **192**: p. 107496.
[68] Li, Y., Y. Xin, B. Sun, C. Man, E. Mouele, L. Petrik, B.J. Bladergroen, and C. Zhang, Inactivation of Cyclotella meneghiniana to prepare biochar by in-liquid pulsed discharge plasma. Biomass and Bioenergy, 2025. **200**: p. 108034.
[69] McGlashan, N., N. Shah, B. Caldecott, and M. Workman, High-level techno-economic assessment of negative emissions technologies. Process Safety and Environmental Protection, 2012. **90**(6): p. 501-510.
[70] Basu, P., *Biomass gasification, pyrolysis and torrefaction: practical design and theory*. 2018: Academic press.
[71] Yusup, S. and N.A. Rashidi, *A Mini Review of Biochar Synthesis, Characterization, and Related Standardization and Legislation*, in *Applications of Biochar for Environmental Safety*, A.A. Abdelhafez and M. Abbas, Editors. 2020, IntechOpen: Rijeka.
[72] Leithaeuser, A., M. Gerber, R. Span, and S. Schwede, Comparison of pyrochar, hydrochar and lignite as additive in anaerobic digestion and NH_4^+ adsorbent. Bioresource Technology, 2022. **361**: p. 127674.
[73] Lee, J.W., B. Hawkins, X. Li, and D.M. Day, *Biochar Fertilizer for Soil Amendment and Carbon Sequestration*, in *Advanced Biofuels and Bioproducts*, J.W. Lee, Editor. 2013, Springer New York: New York, NY. p. 57-68.
[74] Roberts, K.G., B.A. Gloy, S. Joseph, N.R. Scott, and J. Lehmann, Life Cycle Assessment of Biochar Systems: Estimating the Energetic, Economic, and Climate Change Potential. Environmental Science & Technology, 2010. **44**(2): p. 827-833.
[75] Odega, C.A., O.O. Ayodele, S.O. Ogutuga, G.T. Anguruwa, A.E. Adekunle, and C.O. Fakorede, Potential application and regeneration of bamboo biochar for wastewater treatment: A review. Advances in Bamboo Science, 2023. **2**: p. 100012.
[76] Hassan, M., Y. Liu, R. Naidu, S.J. Parikh, J. Du, F. Qi, and I.R. Willett, Influences of feedstock sources and pyrolysis temperature on the properties of biochar and

View Article Online
DOI: 10.1039/D5MA00872G

functionality as adsorbents: A meta-analysis. Science of The Total Environment, 2020. **744**: p. 140714.

[77] Tiwari, A.K., D.B. Pal, and N. Prasad, *Agricultural waste biomass utilization in waste water treatment*, in *Utilization of Waste Biomass in Energy, Environment and Catalysis*. 2022, CRC Press. p. 19-41.

[78] Abdel-Shafy, H.I. and M.S.M. Mansour, Solid waste issue: Sources, composition, disposal, recycling, and valorization. Egyptian Journal of Petroleum, 2018. **27**(4): p. 1275-1290.

[79] Jafri, N., W.Y. Wong, V. Doshi, L.W. Yoon, and K.H. Cheah, A review on production and characterization of biochars for application in direct carbon fuel cells. Process Safety and Environmental Protection, 2018. **118**: p. 152-166.

[80] Shrivastava, P., A. Kumar, P. Tekasakul, S.S. Lam, and A. Palamanit, Comparative Investigation of Yield and Quality of Bio-Oil and Biochar from Pyrolysis of Woody and Non-Woody Biomasses. 2021. **14**(4): p. 1092.

[81] Espíndola, S.P., M. Pronk, J. Zlopasa, S.J. Picken, and M.C.M. van Loosdrecht, Nanocellulose recovery from domestic wastewater. Journal of Cleaner Production, 2021. **280**: p. 124507.

[82] Wu, P., Z. Wang, H. Wang, N.S. Bolan, Y. Wang, and W. Chen, Visualizing the emerging trends of biochar research and applications in 2019: a scientometric analysis and review. Biochar, 2020. **2**(2): p. 135-150.

[83] Rafiq, M.K., R.T. Bachmann, M.T. Rafiq, Z. Shang, S. Joseph, and R. Long, Influence of pyrolysis temperature on physico-chemical properties of corn stover (Zea mays L.) biochar and feasibility for carbon capture and energy balance. PloS one, 2016. **11**(6): p. e0156894.

[84] Ercan, B., K. Alper, S. Ucar, and S. Karagoz, Comparative studies of hydrochars and biochars produced from lignocellulosic biomass via hydrothermal carbonization, torrefaction and pyrolysis. Journal of the Energy Institute, 2023. **109**: p. 101298.

[85] Xiao, R., M.K. Awasthi, R. Li, J. Park, S.M. Pensky, Q. Wang, J.J. Wang, and Z. Zhang, Recent developments in biochar utilization as an additive in organic solid waste composting: A review. Bioresource Technology, 2017. **246**: p. 203-213.

[86] Mohan, D., A. Sarswat, Y.S. Ok, and C.U. Pittman, Organic and inorganic contaminants removal from water with biochar, a renewable, low cost and sustainable adsorbent – A critical review. Bioresource Technology, 2014. **160**: p. 191-202.

[87] Jakab, E., *Chapter 3 - Analytical Techniques as a Tool to Understand the Reaction Mechanism*, in *Recent Advances in Thermo-Chemical Conversion of Biomass*, A. Pandey, T. Bhaskar, M. Stöcker, and R.K. Sukumaran, Editors. 2015, Elsevier: Boston. p. 75-108.

[88] Brewer, C.E., R. Unger, K. Schmidt-Rohr, and R.C. Brown, Criteria to Select Biochars for Field Studies based on Biochar Chemical Properties. BioEnergy Research, 2011. **4**(4): p. 312-323.

[89] Wijitkosum, S. and P. Jiwnok, Elemental Composition of Biochar Obtained from Agricultural Waste for Soil Amendment and Carbon Sequestration. 2019. **9**(19): p. 3980.

[90] Zhang, T., W.P. Walawender, L.T. Fan, M. Fan, D. Daugaard, and R.C. Brown, Preparation of activated carbon from forest and agricultural residues through CO2 activation. Chemical Engineering Journal, 2004. **105**(1): p. 53-59.

[91] Lua, A.C., T. Yang, and J. Guo, Effects of pyrolysis conditions on the properties of activated carbons prepared from pistachio-nut shells. Journal of Analytical and Applied Pyrolysis, 2004. **72**(2): p. 279-287.

[92] Zhang, J., J. Liu, and R. Liu, Effects of pyrolysis temperature and heating time on biochar obtained from the pyrolysis of straw and lignosulfonate. Bioresource Technology, 2015. **176**: p. 288-291.
[93] Chatterjee, R., B. Sajjadi, W.-Y. Chen, D.L. Mattern, N. Hammer, V. Raman, and A. Dorris, Effect of pyrolysis temperature on physicochemical properties and acoustic-based amination of biochar for efficient CO2 adsorption. Frontiers in Energy Research, 2020. **8**: p. 85.
[94] Lehmann, J., M.C. Rillig, J. Thies, C.A. Masiello, W.C. Hockaday, and D. Crowley, Biochar effects on soil biota – A review. Soil Biology and Biochemistry, 2011. **43**(9): p. 1812-1836.
[95] You, S., Y.S. Ok, S.S. Chen, D.C.W. Tsang, E.E. Kwon, J. Lee, and C.-H. Wang, A critical review on sustainable biochar system through gasification: Energy and environmental applications. Bioresource Technology, 2017. **246**: p. 242-253.
[96] Brewer, C.E., K. Schmidt-Rohr, J.A. Satrio, and R.C. Brown, Characterization of biochar from fast pyrolysis and gasification systems. Environmental progress sustainable energy: an Official Publication of the American Institute of Chemical Engineers, 2009. **28**(3): p. 386-396.
[97] Czerwińska, K., M. Śliz, and M. Wilk, Hydrothermal carbonization process: Fundamentals, main parameter characteristics and possible applications including an effective method of SARS-CoV-2 mitigation in sewage sludge. A review. Renewable and Sustainable Energy Reviews, 2022. **154**: p. 111873.
[98] Khan, T.A., A.S. Saud, S.S. Jamari, M.H.A. Rahim, J.-W. Park, and H.-J. Kim, Hydrothermal carbonization of lignocellulosic biomass for carbon rich material preparation: A review. Biomass and Bioenergy, 2019. **130**: p. 105384.
[99] Ahmad, F., E.L. Silva, and M.B.A. Varesche, Hydrothermal processing of biomass for anaerobic digestion – A review. Renewable and Sustainable Energy Reviews, 2018. **98**: p. 108-124.
[100] Maniscalco, M.P., M. Volpe, and A. Messineo, Hydrothermal Carbonization as a Valuable Tool for Energy and Environmental Applications: A Review. 2020. **13**(16): p. 4098.
[101] Fiori, L., D. Basso, D. Castello, and M. Baratieri, Hydrothermal carbonization of biomass: Design of a batch reactor and preliminary experimental results. Chem. Eng. Trans, 2014. **37**(5).
[102] Sun, Y., B. Gao, Y. Yao, J. Fang, M. Zhang, Y. Zhou, H. Chen, and L. Yang, Effects of feedstock type, production method, and pyrolysis temperature on biochar and hydrochar properties. Chemical Engineering Journal, 2014. **240**: p. 574-578.
[103] Liu, Z., A. Quek, S. Kent Hoekman, and R. Balasubramanian, Production of solid biochar fuel from waste biomass by hydrothermal carbonization. Fuel, 2013. **103**: p. 943-949.
[104] Yihunu, E.W., M. Minale, S. Abebe, and M. Limin, Preparation, characterization and cost analysis of activated biochar and hydrochar derived from agricultural waste: a comparative study. SN Applied Sciences, 2019. **1**(8): p. 873.
[105] Weiner, B., I. Baskyr, J. Poerschmann, and F.-D. Kopinke, Potential of the hydrothermal carbonization process for the degradation of organic pollutants. Chemosphere, 2013. **92**(6): p. 674-680.
[106] Gamgoum, R., A. Dutta, R.M. Santos, and Y.W. Chiang, Hydrothermal Conversion of Neutral Sulfite Semi-Chemical Red Liquor into Hydrochar. 2016. **9**(6): p. 435.
[107] Chen, W.-H., B.-J. Lin, Y.-Y. Lin, Y.-S. Chu, A.T. Ubando, P.L. Show, H.C. Ong, J.-S. Chang, S.-H. Ho, A.B. Culaba, A. Pétrissans, and M. Pétrissans, Progress in biomass

torrefaction: Principles, applications and challenges. Progress in Energy and Combustion Science, 2021. **82**: p. 100887.

[108] Sahoo, K., E. Bilek, R. Bergman, and S. Mani, Techno-economic analysis of producing solid biofuels and biochar from forest residues using portable systems. Applied Energy, 2019. **235**: p. 578-590.

[109] Rajapaksha, A.U., M. Vithanage, M. Ahmad, D.-C. Seo, J.-S. Cho, S.-E. Lee, S.S. Lee, and Y.S. Ok, Enhanced sulfamethazine removal by steam-activated invasive plant-derived biochar. Journal of Hazardous Materials, 2015. **290**: p. 43-50.

[110] Rong, S., Y. He, L. Ni, Q. Gao, X. Feng, S. Liu, Y. Zhong, Y. Li, and Z. Liu, Steam-activated biochar for efficient removal of sulfamethoxazole from water: Activation temperature-mediated differences. Journal of Water Process Engineering, 2025. **72**: p. 107462.

[111] Lima, I.M. and W.E. Marshall, Adsorption of selected environmentally important metals by poultry manure-based granular activated carbons. Journal of Chemical Technology Biotechnology: International Research in Process, Environmental Clean Technology, 2005. **80**(9): p. 1054-1061.

[112] Mondal, S., A. Kaustav, and G. and Halder, Optimization of ranitidine hydrochloride removal from simulated pharmaceutical waste by activated charcoal from mung bean husk using response surface methodology and artificial neural network. Desalination and Water Treatment, 2016. **57**(39): p. 18366-18378.

[113] Rangabhashiyam, S. and P. Balasubramanian, The potential of lignocellulosic biomass precursors for biochar production: performance, mechanism and wastewater application-a review. 2019.

[114] Sajjadi, B., W.-Y. Chen, and N.O. Egiebor, A comprehensive review on physical activation of biochar for energy and environmental applications. Reviews in Chemical Engineering, 2019. **35**(6): p. 735-776.

[115] Lyu, H., B. Gao, F. He, C. Ding, J. Tang, and J.C. Crittenden, Ball-Milled Carbon Nanomaterials for Energy and Environmental Applications. ACS Sustainable Chemistry & Engineering, 2017. **5**(11): p. 9568-9585.

[116] Lyu, H., B. Gao, F. He, A.R. Zimmerman, C. Ding, H. Huang, and J. Tang, Effects of ball milling on the physicochemical and sorptive properties of biochar: Experimental observations and governing mechanisms. Environmental Pollution, 2018. **233**: p. 54-63.

[117] Lyu, H., B. Gao, F. He, A.R. Zimmerman, C. Ding, J. Tang, and J.C. Crittenden, Experimental and modeling investigations of ball-milled biochar for the removal of aqueous methylene blue. Chemical Engineering Journal, 2018. **335**: p. 110-119.

[118] Peterson, S.C., M.A. Jackson, S. Kim, and D.E. Palmquist, Increasing biochar surface area: Optimization of ball milling parameters. Powder Technology, 2012. **228**: p. 115-120.

[119] Ahuja, R., A. Kalia, R. Sikka, and C. P, Nano Modifications of Biochar to Enhance Heavy Metal Adsorption from Wastewaters: A Review. ACS Omega, 2022. **7**(50): p. 45825-45836.

[120] Wahi, R., N.F.Q.a. Zuhaidi, Y. Yusof, J. Jamel, D. Kanakaraju, and Z. Ngaini, Chemically treated microwave-derived biochar: An overview. Biomass and Bioenergy, 2017. **107**: p. 411-421.

[121] Li, K., Y. Jiang, X. Wang, D. Bai, H. Li, and Z. Zheng, Effect of nitric acid modification on the lead(II) adsorption of mesoporous biochars with different mesopore size distributions. Clean Technologies and Environmental Policy, 2016. **18**(3): p. 797-805.

[122] Ding, Z., X. Hu, Y. Wan, S. Wang, and B. Gao, Removal of lead, copper, cadmium, zinc, and nickel from aqueous solutions by alkali-modified biochar: Batch and column tests. Journal of Industrial and Engineering Chemistry, 2016. **33**: p. 239-245.
[123] Han, X., L. Chu, S. Liu, T. Chen, C. Ding, J. Yan, L. Cui, and G. Quan, Removal of methylene blue from aqueous solution using porous biochar obtained by KOH activation of peanut shell biochar. BioResources, 2015. **10**(2): p. 2836-2849.
[124] Zhou, Z., J. Xu, L. Zou, X. Wang, Y. Chen, P. Sun, X. Zhu, L. Sheng, and N. Lu, Removal of sulfonamide antibiotics by constructed wetland substrate with NaOH-modified corn straw biochar under different operating conditions. Bioresource Technology, 2024. **410**: p. 131274.
[125] Vithanage, M., A.U. Rajapaksha, M. Zhang, S. Thiele-Bruhn, S.S. Lee, and Y.S. Ok, Acid-activated biochar increased sulfamethazine retention in soils. Environmental Science and Pollution Research, 2015. **22**(3): p. 2175-2186.
[126] Yin, K., J. Wang, X. Tian, N. Yu, X. Zhang, Y. Zhao, Y. Liu, S. Sui, C. Wang, F. Lian, S. Zhai, X. Li, and B. Xing, Effect of biochar-derived dissolved organic matter on tetracycline sorption by KMnO4-modified biochar. Chemical Engineering Journal, 2023. **474**: p. 145872.
[127] Sun, P., Y. Li, T. Meng, R. Zhang, M. Song, and J. Ren, Removal of sulfonamide antibiotics and human metabolite by biochar and biochar/H2O2 in synthetic urine. Water Research, 2018. **147**: p. 91-100.
[128] Pezoti, O., A.L. Cazetta, I.P.A.F. Souza, K.C. Bedin, A.C. Martins, T.L. Silva, and V.C. Almeida, Adsorption studies of methylene blue onto ZnCl2-activated carbon produced from buriti shells (Mauritia flexuosa L.). Journal of Industrial and Engineering Chemistry, 2014. **20**(6): p. 4401-4407.
[129] Zhang, X., Y. Chu, X. Yu, C. Yan, Y. Yang, J. Liu, G. Shen, X. Wang, S. Tao, and X. Wang, Introduction of N-containing moieties by ammonia plasma technique can substantially improve ciprofloxacin removal by biochar and the associated mechanisms: Spectroscopic and site energy distribution analysis. Journal of Hazardous Materials, 2022. **424**: p. 127438.
[130] Lou, J., Y. Wei, M. Zhang, Q. Meng, J. An, and M. Jia, Removal of tetracycline hydrochloride in aqueous by coupling dielectric barrier discharge plasma with biochar. Separation and Purification Technology, 2021. **266**: p. 118515.
[131] Zoroufchi Benis, K., J. Soltan, and K.N. McPhedran, Electrochemically modified adsorbents for treatment of aqueous arsenic: Pore diffusion in modified biomass vs. biochar. Chemical Engineering Journal, 2021. **423**: p. 130061.
[132] Tian, R., H. Dong, J. Chen, R. Li, Q. Xie, L. Li, Y. Li, Z. Jin, S. Xiao, and J. Xiao, Electrochemical behaviors of biochar materials during pollutant removal in wastewater: A review. Chemical Engineering Journal, 2021. **425**: p. 130585.
[133] Xu, L., Y. Qi, S. He, C. Wang, X. Jin, Q. Wang, K. Wang, and P. Jin, Facile synthesis of boron-doped porous biochar as a metal-free adsorbent for efficient removal of aqueous tetracycline antibiotics. Journal of Environmental Sciences, 2025. **152**: p. 235-247.
[134] Cheng, Y., J. Yang, J. Shen, P. Yan, S. Liu, J. Kang, L. Bi, B. Wang, S. Zhao, and Z. Chen, Preparation of P-doped biochar and its high-efficient removal of sulfamethoxazole from water: Adsorption mechanism, fixed-bed column and DFT study. Chemical Engineering Journal, 2023. **468**: p. 143748.
[135] Li, Y., B. Xing, X. Wang, K. Wang, L. Zhu, and S. Wang, Nitrogen-Doped Hierarchical Porous Biochar Derived from Corn Stalks for Phenol-Enhanced Adsorption. Energy & Fuels, 2019. **33**(12): p. 12459-12468.

[136] Wan, Z., Y. Sun, D.C.W. Tsang, E. Khan, A.C.K. Yip, Y.H. Ng, J. Rinklebe, and Y.S. Ok, Customised fabrication of nitrogen-doped biochar for environmental and energy applications. Chemical Engineering Journal, 2020. **401**: p. 126136.
[137] Ahmad, S., L. Liu, S. Zhang, and J. Tang, Nitrogen-doped biochar (N-doped BC) and iron/nitrogen co-doped biochar (Fe/N co-doped BC) for removal of refractory organic pollutants. Journal of Hazardous Materials, 2023. **446**: p. 130727.
[138] Ahmad, S., F. Gao, H. Lyu, J. Ma, B. Zhao, S. Xu, C. Ri, and J. Tang, Temperature-dependent carbothermally reduced iron and nitrogen doped biochar composites for removal of hexavalent chromium and nitrobenzene. Chemical Engineering Journal, 2022. **450**: p. 138006.
[139] Zhu, X., L. Xu, C. Wang, Y. Qi, J. Shi, X. Jin, X. Bai, W. Yan, and P. Jin, Insights into the enhanced simultaneous adsorption and catalytic removal of antibiotics by a novel Fe/B co-doped biochar. Separation and Purification Technology, 2025. **360**: p. 130888.
[140] Cheng, N., B. Wang, M. Chen, Q. Feng, X. Zhang, S. Wang, R. Zhao, and T. Jiang, Adsorption and photocatalytic degradation of quinolone antibiotics from wastewater using functionalized biochar. Environ Pollut, 2023. **336**: p. 122409.
[141] Sudan, S., J. Kaushal, and A. Khajuria, Efficient adsorption of anionic dye (congo red) using copper-carbon dots doped magnetic biochar: kinetic, isothermal, and regeneration studies. Clean Technologies and Environmental Policy, 2024. **26**(2): p. 481-497.
[142] Yao, B., W. Zeng, A. Núñez-Delgado, and Y. Zhou, Simultaneous adsorption of ciprofloxacin and Cu(2+) using Fe and N co-doped biochar: Competition and selective separation. Waste Manag, 2023. **168**: p. 386-395.
[143] Wu, W., J. Zhang, W. Zhu, S. Zhao, Y. Gao, Y. Li, L. Ding, and H. Ding, Novel manganese and nitrogen co-doped biochar based on sodium bicarbonate activation for efficient removal of bisphenol A: Mechanism insight and role analysis of manganese and nitrogen by combination of characterizations, experiments and density functional theory calculations. Bioresour Technol, 2024. **399**: p. 130608.
[144] Liu, Z., P. Zhang, Z. Wei, F. Xiao, S. Liu, H. Guo, C. Qu, J. Xiong, H. Sun, and W. Tan, Porous Fe-doped graphitized biochar: An innovative approach for co-removing per-/polyfluoroalkyl substances with different chain lengths from natural waters and wastewater. Chemical Engineering Journal, 2023. **476**: p. 146888.
[145] Wu, J., T. Wang, Y. Liu, W. Tang, S. Geng, and J. Chen, Norfloxacin adsorption and subsequent degradation on ball-milling tailored N-doped biochar. Chemosphere, 2022. **303**: p. 135264.
[146] Yu, D., Y. He, S. Zeng, H. Tian, and Z. Ji, A novel magnetic S/N co-doped tea residue biochar applied to tetracycline adsorption in water environment. Colloids and Surfaces A: Physicochemical and Engineering Aspects, 2024. **703**: p. 135400.
[147] Ma, Y., L. Yang, L. Wu, P. Li, X. Qi, L. He, S. Cui, Y. Ding, and Z. Zhang, Carbon nanotube supported sludge biochar as an efficient adsorbent for low concentrations of sulfamethoxazole removal. Science of The Total Environment, 2020. **718**: p. 137299.
[148] Hussain, I., N.B. Singh, A. Singh, H. Singh, and S.C. Singh, Green synthesis of nanoparticles and its potential application. Biotechnology Letters, 2016. **38**(4): p. 545-560.
[149] Khalil, M.M.H., E.H. Ismail, K.Z. El-Baghdady, and D. Mohamed, Green synthesis of silver nanoparticles using olive leaf extract and its antibacterial activity. Arabian Journal of Chemistry, 2014. **7**(6): p. 1131-1139.
[150] Ramesh, P., A. Rajendran, and M. Meenakshisundaram, Green synthesis of zinc oxide nanoparticles using flower extract Cassia auriculata. J Nanosci Nanotechnol, 2014. **2**(1): p. 41-45.

[151] Singh, N. and S. Naraa, Biological synthesis and characterization of lead sulfide nanoparticles using bacterial isolates from heavy metal rich sites. Int J Agric Food Sci Technol, 2013. **4**: p. 16-23.
[152] Song, J.Y. and B.S. Kim, Rapid biological synthesis of silver nanoparticles using plant leaf extracts. Bioprocess and Biosystems Engineering, 2009. **32**(1): p. 79-84.
[153] Arabkhani, P., A. Asfaram, and F. Sadegh, Green and low-temperature synthesis of the magnetic modified biochar under the air atmosphere for the adsorptive removal of heavy metal ions from wastewater: CCD-RSM experimental design with isotherm, kinetic, and thermodynamic studies. Environmental Science and Pollution Research, 2023. **30**(57): p. 120085-120102.
[154] Kumar, D. and S.K. Gupta, Green synthesis of novel biochar from Abelmoschus esculentus seeds for direct blue 86 dye removal: Characterization, RSM optimization, isotherms, kinetics, and fixed bed column studies. Environmental Pollution, 2023. **337**: p. 122559.
[155] Dao, T.M. and T. Le Luu, Synthesis of activated carbon from macadamia nutshells activated by H2SO4 and K2CO3 for methylene blue removal in water. Bioresource Technology Reports, 2020. **12**: p. 100583.
[156] Wang, Y., C. Srinivasakannan, H. Wang, G. Xue, L. Wang, X. Wang, and X. Duan, Preparation of novel biochar containing graphene from waste bamboo with high methylene blue adsorption capacity. Diamond and Related Materials, 2022. **125**: p. 109034.
[157] Danish, M. and T. Ahmad, A review on utilization of wood biomass as a sustainable precursor for activated carbon production and application. Renewable and Sustainable Energy Reviews, 2018. **87**: p. 1-21.
[158] Poo, K.-M., E.-B. Son, J.-S. Chang, X. Ren, Y.-J. Choi, and K.-J. Chae, Biochars derived from wasted marine macro-algae (Saccharina japonica and Sargassum fusiforme) and their potential for heavy metal removal in aqueous solution. Journal of Environmental Management, 2018. **206**: p. 364-372.
[159] Nguyen, T.-B., Q.-M. Truong, C.-W. Chen, W.-H. Chen, and C.-D. Dong, Pyrolysis of marine algae for biochar production for adsorption of Ciprofloxacin from aqueous solutions. Bioresource Technology, 2022. **351**: p. 127043.
[160] Ok, Y.S., A. Bhatnagar, D. Hou, T. Bhaskar, and O. Mašek, Advances in algal biochar: Production, characterization and applications. Bioresource technology, 2020. **317**: p. 123982-123982.
[161] Jin, W., Q. Fang, D. Jiang, T. Li, B. Wei, J. Sun, W. Zhang, Z. Zhang, F. Zhang, R.J. Linhardt, H. Wang, and W. Zhong, Structural characteristics and anti-complement activities of polysaccharides from Sargassum hemiphyllum. Glycoconjugate Journal, 2020. **37**(5): p. 553-563.
[162] Bastos, E., M. Schneider, D.P.C. de Quadros, B. Welz, M.B. Batista, P.A. Horta, L.R. Rörig, and J.B. Barufi, Phytoremediation potential of Ulva ohnoi (Chlorophyta): Influence of temperature and salinity on the uptake efficiency and toxicity of cadmium. Ecotoxicology and Environmental Safety, 2019. **174**: p. 334-343.
[163] Hsiao, Y.-H., Y.-H. Wang, W.-S. Lin, Y.-C. Cheng, K. Nagabhushanam, C.-T. Ho, and M.-H. Pan, Molecular Mechanisms of the Anti-obesity Properties of Agardhiella subulata in Mice Fed a High-Fat Diet. Journal of Agricultural and Food Chemistry, 2021. **69**(16): p. 4745-4754.
[164] Mosaffa, E., A. Banerjee, and H. Ghafuri, Sustainable high-efficiency removal of cationic and anionic dyes using new super adsorbent biochar: performance, isotherm, kinetic and thermodynamic evaluation. Environmental Science: Water Research Technology, 2023. **9**(10): p. 2643-2663.

[165] Soltys, L., O. Olkhovyy, T. Tatarchuk, and M. Naushad, Green Synthesis of Metal and Metal Oxide Nanoparticles: Principles of Green Chemistry and Raw Materials. 2021. **7**(11): p. 145.
[166] Chakhtouna, H., H. Benzeid, N. Zari, A.e.k. Qaiss, and R. Bouhfid, Microwave-assisted synthesis of MIL–53(Fe)/biochar composite from date palm for ciprofloxacin and ofloxacin antibiotics removal. Separation and Purification Technology, 2023. **308**: p. 122850.
[167] Mahgoub, S.M., S.A. M., K.A. A., E.Z. E., K. W., E. Doaa, M.E. A., R.A. M., A.A. A., A.H. E., and R. and Mahmoud, Efficient ciprofloxacin removal from water using Zn-MOF and Date seeds-biochar composites: a comprehensive evaluation of greenness, sustainability, and environmental impact. International Journal of Environmental Analytical Chemistry: p. 1-29.
[168] Navarathna, C.M., N.B. Dewage, A.G. Karunanayake, E.L. Farmer, F. Perez, E.B. Hassan, T.E. Mlsna, and C.U. Pittman, Rhodamine B Adsorptive Removal and Photocatalytic Degradation on MIL-53-Fe MOF/Magnetic Magnetite/Biochar Composites. Journal of Inorganic and Organometallic Polymers and Materials, 2020. **30**(1): p. 214-229.
[169] Liu, D., W. Gu, L. Zhou, J. Lei, L. Wang, J. Zhang, and Y. Liu, From biochar to functions: Lignin induced formation of Fe3C in carbon/Fe composites for efficient adsorption of tetracycline from wastewater. Separation and Purification Technology, 2023. **304**: p. 122217.
[170] Ghaedi, S., H. Rajabi, M. Hadi Mosleh, and M. Sedighi, MOF biochar composites for environmental protection and pollution control. Bioresource Technology, 2025. **418**: p. 131982.
[171] Jiang, Y.-C., M.-F. Luo, Z.-N. Niu, S.-Y. Xu, Y. Gao, Y. Gao, W.-J. Gao, J.-J. Luo, and R.-L. Liu, In-situ growth of bimetallic FeCo-MOF on magnetic biochar for enhanced clearance of tetracycline and fruit preservation. Chemical Engineering Journal, 2023. **451**: p. 138804.
[172] Fernández-Andrade, K.J., A.A. Fernández-Andrade, L.Á. Zambrano-Intriago, L.E. Arteaga-Perez, S. Alejandro-Martin, R.J. Baquerizo-Crespo, R. Luque, and J.M. Rodríguez-Díaz, Microwave-assisted MOF@biomass layered nanomaterials: Characterization and applications in wastewater treatment. Chemosphere, 2023. **314**: p. 137664.
[173] Yu, F., J. Pan, Y. Li, Y. Yang, Z. Zhang, J. Nie, and J. Ma, Batch and continuous fixed-bed column adsorption of tetracycline by biochar/MOFs derivative covered with κ-carrageenan/calcium alginate hydrogels. Journal of Environmental Chemical Engineering, 2022. **10**(3): p. 107996.
[174] Mohammadi, A., M. Kazemeini, and S. Sadjadi, Synthesis and physicochemical evaluations of a novel MIL-101(Fe)-PMA-Biochar triple composite photocatalyst activated through visible-light and utilized toward degradation of organic pollutants: optimal operations and kinetics investigations. Photochemical & Photobiological Sciences, 2023. **22**(6): p. 1357-1378.
[175] Zambrano-Intriago, L.A., E.V. Daza-López, A. Fernández-Andrade, R. Luque, C.G. Amorim, A.N. Araújo, J.M. Rodríguez-Díaz, and M.C.B.S.M. Montenegro, Application of a novel hybrid MIL-53(Al)@rice husk for the adsorption of glyphosate in water: Characteristics and mechanism of the process. Chemosphere, 2023. **327**: p. 138457.
[176] Aryee, A.A., Y. Xiao, R. Han, and L. Qu, Uptake of 2,4-dichlorophenoxyacetic acid and tetracycline in single and binary systems onto a biomass-MOF composite:

adsorption and mechanism study. Biomass Conversion and Biorefinery, 2024. **14**(16): p. 18747-18760.

[177] Mahmoud, M.E. and G.A.A. Ibrahim, Cr(VI) and doxorubicin adsorptive capture by a novel bionanocomposite of Ti-MOF@TiO2 incorporated with watermelon biochar and chitosan hydrogel. International Journal of Biological Macromolecules, 2023. **253**: p. 126489.

[178] Liu, J., Q. Zeng, Y. Chen, Z. Dai, W. Jiang, L. Yao, J. Zheng, D. Sun, Y. Wu, and L. Yang, Synthesizing ZIF-8 functionalized biochar by in situ reuse of residual Zn from chemical activation for enhanced tetracycline hydrochloride adsorption removal. Journal of Environmental Chemical Engineering, 2025. **13**(3): p. 116729.

[179] Wang, L., H. Song, L. Yuan, Z. Li, Y. Zhang, J.K. Gibson, L. Zheng, Z. Chai, and W. Shi, Efficient U(VI) Reduction and Sequestration by Ti2CTx MXene. Environmental Science & Technology, 2018. **52**(18): p. 10748-10756.

[180] Dixit, F., K. Zimmermann, R. Dutta, N.J. Prakash, B. Barbeau, M. Mohseni, and B. Kandasubramanian, Application of MXenes for water treatment and energy-efficient desalination: A review. Journal of Hazardous Materials, 2022. **423**: p. 127050.

[181] Bukhari, A., I. Ijaz, A. Nazir, S. Hussain, H. Zain, E. Gilani, A.A. Lfseisi, and H. Ahmad, Functionalization of Shorea faguetiana biochar using Fe(2)O(3) nanoparticles and MXene for rapid removal of methyl blue and lead from both single and binary systems. RSC Adv, 2024. **14**(6): p. 3732-3747.

[182] Liu, F., S. Wang, C. Zhao, and B. Hu, Constructing coconut shell biochar/MXenes composites through self-assembly strategy to enhance U(VI) and Cs(I) immobilization capability. Biochar, 2023. **5**(1): p. 31.

[183] Kumar, A., E. Singh, and S.-L. Lo, Tunable 2D porous Ti3C2Tx MXene@biochar composites synthesized via ultrasound-assisted self-assembly for simultaneous removal of co-existing wastewater contaminants. Separation and Purification Technology, 2025. **355**: p. 129648.

[184] Kumar, A., E. Singh, and S.-L. Lo, MXene/biochar composites for enhanced wastewater reclamation and bioenergy production: A kinetics and thermodynamics study. Chemosphere, 2024. **359**: p. 142268.

[185] Nguyen, T.P., V.D. Nguyen, M.T. Trinh, P.L. Han, T.H. Nguyen, M.T. Nguyen, and A.-T. Vu, Effective biosorptive removal of Pb2+ ions from wastewater using modified lettuce leaves: A novel sustainable and eco-friendly biosorbent. Journal of Hazardous Materials Advances, 2025: p. 100770.

[186] Nguyen Van Doan, N.T.M., Dao Thi Cam Vi, Nguyen Thu Huong, Vu Tuan Cuong, Le Trung Phong, Nguyen Thu Huyen, Vu Anh Tuan, Production of Porous Silica from Rice Husk Using Cetyltrimethylammonium Bromide to Remove Dyes in Aqueous Solution. (2024). JST: Engineering and Technology for Sustainable Development. . JST: Engineering and Technology for Sustainable Development. , 2024. **34**(4): p. 009-016.

[187] Bai, S., S. Zhu, C. Jin, Z. Sun, L. Wang, Q. Wen, and F. Ma, Sorption mechanisms of antibiotic sulfamethazine (SMT) on magnetite-coated biochar: pH-dependence and redox transformation. Chemosphere, 2021. **268**: p. 128805.

[188] Hu, B., Y. Tang, X. Wang, L. Wu, J. Nong, X. Yang, and J. Guo, Cobalt-gadolinium modified biochar as an adsorbent for antibiotics in single and binary systems. Microchemical Journal, 2021. **166**: p. 106235.

[189] Nguyen, V.D. and V.-G. Le, Ultrahigh Pb^{2+} ion adsorption by EDTA-modified super-porous silica aerogel derived from rice husk ash. Environmental Research, 2025. **286**: p. 122803.

[190] Xu, Z., Y. Xiang, H. Zhou, J. Yang, Y. He, Z. Zhu, and Y. Zhou, Manganese ferrite modified biochar from vinasse for enhanced adsorption of levofloxacin: Effects and mechanisms. Environmental Pollution, 2021. **272**: p. 115968.
[191] Cai, P., Q. Huang, and X. Zhang, Microcalorimetric studies of the effects of MgCl2 concentrations and pH on the adsorption of DNA on montmorillonite, kaolinite and goethite. Applied Clay Science, 2006. **32**(1): p. 147-152.
[192] Wu, M., R. Kempaiah, P.-J.J. Huang, V. Maheshwari, and J. Liu, Adsorption and Desorption of DNA on Graphene Oxide Studied by Fluorescently Labeled Oligonucleotides. Langmuir, 2011. **27**(6): p. 2731-2738.
[193] Zhao, J. and Y. Dai, Tetracycline adsorption mechanisms by NaOH-modified biochar derived from waste Auricularia auricula dregs. Environmental Science and Pollution Research, 2022. **29**(6): p. 9142-9152.
[194] Leng, L. and H. Huang, An overview of the effect of pyrolysis process parameters on biochar stability. Bioresource Technology, 2018. **270**: p. 627-642.
[195] Mankomal and H. Kaur, Synergistic effect of biochar impregnated with ZnO nano-flowers for effective removal of organic pollutants from wastewater. Applied Surface Science Advances, 2022. **12**: p. 100339.
[196] Chen, S., C. Qin, T. Wang, F. Chen, X. Li, H. Hou, and M. Zhou, Study on the adsorption of dyestuffs with different properties by sludge-rice husk biochar: Adsorption capacity, isotherm, kinetic, thermodynamics and mechanism. Journal of Molecular Liquids, 2019. **285**: p. 62-74.
[197] Nguyen, T.H., V.D. Nguyen, and A.T. Vu, Synthesis of CS-Fe3O4/GO nanocomposite for adsorption of heavy metal in aqueous environment. Nanotechnology, 2024. **35**(34).
[198] Qiu, B., Q. Shao, J. Shi, C. Yang, and H. Chu, Application of biochar for the adsorption of organic pollutants from wastewater: Modification strategies, mechanisms and challenges. Separation and Purification Technology, 2022. **300**: p. 121925.
[199] Barquilha, C.E.R. and M.C.B. Braga, Adsorption of organic and inorganic pollutants onto biochars: Challenges, operating conditions, and mechanisms. Bioresource Technology Reports, 2021. **15**: p. 100728.
[200] Fan, S., Y. Wang, Z. Wang, J. Tang, J. Tang, and X. Li, Removal of methylene blue from aqueous solution by sewage sludge-derived biochar: Adsorption kinetics, equilibrium, thermodynamics and mechanism. Journal of Environmental Chemical Engineering, 2017. **5**(1): p. 601-611.
[201] Fan, S., J. Tang, Y. Wang, H. Li, H. Zhang, J. Tang, Z. Wang, and X. Li, Biochar prepared from co-pyrolysis of municipal sewage sludge and tea waste for the adsorption of methylene blue from aqueous solutions: Kinetics, isotherm, thermodynamic and mechanism. Journal of Molecular Liquids, 2016. **220**: p. 432-441.
[202] Miri Kafi Abad, S.S.A., P. Javidan, M. Baghdadi, and N. Mehrdadi, Green synthesis of Pd@biochar using the extract and biochar of corn-husk wastes for electrochemical Cr(VI) reduction in plating wastewater. Journal of Environmental Chemical Engineering, 2023. **11**(3): p. 109911.
[203] Mustafa, F.S. and K.H. Hama Aziz, Heterogeneous catalytic activation of persulfate for the removal of rhodamine B and diclofenac pollutants from water using iron-impregnated biochar derived from the waste of black seed pomace. Process Safety and Environmental Protection, 2023. **170**: p. 436-448.
[204] Tsai, W.T. and H.R. Chen, Adsorption kinetics of herbicide paraquat in aqueous solution onto a low-cost adsorbent, swine-manure-derived biochar. International Journal of Environmental Science and Technology, 2013. **10**(6): p. 1349-1356.
[205] Adu-Poku, D., S.A. Saah, P.O. Sakyi, C.K. Bandoh, B. Agyei-Tuffour, D. Azanu, M. Oteng-Peprah, I. Hawawu, S. Azibere, and K.A. Affram, Acid-Activated Biochar for

Efficient Elimination of Amoxicillin From Wastewater. Journal of Chemistry, 2024. **2024**(1): p. 3648098.

[206] Stylianou, M., A. Christou, C. Michael, A. Agapiou, P. Papanastasiou, and D. Fatta-Kassinos, Adsorption and removal of seven antibiotic compounds present in water with the use of biochar derived from the pyrolysis of organic waste feedstocks. Journal of Environmental Chemical Engineering, 2021. **9**(5): p. 105868.

[207] Nguyen, D.T., T.K. Hoang, T.D. Tran, M.H. Nguyen, K.T. Trinh, D.A. Khuong, T. Tsubota, and T.D. Pham, Adsorption characteristics of individual and binary mixture of ciprofloxacin antibiotic and lead(II) on synthesized bamboo-biochar. Environmental Research, 2025. **273**: p. 121225.

[208] Vigneshwaran, S., P. Sirajudheen, M. Nikitha, K. Ramkumar, and S. Meenakshi, Facile synthesis of sulfur-doped chitosan/biochar derived from tapioca peel for the removal of organic dyes: Isotherm, kinetics and mechanisms. Journal of Molecular Liquids, 2021. **326**: p. 115303.

[209] Du, L., W. Xu, S. Liu, X. Li, D. Huang, X. Tan, and Y. Liu, Activation of persulfate by graphitized biochar for sulfamethoxazole removal: The roles of graphitic carbon structure and carbonyl group. Journal of Colloid and Interface Science, 2020. **577**: p. 419-430.

[210] Yan, L., Y. Liu, Y. Zhang, S. Liu, C. Wang, W. Chen, C. Liu, Z. Chen, and Y. Zhang, ZnCl2 modified biochar derived from aerobic granular sludge for developed microporosity and enhanced adsorption to tetracycline. Bioresource Technology, 2020. **297**: p. 122381.

[211] Sayin, F., S.T. Akar, and T. Akar, From green biowaste to water treatment applications: Utilization of modified new biochar for the efficient removal of ciprofloxacin. Sustainable Chemistry and Pharmacy, 2021. **24**: p. 100522.

[212] Fu, Y., F. Wang, H. Sheng, F. Hu, Z. Wang, M. Xu, Y. Bian, X. Jiang, and J.M. Tiedje, Removal of extracellular antibiotic resistance genes using magnetic biochar/quaternary phosphonium salt in aquatic environments: A mechanistic study. Journal of Hazardous Materials, 2021. **411**: p. 125048.

[213] Wu, C., L. Fu, H. Li, X. Liu, and C. Wan, Using biochar to strengthen the removal of antibiotic resistance genes: Performance and mechanism. Science of The Total Environment, 2022. **816**: p. 151554.

[214] Zheng, Y., P. Lv, J. Yang, and G. Xu, Characterization and Adsorption Capacity of Modified Biochar for Sulfamethylimidine and Methylene Blue in Water. ACS Omega, 2023. **8**(33): p. 29966-29978.

[215] Ouyang, E., R. Zhang, W. Fu, R. Zhao, H. Yang, H. Xiang, and W. He, Facile Synthesis of Bamboo Biochar for Efficient Adsorption of Quinolone Antibiotics: Effects and Mechanisms. ACS Omega, 2024. **9**(49): p. 48618-48628.

[216] Xu, K., C. Zhang, X. Dou, W. Ma, and C. Wang, Optimizing the modification of wood waste biochar via metal oxides to remove and recover phosphate from human urine. Environmental Geochemistry and Health, 2019. **41**(4): p. 1767-1776.

[217] Yu, H., L. Gu, L. Chen, H. Wen, D. Zhang, and H. Tao, Activation of grapefruit derived biochar by its peel extracts and its performance for tetracycline removal. Bioresource Technology, 2020. **316**: p. 123971.

[218] Cheng, N., B. Wang, P. Wu, X. Lee, Y. Xing, M. Chen, and B. Gao, Adsorption of emerging contaminants from water and wastewater by modified biochar: A review. Environmental Pollution, 2021. **273**: p. 116448.

[219] Jung, K.-W., S.Y. Lee, and Y.J. Lee, Hydrothermal synthesis of hierarchically structured birnessite-type MnO2/biochar composites for the adsorptive removal of Cu(II) from aqueous media. Bioresource Technology, 2018. **260**: p. 204-212.

[220] Zeng, S. and E. Kan, $FeCl_3$-activated biochar catalyst for heterogeneous Fenton oxidation of antibiotic sulfamethoxazole in water. Chemosphere, 2022. **306**: p. 135554.
[221] Liu, B.-L., M.-M. Fu, L. Xiang, N.-X. Feng, H.-M. Zhao, Y.-W. Li, Q.-Y. Cai, H. Li, C.-H. Mo, and M.-H. Wong, Adsorption of microcystin contaminants by biochars derived from contrasting pyrolytic conditions: Characteristics, affecting factors, and mechanisms. Science of The Total Environment, 2021. **763**: p. 143028.
[222] Lonappan, L., T. Rouissi, S. Kaur Brar, M. Verma, and R.Y. Surampalli, An insight into the adsorption of diclofenac on different biochars: Mechanisms, surface chemistry, and thermodynamics. Bioresource Technology, 2018. **249**: p. 386-394.
[223] Wang, Z., L. Han, K. Sun, J. Jin, K.S. Ro, J.A. Libra, X. Liu, and B. Xing, Sorption of four hydrophobic organic contaminants by biochars derived from maize straw, wood dust and swine manure at different pyrolytic temperatures. Chemosphere, 2016. **144**: p. 285-291.
[224] Liang, J., Y. Fang, Y. Luo, G. Zeng, J. Deng, X. Tan, N. Tang, X. Li, X. He, C. Feng, and S. Ye, Magnetic nanoferromanganese oxides modified biochar derived from pine sawdust for adsorption of tetracycline hydrochloride. Environmental Science and Pollution Research, 2019. **26**(6): p. 5892-5903.
[225] Tang, L., J. Yu, Y. Pang, G. Zeng, Y. Deng, J. Wang, X. Ren, S. Ye, B. Peng, and H. Feng, Sustainable efficient adsorbent: Alkali-acid modified magnetic biochar derived from sewage sludge for aqueous organic contaminant removal. Chemical Engineering Journal, 2018. **336**: p. 160-169.
[226] Nguyen, V.-T., T.-B. Nguyen, C.P. Huang, C.-W. Chen, X.-T. Bui, and C.-D. Dong, Alkaline modified biochar derived from spent coffee ground for removal of tetracycline from aqueous solutions. Journal of Water Process Engineering, 2021. **40**: p. 101908.
[227] Tan, Z., Z. Xueyang, W. Liping, G. Bin, L. Junpeng, F. Ru, Z. Weixin, and N. and Meng, Sorption of tetracycline on H2O2-modified biochar derived from rape stalk. Environmental Pollutants and Bioavailability, 2019. **31**(1): p. 198-207.
[228] Calderón-Franco, D., S. Apoorva, G. Medema, M.C.M. van Loosdrecht, and D.G. Weissbrodt, Upgrading residues from wastewater and drinking water treatment plants as low-cost adsorbents to remove extracellular DNA and microorganisms carrying antibiotic resistance genes from treated effluents. Science of The Total Environment, 2021. **778**: p. 146364.
[229] Wang, C., T. Wang, W. Li, J. Yan, Z. Li, R. Ahmad, S.K. Herath, and N. Zhu, Adsorption of deoxyribonucleic acid (DNA) by willow wood biochars produced at different pyrolysis temperatures. Biology and Fertility of Soils, 2014. **50**(1): p. 87-94.
[230] Lu, Q., K. Yin, J. Wang, X. Zhang, X. Tian, X. Ma, Y. Zhao, S. Sun, H. Yuan, S. Zhai, H. Zheng, and B. Xing, Characteristics of chemical aged biochars and their adsorption behaviors for norfloxacin. Journal of Environmental Chemical Engineering, 2024. **12**(5): p. 113638.
[231] Liu, X., D. Wang, J. Tang, F. Liu, and L. Wang, Effect of dissolved biochar on the transfer of antibiotic resistance genes between bacteria. Environmental Pollution, 2021. **288**: p. 117718.
[232] Deng, Y., M. Wang, Y. Yang, X. Li, W. Chen, and T. Ao, Enhanced adsorption performance of sulfamethoxazole and tetracycline in aqueous solutions by $MgFe_2O_4$-magnetic biochar. Water Science and Technology, 2022. **86**(3): p. 568-583.
[233] Badshah, K., Q. Ali, A.A. Khan, R. Ahmad, and I. Ahmad, Experimental and DFT Studies of Antibiotics Removal Through Activated Carbon: A Step-by-Step Adsorption Process at Atomic Level. ChemistrySelect, 2024. **9**(44): p. e202402422.

[234] Zhang, X., J. Hou, S. Zhang, T. Cai, S. Liu, W. Hu, and Q. Zhang, Standardization and micromechanistic study of tetracycline adsorption by biochar. Biochar, 2024. **6**(1): p. 12.
[235] Bai, S., Y. Zhou, M. Qian, J. Xia, Z. Sun, Y. Wang, X. Huang, and S. Zhu, Mechanistic insights to sorptive removal of four sulfonamide antibiotics from water using magnetite-functionalized biochar. Biochar, 2023. **5**(1): p. 80.
[236] Ezzahi, K., I. Rabichi, H. Befenzi, E. Record, T. Bouzid, A. Yaacoubi, A. Baçaoui, Y. Habibi, and L. El Fels, Optimization, characterization, and DFT study of activated-biochar from lignocellulosic biomass for fluoroquinolone antibiotic adsorption. Results in Engineering, 2025. **27**: p. 106540.
[237] Ren, H., X. Ma, B. Ma, X. Bai, H. Wang, Z. Ma, S. Gu, and J. Wang, DFT-Validated adsorption mechanisms of metronidazole on CO_2-activated almond shell biochar for antibiotic wastewater treatment. Desalination and Water Treatment, 2025. **324**: p. 101414.
[238] Jiang, H. and H. Hu, Sustainable synergistic adsorption of tetracycline in water by biochar and microplastics: Exploration of the mechanism of DFT. Journal of Water Process Engineering, 2024. **66**: p. 105998.
[239] Chen, Q., J. Zheng, J. Xu, Z. Dang, and L. Zhang, Insights into sulfamethazine adsorption interfacial interaction mechanism on mesoporous cellulose biochar: Coupling DFT/FOT simulations with experiments. Chemical Engineering Journal, 2019. **356**: p. 341-349.
[240] Liu, X., P. Huang, W. Ma, F. Jin, and L. Tai, Unveiling adsorption mechanisms and regeneration challenges of durian peel biochar for ciprofloxacin removal: Batch experiments and DFT study. Journal of Water Process Engineering, 2025. **75**: p. 107991.
[241] Peng, B., L. Chen, C. Que, K. Yang, F. Deng, X. Deng, G. Shi, G. Xu, and M. Wu, Adsorption of Antibiotics on Graphene and Biochar in Aqueous Solutions Induced by π-π Interactions. Scientific Reports, 2016. **6**(1): p. 31920.
[242] Hu, W., Y. Niu, T. Shen, K. Dong, and D. Wang, Magnetic biochar prepared by a dry process for the removal of sulfonamides antibiotics from aqueous solution. Journal of Molecular Liquids, 2024. **400**: p. 124576.
[243] Li, Y., B. Wang, H. Shang, Y. Cao, C. Yang, W. Hu, Y. Feng, and Y. Yu, Influence of adsorption sites of biochar on its adsorption performance for sulfamethoxazole. Chemosphere, 2023. **326**: p. 138408.
[244] Zhao, H., Z. Wang, Y. Liang, T. Wu, Y. Chen, J. Yan, Y. Zhu, and D. Ding, Adsorptive decontamination of antibiotics from livestock wastewater by using alkaline-modified biochar. Environmental Research, 2023. **226**: p. 115676.
[245] Nasiri, A., N. Golestani, S. Rajabi, and M. Hashemi, Facile and green synthesis of recyclable, environmentally friendly, chemically stable, and cost-effective magnetic nanohybrid adsorbent for tetracycline adsorption. Heliyon, 2024. **10**(2).
[246] Thakur, A., A. Kumar, and A. Singh, Adsorptive removal of heavy metals, dyes, and pharmaceuticals: Carbon-based nanomaterials in focus. Carbon, 2024. **217**: p. 118621.
[247] Zhou, Y., Z. Wang, W. Hu, Q. Zhou, and J. Chen, Norfloxacin adsorption by urban green waste biochar: characterization, kinetics, and mechanisms. Environmental Science and Pollution Research, 2024. **31**(20): p. 29088-29100.
[248] Dilpazeer, F., M. Munir, M.Y.J. Baloch, I. Shafiq, J. Iqbal, M. Saeed, M.M. Abbas, S. Shafique, K.H.H. Aziz, A. Mustafa, and I. Mahboob, A Comprehensive Review of the Latest Advancements in Controlling Arsenic Contaminants in Groundwater. 2023. **15**(3): p. 478.

[249] Amalina, F., S. Krishnan, A.W. Zularisam, and M. Nasrullah, Biochar and sustainable environmental development towards adsorptive removal of pollutants: Modern advancements and future insight. Process Safety and Environmental Protection, 2023. **173**: p. 715-728.
[250] Zhao, X., G. Zhu, J. Liu, J. Wang, S. Zhang, C. Wei, L. Cao, S. Zhao, and S. Zhang, Efficient Removal of Tetracycline from Water by One-Step Pyrolytic Porous Biochar Derived from Antibiotic Fermentation Residue. 2024. **14**(17): p. 1377.
[251] Aziz, S., S. Anbreen, I. Iftikhar, T. Fatima, A. Iftikhar, and L. Ali, Green technology: synthesis of iron-modified biochar derived from pine cones to remove azithromycin and ciprofloxacin from water. 2024. **Volume 12 - 2024**.
[252] Sen, U., B. Esteves, T. Aguiar, and H. Pereira, Removal of Antibiotics by Biochars: A Critical Review. Applied Sciences, 2023. **13**(21): p. 11963.
[253] MacKay, A.A. and D. Vasudevan, Polyfunctional Ionogenic Compound Sorption: Challenges and New Approaches To Advance Predictive Models. Environmental Science & Technology, 2012. **46**(17): p. 9209-9223.
[254] Wang, K., R. Yao, D. Zhang, N. Peng, P. Zhao, Y. Zhong, H. Zhou, J. Huang, and C. Liu, Tetracycline Adsorption Performance and Mechanism Using Calcium Hydroxide-Modified Biochars. Toxics, 2023. **11**(10).
[255] Chen, Y., J. Shi, Q. Du, H. Zhang, and Y. Cui, Antibiotic removal by agricultural waste biochars with different forms of iron oxide. RSC Advances, 2019. **9**(25): p. 14143-14153.
[256] Xu, Q., Q. Zhou, M. Pan, and L. Dai, Interaction between chlortetracycline and calcium-rich biochar: Enhanced removal by adsorption coupled with flocculation. Chemical Engineering Journal, 2020. **382**: p. 122705.
[257] Zhang, L., W. Yang, Y. Chen, and L. Yang, Removal of Tetracycline from Water by Biochar: Mechanisms, Challenges, and Future Perspectives. 2025. **17**(13): p. 1960.
[258] Jia, Y., Y. Ou, S.K. Khanal, L. Sun, W.-s. Shu, and H. Lu, Biochar-Based Strategies for Antibiotics Removal: Mechanisms, Factors, and Application. ACS ES&T Engineering, 2024. **4**(6): p. 1256-1274.
[259] Wei, J., Y. Liu, J. Li, Y. Zhu, H. Yu, and Y. Peng, Adsorption and co-adsorption of tetracycline and doxycycline by one-step synthesized iron loaded sludge biochar. Chemosphere, 2019. **236**: p. 124254.
[260] Tang, Y., Y. Li, L. Zhan, D. Wu, S. Zhang, R. Pang, and B. Xie, Removal of emerging contaminants (bisphenol A and antibiotics) from kitchen wastewater by alkali-modified biochar. Science of The Total Environment, 2022. **805**: p. 150158.
[261] Ge, Q., P. Li, M. Liu, G.-m. Xiao, Z.-q. Xiao, J.-w. Mao, and X.-k. Gai, Removal of methylene blue by porous biochar obtained by KOH activation from bamboo biochar. Bioresources and Bioprocessing, 2023. **10**(1): p. 51.
[262] Alsaiari, N.S., M.S. Alsaiari, F.M. Alzahrani, A. Amari, and M.A. Tahoon, Synthesis, characterization, and application of the novel nanomagnet adsorbent for the removal of Cr(vi) ions. 2023. **62**(1).
[263] Babić, S., M. Periša, and I. Škorić, Photolytic degradation of norfloxacin, enrofloxacin and ciprofloxacin in various aqueous media. Chemosphere, 2013. **91**(11): p. 1635-1642.
[264] Lian, F., W. Yu, Q. Zhou, S. Gu, Z. Wang, and B. Xing, Size Matters: Nano-Biochar Triggers Decomposition and Transformation Inhibition of Antibiotic Resistance Genes in Aqueous Environments. Environmental Science & Technology, 2020. **54**(14): p. 8821-8829.

[265] Fang, J., L. Jin, Q. Meng, D. Wang, and D. Lin, Interactions of extracellular DNA with aromatized biochar and protection against degradation by DNase I. Journal of Environmental Sciences, 2021. **101**: p. 205-216.
[266] Tan, Z., S. Yuan, M. Hong, L. Zhang, and Q. Huang, Mechanism of negative surface charge formation on biochar and its effect on the fixation of soil Cd. Journal of Hazardous Materials, 2020. **384**: p. 121370.
[267] Li, N., X. Zhu, Y. Miao, Z. Wang, C.S.K. Lin, and C. Li, Meta-analysis and empirical research on the effectiveness of biochar in remediating tetracyclines pollution in water bodies. Bioresource Technology, 2025. **435**: p. 132917.
[268] Zhang, F., J. Wang, Y. Tian, C. Liu, S. Zhang, L. Cao, Y. Zhou, and S. Zhang, Effective removal of tetracycline antibiotics from water by magnetic functionalized biochar derived from rice waste. Environ Pollut, 2023. **330**: p. 121681.
[269] Yang, Z., R. Xing, W. Zhou, and L. Zhu, Adsorption characteristics of ciprofloxacin onto g-MoS_2 coated biochar nanocomposites. Frontiers of Environmental Science & Engineering, 2020. **14**(3): p. 41.
[270] Rajapaksha, A.U., M. Vithanage, M. Zhang, M. Ahmad, D. Mohan, S.X. Chang, and Y.S. Ok, Pyrolysis condition affected sulfamethazine sorption by tea waste biochars. Bioresource Technology, 2014. **166**: p. 303-308.
[271] Duan, M., G. Liu, B. Zhou, X. Chen, Q. Wang, H. Zhu, and Z. Li, Effects of modified biochar on water and salt distribution and water-stable macro-aggregates in saline-alkaline soil. Journal of Soils and Sediments, 2021. **21**(6): p. 2192-2202.
[272] Guo, X., H. Dong, C. Yang, Q. Zhang, C. Liao, F. Zha, and L. Gao, Application of goethite modified biochar for tylosin removal from aqueous solution. Colloids and Surfaces A: Physicochemical and Engineering Aspects, 2016. **502**: p. 81-88.
[273] Premarathna, K.S.D., A.U. Rajapaksha, N. Adassoriya, B. Sarkar, N.M.S. Sirimuthu, A. Cooray, Y.S. Ok, and M. Vithanage, Clay-biochar composites for sorptive removal of tetracycline antibiotic in aqueous media. Journal of Environmental Management, 2019. **238**: p. 315-322.
[274] Li, J., G. Yu, L. Pan, C. Li, F. You, and Y. Wang, Ciprofloxacin adsorption by biochar derived from co-pyrolysis of sewage sludge and bamboo waste. Environmental Science and Pollution Research, 2020. **27**(18): p. 22806-22817.
[275] Huang, P., C. Ge, D. Feng, H. Yu, J. Luo, J. Li, P.J. Strong, A.K. Sarmah, N.S. Bolan, and H. Wang, Effects of metal ions and pH on ofloxacin sorption to cassava residue-derived biochar. Science of The Total Environment, 2018. **616-617**: p. 1384-1391.
[276] Kabir, E., K.-H. Kim, and E.E. Kwon, Biochar as a tool for the improvement of soil and environment. Frontiers in Environmental Science, 2023. **Volume 11 - 2023**.
[277] Keiluweit, M., P.S. Nico, M.G. Johnson, and M. Kleber, Dynamic Molecular Structure of Plant Biomass-Derived Black Carbon (Biochar). Environmental Science & Technology, 2010. **44**(4): p. 1247-1253.
[278] Li, Y., D. Chi, Y. Sun, X. Wang, M. Tan, Y. Guan, Q. Wu, and H. Zhou, Synthesis of struvite-enriched slow-release fertilizer using magnesium-modified biochar: Desorption and leaching mechanisms. Science of The Total Environment, 2024. **926**: p. 172172.
[279] Dou, S., X.-X. Ke, Z.-D. Shao, L.-B. Zhong, Q.-B. Zhao, and Y.-M. Zheng, Fish scale-based biochar with defined pore size and ultrahigh specific surface area for highly efficient adsorption of ciprofloxacin. Chemosphere, 2022. **287**: p. 131962.
[280] Feng, Y., Q. Liu, Y. Yu, Q. Kong, L.-l. Zhou, Y.-d. Du, and X.-f. Wang, Norfloxacin removal from aqueous solution using biochar derived from luffa sponge. Journal of Water Supply: Research Technology—AQUA, 2018. **67**(8): p. 703-714.

[281] Yan, B., C.H. Niu, and J. Wang, Kinetics, electron-donor-acceptor interactions, and site energy distribution analyses of norfloxacin adsorption on pretreated barley straw. Chemical Engineering Journal, 2017. **330**: p. 1211-1221.
[282] Chen, M., Z. Yan, J. Luan, X. Sun, W. Liu, and X. Ke, π-π electron-donor-acceptor (EDA) interaction enhancing adsorption of tetracycline on 3D PPY/CMC aerogels. Chemical Engineering Journal, 2023. **454**: p. 140300.
[283] Li, Y., Z. Cheng, H. Shang, Y. Chen, S. Li, X. Wei, T. Wang, W. Zhou, and Y. Yu, Design of functional groups on biochar for sulfamethoxazole adsorption from adsorption efficiency and adsorption mechanism. Journal of Environmental Chemical Engineering, 2025. **13**(3): p. 116874.
[284] Pap, S., L. Shearer, and S.W. Gibb, Sustainable remediation of macrolide antibiotic from water using a novel Fe oxide/biochar nanocomposite: Adsorption behaviour and mechanistic analysis. Journal of Environmental Chemical Engineering, 2025. **13**(1): p. 115208.
[285] Zhang, Y., Y. Gong, G. Shi, X. Liu, M. Dai, and L. Ding, Removal of Quinolone Antibiotics from Wastewater by the Biochar-Based Sludge Adsorbent. 2023. **9**(8): p. 752.
[286] Son Tran, V., H. Hao Ngo, W. Guo, T. Ha Nguyen, T. Mai Ly Luong, X. Huan Nguyen, T. Lan Anh Phan, V. Trong Le, M. Phuong Nguyen, and M. Khai Nguyen, New chitosan-biochar composite derived from agricultural waste for removing sulfamethoxazole antibiotics in water. Bioresource Technology, 2023. **385**: p. 129384.
[287] Huang, J., A.R. Zimmerman, H. Chen, and B. Gao, Ball milled biochar effectively removes sulfamethoxazole and sulfapyridine antibiotics from water and wastewater. Environmental Pollution, 2020. **258**: p. 113809.
[288] Geng, X., S. Lv, J. Yang, S. Cui, and Z. Zhao, Carboxyl-functionalized biochar derived from walnut shells with enhanced aqueous adsorption of sulfonamide antibiotics. Journal of Environmental Management, 2021. **280**: p. 111749.
[289] Diao, Y., R. Shan, M. Li, J. Gu, H. Yuan, and Y. Chen, Efficient Adsorption of a Sulfonamide Antibiotic in Aqueous Solutions with N-doped Magnetic Biochar: Performance, Mechanism, and Reusability. ACS Omega, 2023. **8**(1): p. 879-892.
[290] Wang, Y., J. Lu, J. Wu, Q. Liu, H. Zhang, and S. Jin, Adsorptive Removal of Fluoroquinolone Antibiotics Using Bamboo Biochar. 2015. **7**(9): p. 12947-12957.
[291] Jiang, H., X. Li, J. Bai, W. Pan, Z. Luo, and Y. Dai, Removal of ciprofloxacin lactate by phosphoric acid activated biochar: Urgent consideration of new antibiotics for human health. Chemical Engineering Science, 2024. **283**: p. 119403.
[292] Yao, B., W. Zeng, A. Núñez-Delgado, and Y. Zhou, Simultaneous adsorption of ciprofloxacin and Cu^{2+} using Fe and N co-doped biochar: Competition and selective separation. Waste Management, 2023. **168**: p. 386-395.
[293] Saremi, F., M.R. Miroliaei, M. Shahabi Nejad, and H. Sheibani, Adsorption of tetracycline antibiotic from aqueous solutions onto vitamin B6-upgraded biochar derived from date palm leaves. Journal of Molecular Liquids, 2020. **318**: p. 114126.
[294] Xiang, W., Y. Wan, X. Zhang, Z. Tan, T. Xia, Y. Zheng, and B. Gao, Adsorption of tetracycline hydrochloride onto ball-milled biochar: Governing factors and mechanisms. Chemosphere, 2020. **255**: p. 127057.
[295] Deng, Y., M. Wang, Y. Yang, X. Li, W. Chen, and T. Ao, Enhanced adsorption performance of sulfamethoxazole and tetracycline in aqueous solutions by $MgFe_2O_4$-magnetic biochar. Water Sci Technol, 2022. **86**(3): p. 568-583.
[296] Meseguer, V.F., J.F. Ortuño, M.I. Aguilar, M. Lloréns, A.B. Pérez-Marín, and E. Fuentes, Ciprofloxacin Uptake from an Aqueous Solution via Adsorption with K2CO3-Activated Biochar Derived from Brewing Industry Bagasse. 2024. **12**(1): p. 199.

[297] Fan, X., Z. Qian, J. Liu, N. Geng, J. Hou, and D. Li, Investigation on the adsorption of antibiotics from water by metal loaded sewage sludge biochar. Water Science and Technology, 2020. **83**(3): p. 739-750.
[298] Nguyen, V.-T., T.-B. Nguyen, N.D. Dat, T.-K.Q. Vo, X.C. Nguyen, V.-C. Dinh, T.-N.-C. Le, T.-G.-H. Duong, M.-H. Bui, and X.-T. Bui, Preliminary study of doxycycline adsorption from aqueous solution on alkaline modified biochar derived from banana peel. Environmental Engineering Research, 2024. **29**(3).
[299] Li, Z., Z. Wang, X. Wu, M. Li, and X. Liu, Competitive adsorption of tylosin, sulfamethoxazole and Cu(II) on nano-hydroxyapatitemodified biochar in water. Chemosphere, 2020. **240**: p. 124884.
[300] Wang, H., X. Lou, Q. Hu, and T. Sun, Adsorption of antibiotics from water by using Chinese herbal medicine residues derived biochar: Preparation and properties studies. Journal of Molecular Liquids, 2021. **325**: p. 114967.
[301] Zeng, Z., S. Ye, H. Wu, R. Xiao, G. Zeng, J. Liang, C. Zhang, J. Yu, Y. Fang, and B. Song, Research on the sustainable efficacy of g-MoS_2 decorated biochar nanocomposites for removing tetracycline hydrochloride from antibiotic-polluted aqueous solution. Science of The Total Environment, 2019. **648**: p. 206-217.
[302] Liang, H., C. Zhu, A. Wang, and F. Chen, Facile preparation of $NiFe_2O_4$/biochar composite adsorbent for efficient adsorption removal of antibiotics in water. Carbon Research, 2024. **3**(1): p. 2.
[303] Zeng, Z.-w., X.-f. Tan, Y.-g. Liu, S.-r. Tian, G.-m. Zeng, L.-h. Jiang, S.-b. Liu, J. Li, N. Liu, and Z.-h. Yin, Comprehensive Adsorption Studies of Doxycycline and Ciprofloxacin Antibiotics by Biochars Prepared at Different Temperatures. 2018. **Volume 6 - 2018**.
[304] Nguyen, T.K., T.B. Nguyen, W.H. Chen, C.W. Chen, A. Kumar Patel, X.T. Bui, L. Chen, R.R. Singhania, and C.D. Dong, Phosphoric acid-activated biochar derived from sunflower seed husk: Selective antibiotic adsorption behavior and mechanism. Bioresour Technol, 2023. **371**: p. 128593.
[305] Zou, C., Q. Wu, Z. Gao, Z. Xu, and F. Nie, The magnetic porous biochar prepared by K_2FeO_4-promoted oxidative pyrolysis of bagasse for adsorption of antibiotics in the aqueous solution. Biomass Conversion and Biorefinery, 2024. **14**(13): p. 14189-14205.
[306] Liao, X., C. Chen, Z. Liang, Z. Zhao, and F. Cui, Selective adsorption of antibiotics on manganese oxide-loaded biochar and mechanism based on quantitative structure–property relationship model. Bioresource Technology, 2023. **367**: p. 128262.
[307] Fan, Z., J. Fang, G. Zhang, L. Qin, Z. Fang, and L. Jin, Improved Adsorption of Tetracycline in Water by a Modified Caulis spatholobi Residue Biochar. ACS Omega, 2022. **7**(34): p. 30543-30553.
[308] Choi, Y.-K., R. Srinivasan, and E. Kan, Facile and Economical Functionalized Hay Biochar with Dairy Effluent for Adsorption of Tetracycline. ACS Omega, 2020. **5**(27): p. 16521-16529.
[309] Gao, J., Y. Zhou, X. Yang, Y. Yao, J. Qi, Z. Zhu, Y. Yang, D. Fang, L. Zhou, and J. Li, Dyeing sludge-derived biochar for efficient removal of antibiotic from water. Science of The Total Environment, 2024. **912**: p. 169035.
[310] Huang, B., D. Huang, Q. Zheng, C. Yan, J. Feng, H. Gao, H. Fu, and Y. Liao, Enhanced adsorption capacity of tetracycline on porous graphitic biochar with an ultra-large surface area. RSC advances, 2023. **13**(15): p. 10397-10407.
[311] Ling, C., Y. Song, Y. Zhu, R. Hong, T. Dong, J. Han, and Y. Feng, Highly Efficient Adsorption of Sulfamethoxazole and Ciprofloxacin by a Novel Bowl-Shaped Nitrogen-Doped Pyrolytic Carbon and the Underlying Structural-Property Mechanism. ACS ES&T Water, 2025. **5**(2): p. 871-880.

[312] Li, Y., H. Shang, Y. Cao, C. Yang, Y. Feng, and Y. Yu, High performance removal of sulfamethoxazole using large specific area of biochar derived from corncob xylose residue. Biochar, 2022. **4**(1): p. 11.
[313] Ma, X., Y. Cao, J. Deng, J. Shao, X. Feng, W. Li, S. Li, and R. Zhang, Synergistic enhancement of N, S co-modified biochar for removal of tetracycline hydrochloride from aqueous solution: Tunable micro-mesoporosity and chemisorption sites. Chemical Engineering Journal, 2024. **492**: p. 152189.
[314] Luo, P., W. Zhang, D. Xiao, J. Hu, N. Li, and J. Yang, Biochar-Based Fertilizers: Advancements, Applications, and Future Directions in Sustainable Agriculture—A Review. 2025. **15**(5): p. 1104.
[315] Dong, M., M. Jiang, L. He, Z. Zhang, W. Gustave, M. Vithanage, N.K. Niazi, B. Chen, X. Zhang, H. Wang, and F. He, Challenges in safe environmental applications of biochar: identifying risks and unintended consequence. Biochar, 2025. **7**(1): p. 12.
[316] Antonangelo, J.A., X. Sun, and H.d.J. Eufrade-Junior, Biochar impact on soil health and tree-based crops: a review. Biochar, 2025. **7**(1): p. 51.

No primary research results, software or code have been included and no new data were generated or analysed as part of this review.

View Article Online
DOI: 10.1039/D5MA00872G